Investigating the Role of Experience-Activated Neurons in Sleep-Dependent Memory Consolidation

by

Brittany C. Clawson

A dissertation submitted in partial fulfillment
of the requirements for the degree of
Doctor of Philosophy
(Molecular, Cellular, and Developmental Biology)
in the University of Michigan
2020

Doctoral Committee:

Associate Professor Sara J. Aton, Chair
Assistant Professor Dawen Cai
Assistant Professor Monica Dus
Professor Richard Hume
Assistant Professor Natalie Tronson

Brittany Clawson

clabri@umich.edu

ORCID iD: 0000-0003-4916-4201

Dedication

To knowing more.

Acknowledgements

Thank you to my labmates, friends, and fiancé! This wouldn't have been possible without you all!

A special thanks to Sha for keeping our lab running and always making us feel at home!

Thank you, Sara! You have provided extensive guidance and support!

Thank you to my committee for your feedback over the years.

Thank you to all of my students – I couldn't have finished this thesis without you! Emily, Laura, Amy, James, and John – you are destined for great things!

Last but not, least, thank you to my funding sources – the National Science Foundation and Rackham Graduate School.

TABLE OF CONTENTS

List of Figures

List of Abbreviations

REM	Rapid Eye Movement
NREM	Non-Rapid Eye Movement
SWS	Slow Wave Sleep
EEG	Electroencephalogram
EMG	Electromyogram
LFP	Local Field Potential
LGN	Lateral Geniculate Nucleus
TRN	Thalamic Reticular Nucleus
V1	Primary Visual Cortex
TC	Thalamocortical
CT	Corticothalamic
SHY	Synaptic Homeostasis Hypothesis
OSRP	Orientation Specific Response Potentiation
VEP	Visually Evoked Potential
LTP	Long Term Potentiation
RI	Responsiveness Index
OSI	Orientation Specificity Index
ISI	Interspike Interval
DB	Davies-Bouldin
SD	Sleep Deprivation

ESD	Early Sleep Deprivation
LSD	Late Sleep Deprivation
CCG	Cross-correlogram
PCA	Principal Components Analysis
SFC	Spike Field Coherence
PSD	Power Spectral Density
FR	Firing Rate
CT0/CT12	Circadian Time 0 / Circadian Time 12
ChR2	Channelrhodopsin-2
ArchT	Archaerhodopsin-T
GFP	Green Fluorescent Protein
TRAP	Targeted Recombination in Activated Populations
ZT0/ZT12	Zeitgeber Time 0/12

Abstract

Sleep is critical for memory consolidation, yet the mechanisms which underlie this process are not well understood. There are two main hypotheses on how sleep promotes memory consolidation: the Sleep Homeostasis Hypothesis (SHY) and Active System Consolidation (ASC). SHY posits that during waking experience, the brain forms new memories—creating and strengthening synapses. Unregulated, this process could reach a point of saturation, which would be metabolically expensive and occlude new memory formation. SHY hypothesizes that during sleep, synapses are uniformly scaled, eliminating weak connections while stronger synapses (important memories) persist. In contrast, ASC postulates that sleep synchronizes neural firing, selectively activating (and strengthening) synaptic connections for specific memories—promoting consolidation. Thus, according to the two hypotheses, different synaptic changes are expected across sleep.

Unresolved discrepancies between ACS and SHY may be due to technical limitations. Until recently, techniques have been unavailable to characterize and manipulate the neurons involved in a specific memory. Experimental outcomes have historically relied on data averaged across the neurons in a given brain structure. This lack of resolution has been a major barrier to understanding how sleep promotes memory consolidation. To move beyond these limitations, this thesis employs both in vivo recording of neurons (allowing tracking of memory encoding neurons across behavioral states) and recently developed engram, or memory trace, tools (allowing us to manipulate

the activity of neurons encoding a specific memory). These experimental strategies aim to clarify whether SHY or ASC (or both) occur in primary visual cortex (V1) during post learning sleep, and whether this consolidation is dependent on sleep-specific memory reactivation.

Using neuronal firing rates as a measure of plasticity, we examined the activity of V1 neurons across sleep, sleep deprivation, and post-learning sleep. The learning paradigm used is orientation-specific response potentiation (OSRP) which manifests as selective increases in V1 neuronal responses to a specific orientated grating. All sleep conditions showed an upregulation in the activity of low firing rate neurons and a downregulation of the activity of high firing rate neurons. These low firing rate neurons convey more visual information and selectively express OSRP. This suggests that sleep selectively upregulates the activity of neurons involved in sensory experience while simultaneously downregulating the activity those that are not.

To evaluate the necessity of memory reactivation during sleep for consolidation, we used engram technology to selectively manipulate neurons activated by a specific visual stimulus. We combined visually-cued conditioning to oriented gratings with engram labelling to create a tractable system for manipulating a specific memory during sleep. We show that the TRAP (targeted recombination in active populations) engram mouse line can be used to drive transgene expression in a specific oriented grating ensemble in primary visual cortex. We then inhibit this ensemble during post-conditioning sleep causing impaired consolidation. This was done in a content specific manner without altering sleep architecture or oscillations - indicating that reactivation specifically is necessary for sleep dependent memory consolidation.

This work unites two long standing hypotheses regarding sleep function for brain circuitry - SHY and ASC. The data support a comprehensive model in which sleep selectively reactivates neurons encoding relevant information. This upregulates their activity, while simultaneously decreasing activity in neurons whose information content is not salient. Future work will be needed to understand the molecular, cellular, and network mechanisms which drive these changes in specific cell populations.

Chapter 1

Introduction

1.1 The neurobiology of sleep

From honeybees to human beings, sleep is an evolutionarily conserved process[1,2]. Although its manifestations differ greatly across organisms, sleep has three key features: reduced physical activity, reduced responsiveness to sensory stimuli (i.e., level of consciousness), and homeostatic regulation[1]. Sleep can be identified in organisms of varying complexity living in wildly different ecosystems. In simpler organisms like jellyfish and sea sponges sleep is generally observed as periods of relative quiescence[3,4]. In organisms with more complex nervous systems, sleep begins to manifest as synchronous changes in neuronal and systems-level activity[5].

Sleep-specific occurrence of rhythmic brain network activity has been observed in organisms from fruit flies to humans[5,6]. In mammals, sleep-associated brain activity patterns and altered neuromodulator release characterize the two major stages of mammalian sleep: non-rapid eye movement (NREM) sleep and rapid eye movement (REM) sleep[7]. NREM (also referred to as slow-wave sleep; SWS) is defined by large slow oscillations in thalamocortical activity (including slow wave activity [<1 Hz], delta waves [0.5-4 Hz], and sleep spindles [7-15 Hz][8]. During NREM there are low levels of acetylcholine (ACH), dopamine (DA), serotonin (5-HT), and norepinephrine (NE) released throughout the brain[9,10]. REM sleep is defined by rapid eye movements, muscle atonia, theta-frequency (4-12 Hz) rhythms in the hippocampus and associated structures, and a

lack of NREM-associated oscillations[8]. This state is accompanied by very high levels of ACH release, and very low levels of DA, NE and 5-HT release[9,10]. In contrast to these two sleep states, the wake state is characterized by low-amplitude, high-frequency rhythms in many brain circuits, and relatively high release of ACH, NE, DA, and 5-HT.

1.2 Sleep, cognition and memory

For almost a century we have known that sleep is necessary for memory consolidation. In their landmark study, Jenkins and Dallenbach, had participants memorize a list of nonsense syllables[11]. Participants that were allowed to sleep retained a larger number of syllables compared those that remained awake. Since then, numerous studies have shown sleep's effect on various memory types including motor, visual, verbal, and spatial memory[7,8,12]. These effects appear to be conserved across species. For example, sleep deprivation in honeybees leads to a degradation in the ability to remember and communicate food locations[2,13].

Disordered sleep has been indicated as a potential contributing factor in a number of cognitive impairment disorders such as schizophrenia, major depression, and post-traumatic stress disorder. In these disorders, changes in memory and executive dysfunction correlate with changes in sleep architecture or quality[14–17]. Given sleep's essential entanglement in cognition, it is key that a mechanistic link between the two is discerned.

1.3 Hypothesized synaptic changes during sleep-dependent memory consolidation SHY vs ASC

There are two main hypotheses regarding synaptic changes underlying memory functions of sleep: the Sleep Homeostasis Hypothesis (SHY) and Active System Consolidation (ASC)[7,18–20]. SHY posits that the brain forms new memories by

strengthening synapses throughout the day. Unregulated, this process will eventually reach a point where 1), maintaining large numbers of strong synapses is metabolically too expensive to sustain and 2) forming new memories is no longer possible. SHY proposes that during sleep, the strength of synapses is scaled back throughout the entire brain, with roughly uniform changes in strength at each synapse[18]. This process eliminates weak connections, while maintaining strong memory related synapses. In contrast, the ASC hypothesis proposes that brain activity patterns during sleep synchronize neuronal firing in a manner that selectively reactivates and strengthens synaptic connections previously activated by memory formation[7,20]. This process would promote long term memory storage by selectively strengthening important connections between specific neurons engaged by learning. As opposition to mechanisms invoked by SHY, ASC proposes that specific synapses are selectively strengthened during sleep to reinforce memory. Ultimately, these two hypotheses differ in whether sleep is viewed as a permissive or instructive—protecting the consolidation process and reducing noise (SHY) or actively contributing to consolidation (ASC)[21].

Each of the two hypotheses draw on prior data, suggesting changes in synaptic strength occur across sleep. Strengthening or weakening of synapses can be measured as differences in protein expression, structure, and/or function of connections between neurons[22]. Proponents of SHY have emphasized data suggesting that synaptic strengthening occurs during prolonged wake and weakening during sleep. Synaptic expression of long term potentiation (LTP) proteins has been shown to increase during sleep deprivation (SD)[23,24]; in comparison, synaptic expression of these proteins goes down after a period of sleep. In contrast, literature supporting ASC has shown an

upregulation of LTP related mRNAs and proteins (including zif268, Arc, and BDNF) during post-learning sleep[25–27]. Similarly, conflicting data are seen with regard to electrophysiological measurements and synaptic structural plasticity. In support of SHY, the frequency of cortical neuronal firing and excitatory postsynaptic currents increase during wake and SD[23,28]. SD also leads to a net increase in formation of new spines relative to a similar period of *ad lib* sleep[29,30] In support of ASC, SD has been shown to disrupt many forms of LTP[31–37]. Post-learning SD also disrupts spine formation in learning-activated cortical pyramidal neurons, which occurs during sleep in an activity-dependent manner[38].

While the SHY and ASC hypotheses are not mutually exclusive, supporters of SHY and ASC have faced difficulties reconciling these seemingly conflicting data. One plausible explanation of these discrepancies is that comparisons have been made across data gathered in different brain regions, in different contexts (e.g., learning vs. not learning), and with different methodology for SD[39]. Furthermore, prior work on sleep's role in synaptic plasticity has drawn on data from large mixed cell populations, and even whole brain structures (e.g. neocortex or hippocampus). With such measures, it is likely that the sparser memory specific synaptic signal is small relative to that from synapses not engaged in the process of memory consolidation. It is plausible that this has contributed to discrepant data in the field.

1.4 Replay of memories during sleep

One instructive mechanism by which sleep may specifically strengthen memories is the reactivation or replay of neuronal activity from learning experiences. Reactivation of experience-activated neurons during sleep has been observed since 1989, when

Pavlides and Winson found that place cell neurons active in the rat hippocampus during exploration of a novel environment showed greater activity during subsequent sleep[40]. Subsequent studies have found that pairwise temporal correlations of firing between hippocampal place cells during experience are preserved during subsequent sleep[41–43]. Thus, across a population of place cell neurons, sequential firing during spatial navigation can be re-iterated (i.e., sequentially replayed) during sleep. These sequences of activity have been observed in quiet wake, REM, and NREM, in the context of specific network oscillations[44,45]. Within REM sleep, replay occurs in real time phase-coordinated with the theta oscillations[46]. Meanwhile, in NREM sleep, often occurs at a time compressed manner, frequently coordinated with sharp wave ripples[46,47]. Further, these replay events and oscillations coordinate into a synchronized interregional triple rhythm. The triple rhythm consists of coordinated oscillatory activity between sleep spindles, sharp wave ripples, and slow waves[48]. The precisely coordinated symphony of electrical activity leads to plasticity that may underlie sleep dependent memory consolidation.

Replay and reactivation are widely hypothesized to be causally linked to memory consolidation, based on several lines of circumstantial evidence. For example, the extent to which these phenomena occur in the hippocampus during sleep is influenced by the novelty and extent of prior learning experience[45,49,50]. Moreover, network oscillations associated with the occurrence of sequential replay are enhanced (in both frequency of occurrence, and amplitude)—both in the hippocampus and thalamocortical circuits—during sleep following learning[51,52].The simultaneous upregulation of both replay events and ripples suggests that enhanced replay may support enhanced memory consolidation.

Later work confirmed that the replay associated with sharp wave ripples was predictive of memory performance.

Recent work has aimed at testing the causal role for sleep-associated neuronal reactivation and replay in memory. For example, Girardeau et al trained rats on a spatial learning task and then disrupted hippocampal activity (in the context of NREM network oscillations associated with sequential replay) during periods of post-learning sleep[53]. This intervention, when continued over several days, led to minor deficits in learning. Similarly, Ego-Stengel and Wilson disrupted activity during NREM hippocampal oscillations using electrical stimulation and also found spatial memory deficits[54]. More recently, optogenetic inhibition of all hippocampal pyramidal neurons during NREM oscillations (or during online detection of ensemble replay, regardless of state) has been used as a strategy to disrupt replay occurrence[55,56]. While all of these manipulations almost certainly interfere with the occurrence of neuron-specific reactivation and replay, they also transiently cause large-scale disruption of virtually all hippocampal activity. Thus, it is unclear that memory deficits associated with these network-wide manipulations are due to the necessity of sleep-dependent memory trace reactivation for the process of memory consolidation.

1.5 Probing instructive network mechanisms for sleep-dependent memory consolidation in the visual system

While the majority of work on reactivation and replay has been done in the hippocampal system, memory replay during sleep has been observed in primary visual cortex (V1)[57]. The visual system provides a tractable plasticity for studying both memory reactivation and neuron-specific alterations. This plasticity is called Orientation Specific Response Potentiation (OSRP) - in which primary visual cortical neurons shift their tuning

towards a specific orientation after one extended viewing of that specific orientation. This phenomena has been observed in humans, nonhuman primates, and mice[52,58–64]. This is a one trial, sleep-dependent plasticity that requires LTP[61,63]. These features suggest that sleep may be facilitating some form synaptic strengthening.

Work from the Aton Lab measures OSRP using long term *in vivo* electrophysiology[52,58,61]. This technique allows for continuous recording of individual neurons' firing across learning experiences during wake and subsequent sleep. In combination with measures of learned animal behavior, such recordings allow us to infer which neurons' activity are affected by learning, and which sleep-dependent changes in their activity are correlated with memory formation. This work has demonstrated that plastic changes correlate with changes in the network activity sleep and are facilitated by thalamocortical transfer of information[52,58,61].

Prior work has relied on average measures of plasticity across neurons. While averages have given us an idea of how this plasticity is occurring across an entire population, recent findings suggest that sleep alters neurons in a heterogeneous manner that may be masked in averaged data[65,66]. These studies suggest that sleep differentially alters the activity of neurons – selectively increasing the firing rates of sparsely firing neurons and decreasing those of faster firing neurons. While these changes are dependent on waking firing rates, the authors did not correlate these firing rates with learning or memory. This leaves an open question: does sleep selectivity upregulate activity in OSRP encoding neurons while simultaneously downregulating the activity of uninvolved neurons?

1.6 Outline

To expand upon and unite the work of both the OSRP and memory reactivation fields, this thesis aims to address two main questions. Q1. Does sleep selectively upregulate the activity of neurons involved in sensory experience while simultaneously downregulating the activity of those that are not? Q2. Is reactivation necessary for sleep-dependent memory consolidation? As shown in Figure 1.1, we hypothesize that OSRP upregulates the activity of neurons involved in experience (via ASC) while unrelated neuronal activity is simultaneously downregulated (via SHY), and this consolidation may be mediated by sleep-specific memory reactivation.

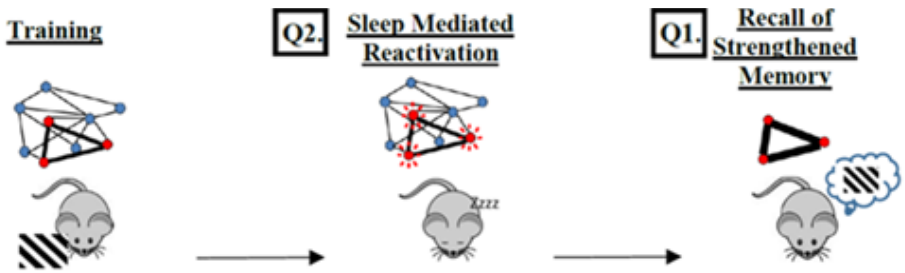

Figure 1.1 Potential mechanism for sleep-dependent memory consolidation. Red nodes represent cells activated by the visual experience; blue nodes are unrelated cells. The thickness of the line represents the strength of the connection. I will test the necessity of reactivation across sleep (Q2) and the specific strengthening of memory related connections accompanied by downscaling of unrelated synapses.

In Chapter 3, using long term *in vivo* electrophysiology, we will examine how sleep differentially alters the activity of memory encoding neurons during OSRP. This work will address the sleep-specific renormalization of firing rates - comparing changes across control sleep, post-learning sleep, and sleep deprivation. Analyzing these changes across the distribution of neurons will illuminate the heterogeneity of sleep's effects. Furthermore, examining changes in population coupling, visual response properties, and plastic changes will elucidate if firing rate renormalization may facilitate OSRP.

In Chapter 4 we will address the potential necessity of reactivation of learning-activated ensembles for sleep dependent memory consolidation. We will begin by testing the sleep-dependence of visually-cued fear conditioning to oriented gratings - assaying it's viability as a single trial sleep-dependent learning paradigm based on the same visual substrates as OSRP. Then, using recently developed genetic tools that allow selective manipulation of memory-encoding neurons, we will test if this technology is capable of labelling orientation-specific ensembles. In the final experiments we will inhibit this orientation-specific ensemble during post-conditioning sleep to assay the necessity of reactivation for sleep-dependent memory consolidation.

In addition to the data Chapters 3 and 4, Chapter 2 contains a review on a discrete sleep-specific oscillation known as the sleep spindle. This 12-15 Hz oscillation is a hallmark of NREM sleep, and has been correlated with cognitive function and learning. This review outlines how the function of this oscillation and how it changes across development, adulthood, and aging.

1.7 References

1. Cirelli, C. & Tononi, G. Is sleep essential? *PLoS Biol.* **6**, 1605–1611 (2008).

2. Klein, B. A., Klein, A., Wray, M. K., Mueller, U. G. & Seeley, T. D. Sleep deprivation impairs precision of waggle dance signaling in honey bees. *Proc. Natl. Acad. Sci. U. S. A.* **107**, 22705–22709 (2010).

3. Nath, R. *et al.* The Jellyfish Cassiopea Exhibits a Sleep-Like State. *Curr. Biol.* **27**, 2984–2990 (2017).

4. Nickel, M. Kinetics and rhythm of body contractions in the sponge Tethya wilhelma (Porifera: Demospongiae). *J. Exp. Biol.* **207**, 4515–4524 (2004).

5. Cirelli, C. The genetic and molecular regulation of sleep: From fruit flies to humans. *Nat. Rev. Neurosci.* **10**, 549–560 (2009).

6. Nitz, D. A., Van Swinderen, B., Tononi, G. & Greenspan, R. J. Electrophysiological correlates of rest and activity in Drosophila melanogaster. *Curr. Biol.* **12**, 1934–1940 (2002).

7. Diekelmann, S. & Born, J. The memory function of sleep. *Nat Rev Neurosci* **11**, 114–126 (2010).

8. Rasch, B. & Born, J. About Sleep's Role in Memory. *Physiol. Rev.* **93**, 681–766 (2013).

9. Watson, C. J., Baghdoyan, H. A. & Lydic, R. Neuropharmacology of sleep and wakefulness. *Sleep Med. Clin.* **5**, 513–528 (2010).

10. Lyamin, O. I. *et al.* Monoamine Release during Unihemispheric Sleep and Unihemispheric Waking in the Fur Seal. *Sleep* **39**, 625–636 (2016).

11. Jenkins, J. G. & Dallenbach, K. M. Obliviscence during Sleep and Waking. *Am. J. Psychol.* **35**, 605–612 (1924).

12. Frankland, P. W. & Bontempi, B. The organization of recent and remote memories. *Nat. Rev. Neurosci.* **6**, 119–30 (2005).

13. Beyaert, L., Greggers, U. & Menzel, R. Honeybees consolidate navigation memory during Sleep. *J. Exp. Biol.* **215**, 3981–3988 (2012).

14. Manoach, D. S. & Stickgold, R. Sleep, Memory and Schizophrenia. *Sleep Med.* **16**, 553–554 (2015).

15. Dow, B. M., Kelsoe, J. R. & Gillin, J. C. Sleep and dreams in Vietnam PTSD and

depression. *Biol. Psychiatry* **39**, 42–50 (1996).

16. Kalmbach, D. A., Pillai, V., Cheng, P., Arnedt, J. T. & Drake, C. L. Shift work disorder, depression, and anxiety in the transition to rotating shifts: The role of sleep reactivity. *Sleep Med.* **16**, 1532–1538 (2015).

17. Goldstein, A. N. & Walker, M. P. The Role of Sleep in Emotional Brain Function. *Annu. Rev. Clin. Psychol. Vol 10* **10**, 679–708 (2014).

18. Tononi, G. & Cirelli, C. Sleep and synaptic homeostasis : a hypothesis. **62**, 143–150 (2003).

19. Tononi, G. & Cirelli, C. Sleep function and synaptic homeostasis. 49–62 (2006). doi:10.1016/j.smrv.2005.05.002

20. Puentes-Mestril, C. & Aton, S. J. Linking network activity to synaptic plasticity during sleep: Hypotheses and recent data. *Front. Neural Circuits* **11**, 1–18 (2017).

21. Ellenbogen, J. M., Hulbert, J. C., Stickgold, R., Dinges, D. F. & Thompson-Schill, S. L. Interfering with Theories of Sleep and Memory: Sleep, Declarative Memory, and Associative Interference. *Curr. Biol.* **16**, 1290–1294 (2006).

22. Lynch, M. Long-term potentiation and memory. *Physiol. Rev.* **84**, 87–136 (2004).

23. Vyazovskiy, V. V., Cirelli, C., Pfister-Genskow, M., Faraguna, U. & Tononi, G. Molecular and electrophysiological evidence for net synaptic potentiation in wake and depression in sleep. *Nat. Neurosci.* **11**, 200–208 (2008).

24. Cirelli, C., Gutierrez, C. M. & Tononi, G. Extensive and Divergent Effects of Sleep and Wakefulness on Brain Gene Expression. *Neuron* **41**, 35–43 (2004).

25. Ribeiro, S. *et al.* Induction of Hippocampal Long-Term Potentiation during Waking Leads to Increased Extrahippocampal zif-268 Expression during Ensuing Rapid-Eye-Movement Sleep. *Neuroscience* **22**, 10914–10923 (2002).

26. Aton, S. J. *et al.* Mechanisms of Sleep-Dependent Consolidation of Cortical Plasticity. *Neuron* **61**, 454–466 (2009).

27. Seibt, J. *et al.* Protein synthesis during sleep consolidates cortical plasticity in vivo. *Curr. Biol.* **22**, 676–682 (2012).

28. Liu, Z. W., Faraguna, U., Cirelli, C., Tononi, G. & Gao, X. B. Direct evidence for wake-related increases and sleep-related decreases in synaptic strength in rodent cortex. *J. Neurosci.* **30**, 8671–8675 (2010).

29. Maret, S., Faraguna, U., Nelson, A. B., Cirelli, C. & Tononi, G. Sleep and wake

modulate spine turnover in the adolescent mouse cortex. *Nat. Methods* **14**, 1418–1420 (2012).

30. Vivo, L. De *et al.* Ultrastructural evidence for synaptic scaling across the wake/sleep cycle. *Science (80-.).* **355**, 507–510 (2017).

31. Vecsey, C. G. *et al.* Sleep deprivation impairs cAMP signalling in the hippocampus. *Nature* **461**, 1122–1125 (2009).

32. Tartar, J. L. *et al.* Hippocampal Synaptica Plasticity and Spatial Learning are Impaired in a Rat Model of Sleep Fragmentation. *Eur. J. Neurosci.* **23**, 2739–2748 (2006).

33. Chauvette, S., Seigneur, J. & Timofeev, I. Sleep Oscillations in the Thalamocortical System Induce Long-Term Neuronal Plasticity. *Neuron* **75**, 1105–1113 (2012).

34. Campbell, I. G., Guinan, M. J. & Horowitz, J. M. Sleep deprivation impairs long-term potentiation in rat hippocampal slices. *J. Neurophysiol.* **88**, 1073–1076 (2002).

35. Braunewell, K. H. & Manahan-Vaughan, D. Long-term depression: a cellular basis for learning? *Rev. Neurosci.* **12**, 121–40 (2001).

36. Kopp, C., Longordo, F., Nicholson, J. R. & Lüthi, A. Insufficient sleep reversibly alters bidirectional synaptic plasticity and NMDA receptor function. *J. Neurosci.* **26**, 12456–12465 (2006).

37. Florian, C., Vecsey, C. G., Halassa, M. M., Haydon, P. G. & Abel, T. Astrocyte-derived adenosine and A1 receptor activity contribute to sleep loss-induced deficits in hippocampal synaptic plasticity and memory in mice. *J. Neurosci.* **31**, 6956–6962 (2011).

38. Yang, G., Lai, C., Cichon, J., Li, W. & Gan, W. Sleep promotes branch-specific formation of dendritic spines after learning. *Science (80-.).* **344**, 1173–1178 (2014).

39. Genzel, L., Kroes, M. C. W., Dresler, M. & Battaglia, F. P. Light sleep versus slow wave sleep in memory consolidation: A question of global versus local processes? *Trends Neurosci.* **37**, 10–19 (2014).

40. Pavlides, C. & Winson, J. Influences of Hippocampal Place Cell Firing in the Awake State on the Activity of These Cells During Subsequent Sleep Episodes. *Neuroscience* **9**, 2907–2918 (1989).

41. Nadasdy, Z., Hirase, H., Czurko, A., Csicsvari, J. & Buzsáki, G. Replay and Time Compression of Recurring Spike Sequences in the Hippocampus. *Neuroscience* **19**, 9497–9507 (1999).

42. Wilson, M. A. & Mcnaughton, B. L. Reactivation of Hippocampal Ensemble Memories During Sleep. *Science (80-.).* **265**, 676–679 (1994).

43. Skaggs, W. E. & McNaughton, B. L. Replay of neuronal firing sequences in rat hippocampus during sleep following spatial experience. *Science (80-.).* **271**, 1870–1873 (1996).

44. Foster, D. J. Replay Comes of Age. *Annu. Rev. Neurosci.* **40**, 581–602 (2017).

45. Foster, D. J. & Wilson, M. A. Reverse replay of behavioural sequences in hippocampal place cells during the awake state. *Nature* **440**, 680–683 (2006).

46. Louie, K. & Wilson, M. A. Temporally Structured Replay of Awake Hippocampal Ensemble Activity during Rapid Eye Movement Sleep. *Neuron* **29**, 145–156 (2001).

47. Lee, A. K. & Wilson, M. A. Memory of sequential experience in the hippocampus during slow wave sleep. *Neuron* **36**, 1183–1194 (2002).

48. Latchoumane, C., Ngo, H. V. V., Born, J. & Shin, H.-S. Thalamic Spindles Promote Memory Formation during Sleep through Triple Phase-Locking of Article Thalamic Spindles Promote Memory Formation during Sleep through Triple Phase-Locking of Cortical, Thalamic, and Hippocampal Rhythms. *Neuron* **95**, 1–12 (2017).

49. Wilson, M. A. & Mcnaughton, B. L. Reactivation of Hippocampal Ensemble Memories During Sleep. *Science (80-.).* **265**, 5–8 (1994).

50. Jackson, J. C., Johnson, A. & Redish, A. D. Hippocampal sharp waves and reactivation during awake states depend on repeated sequential experience. *J. Neurosci.* **26**, 12415–12426 (2006).

51. Ognjanovski, N. *et al.* Parvalbumin-expressing interneurons coordinate hippocampal network dynamics required for memory consolidation. *Nat. Commun.* **8**, 1–13 (2017).

52. Durkin, J. *et al.* Cortically coordinated NREM thalamocortical oscillations play an essential , instructive role in visual system plasticity. *Proc. Natl. Acad. Sci.* 2–7 (2017). doi:10.1073/pnas.1710613114

53. Girardeau, G., Benchenane, K., Wiener, S. I., Buzsáki, G. & Zugaro, M. B. Selective suppression of hippocampal ripples impairs spatial memory. *Nat. Neurosci.* **12**, 1222–1223 (2009).

54. Ego-Stengel, V. & Wilson, M. A. Disruption of ripple-associated hippocampal activity during rest impairs spatial learning in the rat. *Hippocampus* **20**, 1–10 (2010).

55. van de Ven, G. M., Trouche, S., McNamara, C. G., Allen, K. & Dupret, D.

Hippocampal Offline Reactivation Consolidates Recently Formed Cell Assembly Patterns during Sharp Wave-Ripples. *Neuron* **92**, 968–974 (2016).

56. Gridchyn, I. *et al.* Assembly-Specific Disruption of Hippocampal Replay Leads to Selective Memory Deficit Article Assembly-Specific Disruption of Hippocampal Replay Leads to Selective Memory Deficit. *Neuron* 1–10 (2020). doi:10.1016/j.neuron.2020.01.021

57. Ji, D. & Wilson, M. A. Coordinated memory replay in the visual cortex and hippocampus during sleep. *Nat. Neurosci.* **10**, 100–107 (2007).

58. Durkin, J. & Aton, S. J. Sleep-Dependent Potentiation in the Visual System Is at Odds with the Synaptic Homeostasis Hypothesis. *Sleep* **39**, 155–159 (2016).

59. Jehee, J. F. M., Ling, S., Swisher, J. D., van Bergen, R. S. & Tong, F. Perceptual learning selectively Refines orientation representations in early visual cortex. *J. Neurosci.* **32**, 16747–16753 (2012).

60. Adab, H. Z., Popivanov, I. D., Vanduffel, W. & Vogels, R. Perceptual Learning of Simple Modifies Stimulus Representations in Posterior Inferior Temporal Cortex. *J. Cogn. Neurosci.* **26**, 2187–2200 (2014).

61. Aton, S. J., Suresh, A., Broussard, C. & Frank, M. G. Sleep Promotes Cortical Response Potentiation Following Visual Experience. *Sleep* **37**, 1163–1170 (2014).

62. Zivari Adab, H. & Vogels, R. Practicing coarse orientation discrimination improves orientation signals in macaque cortical area V4. *Curr. Biol.* **21**, 1661–1666 (2011).

63. Cooke, S. F., Komorowski, R. W., Kaplan, E. S., Gavornik, J. P. & Bear, M. F. Visual recognition memory, manifested as long-term habituation, requires synaptic plasticity in V1. *Nat. Neurosci.* **18**, 262–271 (2015).

64. Frenkel, M. Y. *et al.* Instructive Effect of Visual Experience in Mouse Visual Cortex. *Neuron* **51**, 339–349 (2006).

65. Watson, B. O., Levenstein, D., Greene, J. P., Gelinas, J. N. & Buzsáki, G. Network Homeostasis and State Dynamics of Neocortical Sleep. *Neuron* **90**, 839–852 (2016).

66. Miyawaki, H. & Diba, K. Regulation of hippocampal firing by network oscillations during sleep. *Curr. Biol.* **26**, 893–902 (2016).

CHAPTER II

Form and Function of Sleep Spindles Across the Lifespan

*This chapter includes the review article: **Clawson, B.C**., Durkin, J., Aton, S.J. (2016). Form and function of sleep spindles across lifespan. Neural Plasticity, e6936381.*

2.1 Abstract

Since the advent of EEG recordings, sleep spindles have been identified as hallmarks of non- REM sleep. Despite a broad general understanding of mechanisms of spindle generation gleaned from animal studies, the mechanisms underlying certain features of spindles in the human brain, such as “global” vs. “local” spindles, are largely unknown. Neither the topography nor the morphology of sleep spindles remains constant throughout the lifespan. It is likely that changes in spindle phenomenology during development and aging are the result of dramatic changes in brain structure and function. Across various developmental windows, spindle activity is correlated with general cognitive aptitude, learning, and memory, however these correlations vary in strength, and even direction, depending on age and metrics used. Understanding these differences across the lifespan should further clarify how these oscillations are generated, and their function, under a variety of circumstances. We discuss these issues, and their translational implications for human cognitive function. Because sleep spindles are similarly affected in disorders of neurodevelopment (such as schizophrenia) and during aging (such as neurodegenerative conditions), both types of disorders may benefit from therapies based on a better understanding of spindle function.

2.2 Introduction: Why "spindle"? Generation and termination of a very conspicuous waveform

Sleep spindles were the first features of sleep described in human EEG recordings [1,2]. Their name reflects the waxing-and-waning nature of the 7-15 Hz spindle oscillation itself, which emerges, crests, and disappears over the course approximately 1 s. These events occur at intervals during non-rapid eye movement (NREM) sleep. GABAergic neurons in the TRN play a critical role in the generation of these oscillations. Neurons in the TRN generate highly synchronized bursts at the outset of a spindle (**Figure 2.1A**). These bursts can be generated in NREM due to a relative hyperpolarization in TRN neuronal membrane potential. This is due at least in part to reduced noradrenergic and serotonergic signaling [3]. Under these conditions, a relatively small amount of glutamatergic input (acting on ionotropic [primarily GluR4] receptors [4]) is sufficient to activate T-type calcium channels [5], the kinetics of which causes a transient depolarization to spike threshold. After this calcium spike, the resting membrane potential undergoes an afterhyperpolarization, mediated in part by calcium-activated, small-conductance potassium (SK2) channels (reviewed in [6]). Importantly, many TRN neurons are intrinsically capable of generating multiple cycles of membrane oscillations and firing bursts, which are facilitated by both Ca(V)3.3 T-type calcium channels [5] and Kv3-class voltage-gated potassium channels [7]. In the absence of ionotropic glutamatergic input, these oscillations can be initiated by mGluR activation and synchronized across the TRN via gap junction communication [8].

Despite the fact that some TRN neurons can generate spindle-frequency oscillations in a seemingly cell-autonomous manner, sleep spindles are a network event. TRN bursts lead to transient GABA-mediated hyperpolarization in neighboring

glutamatergic TC neurons elsewhere in the thalamus (**Figure 2.1A**). This hyperpolarization initiates a series of postsynaptic events in TC neurons: 1) firing becomes suppressed through GABA receptor-mediated inhibition, 2) due to membrane hyperpolarization, I_h (hyperpolarization-activated cation current) is activated and I_t (T-type calcium current) is disinhibited, 3) due to activation of these currents, the membrane rapidly depolarizes, leading to a burst of action potentials [9]. This rebound burst results in a volley of excitatory input to TC targets in both the cortex and TRN, where it sets off the next burst of firing in TRN neurons.

While spindle oscillation generation relies on intrathalamic mechanisms, spindles can be driven from outside the thalamus. In particular, synchronous bursts of TRN firing are often initiated by excitatory input from layer 6 CT neurons, a major source of input to the TRN [10,11] (**Figure 2.1A**). Indeed, some of the earliest descriptions of spindles noted their propensity to be initiated by sensory (*e.g.*, auditory) input during sleep [1], consistent with initiation through either thalamic or cortical excitatory pathways.

Although the mechanism of pacemaking during spindles is well-understood at the cellular level, it is less clear how the conspicuous, spindle-shaped oscillation envelope that defines these events is generated. The waxing phase of spindle oscillations is generally thought to be caused by increasing activation of cortical neurons with each successive volley of excitatory TC input [12] (**Figure 2.1A**), leading to greater CT excitatory feedback, which synchronizes successive cycles of activity among neurons in the thalamus [6]. There are multiple theories regarding the waning and termination of spindles, each focused on changes in different parts of the CT-TRN-TC network. A number of studies have indicated that TC neurons gradually depolarize across successive spindle

oscillation cycles. This eventually prevents activation of hyperpolarization-activated currents and associated burst firing [13,14]. This effect may be due in part to disinhibition; the level of activity in TRN GABAergic neurons changes during the waning phase of spindle oscillations. TRN neurons become less active (firing fewer spikes per burst) with successive cycles of spindle oscillations [15]; this may be due in part to an increase in GABAergic signaling between TRN neurons as spindle oscillations progress [16,17]. At the same time, TC neurons fire more spikes per burst across successive cycles. After-depolarization (mediated by Ca-activated I_h current) in TC neurons lasts several (*i.e.*, 5-20) seconds, resulting in "refractory" periods between spindles, and setting an upper limit on their frequency [14]. Indeed, Bal and McCormick [13] demonstrated that when I_h current is blocked in *ex vivo* slices, TC neurons generate spindle-frequency oscillations which are continuous in nature, rather than spindle-shaped. Taken together, this suggests that excitatory TC input both increases and becomes less rhythmic as spindles wane and terminate. Feedback from excitatory CT neurons also appears to play a role in terminating spindles. Similar to TC neurons, CT neurons both increase their firing rate, and fire in a less synchronous manner, across the waning phase [18]. This change in CT input could disrupt intrathalamic oscillations due to either desynchrony or neuronal depolarization (and thus disruption of thalamic bursting). Furthermore, increased CT input may play a role in termination by promoting greater intra-TRN inhibitory signaling (which would both inhibit TRN neuronal firing and desynchronize burst of firing between TRN neurons) with each successive cycle of the oscillation [16,17]. These CT-TRN-TC changes seem to occur nearly simultaneously *in vivo*. Thus while changes in each part of the circuit likely

contribute to spindle waning and termination, it remains unclear which comes first in the sequence of events leading to termination.

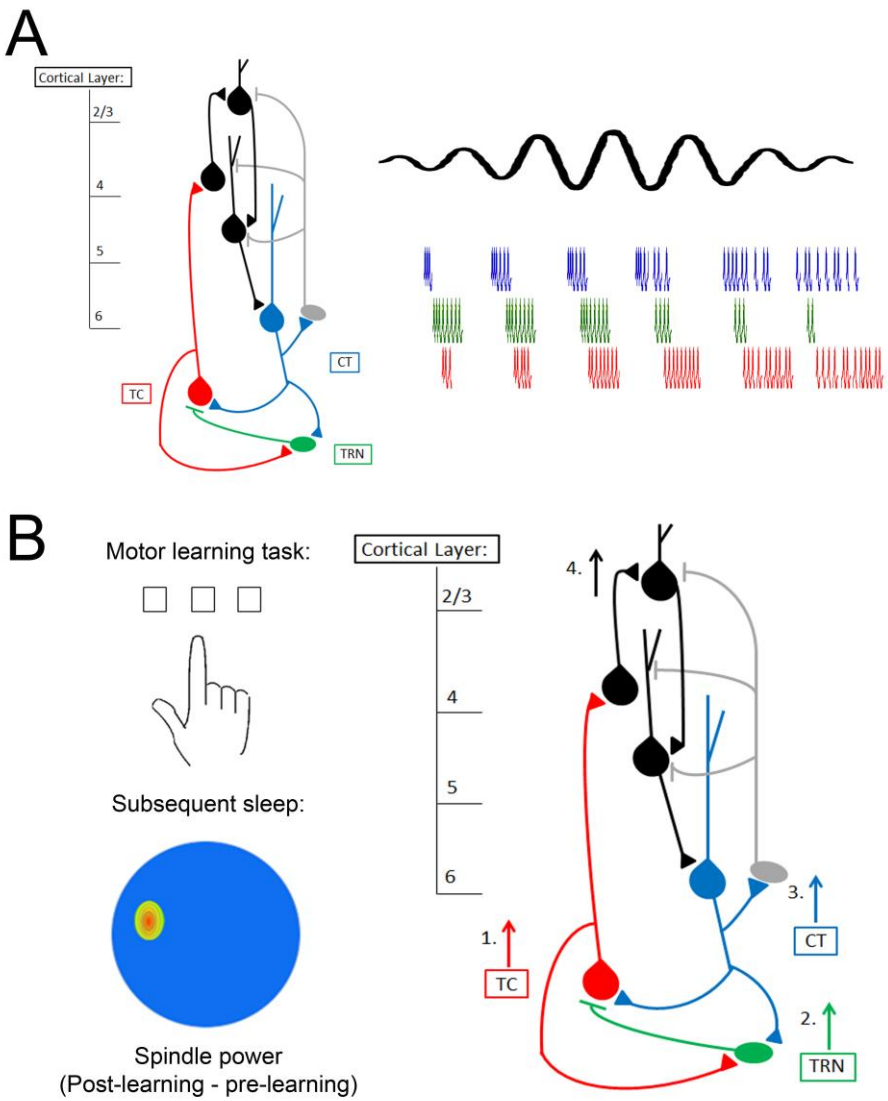

Figure 2.1: Spindles generation within the CT-TRN-TC circuit. (A) Sleep spindles are generated through reciprocal interactions of the TRN (**green**) and TC (**red**) neurons. Spindles can be initiated by excitatory input from CT (**blue**) neurons, which also synchronize spindle oscillations across the thalamocortical network. Representative raster plots (**right**) show the order and organization of firing for CT, TRN, and TC neurons, respectively. As the spindle oscillation wanes, increasing excitation of TC and CT neurons prevents hyperpolarization activated currents in the TRN from driving bursting in TRN neurons, and CT input desynchronizes. **(B)** The CT-TRN-TC circuit may also generate local spindles following waking experience. For example, training on a motor task leads to increased sleep spindles over the contralateral motor cortex during subsequent sleep (**left**; adapted from [58]). There are several possible mechanisms by which changes to CT-TRN-TC circuitry during waking could cause subsequent local spindle increases (**right**). TC projections may show changes to dynamics (*e.g.*, firing rate or bursting) based on prior waking experience (**1**). Experience may alter TRN excitability or bursting during subsequent sleep (**2**). CT feedback may be altered by experience to increase synchronization or amplification of spindles (**3**). Finally, intracortical plasticity could amplify spindles locally (**4**).

2.3 Where do they come from, where do they go? Spindle topology, synchronization, and propagation

Early reports suggested that spindles occurred independently in different cortical areas (*i.e.*, frontal vs. occipital [2]. More recent studies on the topography of spindle occurrence (*i.e*., using high density EEG) have indicated that in humans and other mammalian species, spindles occur nearly simultaneously across many cortical areas [19-22]. However, these studies have demonstrated notable exceptions, in which "local" spindles occur independently at specific recording sites. Moreover, spindles occurring across the cortex are not completely coherent; the oscillations are not always phase-locked, and do not always have the same intrinsic frequency. Rather, across multiple species [23-25], the frequency of oscillations shows an anteroposterior gradient, with spindles in frontal cortex showing a lower peak frequency (9-12 Hz) relative to those occurring at more posterior sites (13-15 Hz) [26] (although this does not appear to be true for mice, possibly due to differences in brain anatomy [22]). Furthermore, spindles do not initiate in perfect synchrony. Faster centroparietal spindles begin several hundred milliseconds earlier than slower spindles occurring in frontal cortex [20]. Experimental cortical stimulation is sufficient to generate "traveling" spindle oscillations that propagate outward from the stimulation site [21]. It seems likely that during natural sleep spindle oscillations, posterior-to-anterior propagation of spindles is mediated (at least in part) through CT connections, which support information transfer between neighboring cortical areas via the thalamus [27-29].

The more recent application of magnetoencephalography (MEG) to studying sleep oscillations has further complicated the picture of spindle generation and synchronization. Early studies [30,31] demonstrated that spindle oscillations could be detected (either across

the cortex, or in a specific cortical location) in one modality but not the other (*e.g.*, present in MEG and not simultaneously present in EEG). Subsequent data suggested that MEG frequently detects spindles that are not present in EEG, while the reverse is seldom true [32]. Additionally, within individual spindles, MEG waveforms are more variable between brain areas than EEG waveforms, with highly divergent oscillation phases, amplitudes, and periodicities among cortical recording sites [33].

Why are there such differences between MEG and EEG? MEG has better spatial resolution than EEG for superficial (cortical) brain activity, since magnetic fields suffer less distortion by the skull and scalp than electric fields. MEG and EEG may also have different sensitivities for detecting oscillations generated by anatomically different TC connections. Local spindle generation has been ascribed to highly focal projections of thalamic "core" ("C-type") neurons, which send dense, spatially-limited, and fast glutamatergic input to cortical layer 4. Such projections predominate in sensory cortical areas. In contrast, more diffuse "matrix" ("M-type") projections provide slow glutamatergic input to large patches of layer 1 [34]. Available data suggests that MEG would be more sensitive to oscillations generated through the former pathway, while EEG would be more sensitive to oscillations generated through the latter [33,35,36].

While the general phenomenon of global vs. local spindling has been primarily characterized as a cortical phenomenon, this may be due to methodological limitations. Most evidence of local spindling comes from high-density EEG and MEG recording, neither of which is useful for detecting thalamic signals. There is limited evidence that local spindles could be present the level of the thalamus, in TC or even TRN neurons. Decortication leads to gross desynchrony of spindles across TC sites *in vivo* [21]. Spindles

recorded *ex vivo* in isolated thalamic slices are generally not synchronized [37], and stimulation of corticothalamic axons is sufficient to synchronize spindles within the slice [38]. Together, these experiments suggest that CT feedback is critical for synchrony. This is further supported by the recent finding that cortical EEG signals phase-lead thalamic EEG signals during NREM spindles *in vivo* [22]. However, because there are limited studies in which multi-site thalamic recording has been carried out *in vivo*, it remains unclear how coherent thalamic spindle oscillations are during natural sleep, or whether "local" oscillations are present.

Given all of the contributions of corticothalamic, intrathalamic and thalamocortical circuitry to maintaining coherent sleep spindles, what circumstances give rise to local spindles? The anatomy of TC and CT projections plays a role - spindles are coherent between TC nuclei and the cortical areas they project to, but not between thalamic and cortical sites which are not functionally connected [39]. However it remains unclear why they should occur synchronously in two cortical areas at certain times, and asynchronously at others. What is clear is that spindles can be more pronounced in specific cortical areas based on prior (wakeful) activity in those areas. This can be seen, for example, following training on a visual texture discrimination task, in which psychophysical discrimination thresholds decrease for a specific retinotopic area of the visual cortex. This retinotopically-specific improvement is dependent on post-training sleep [40,41], and during post-training sleep MEG spindle power is significantly increased in these trained retinotopic areas [42]. To date, evidence for "use-dependent" local spindle generation has primarily come from recordings in primary sensory or motor cortical areas, where C-type TC projections are most abundant.

There are several physiological reasons for why circuit activation in sensory and motor cortices might preferentially lead to local spindling, which are by no means mutually exclusive. One possibility is that C-type TC relay neurons projecting to these cortical areas show some hysteresis of activity or excitability, which translates to modality-specific changes in their subsequent dynamics in the hours following learning (**Figure 2.1B, red arrow**). Indeed, experience-dependent changes in both membrane excitability and auditory responses have been recorded in TC neurons following behavioral conditioning to specific sounds [43]. A second possibility is that TRN neurons, which show topography similar to TC and cortical neurons [44,45], show changes in firing properties, bursting, or intrinsic excitability based on experience-dependent alterations in input from thalamic and cortical neurons (**Figure 2.1B, green arrow**) [46]. A third possibility is that the CT input returning *from* sensory and motor areas (*i.e.*, those receiving C-type TC input [47]) is altered by learning in a manner which promotes local spindle amplification, or greater local spindle coherence (**Figure 2.1B, blue arrow**) [38]. Plasticity of CT synapses on sensory relay neurons is well described [48,49]. Importantly, CT feedback to thalamus could also vary as a function of cortical location, in a manner analogous to (and indeed paralleling) C- and M-type TC pathways. As discussed above, CT feedback from layer 6 sends input to both TC and TRN neurons. A subset of layer 5 neurons also send input to thalamus, but in contrast to layer 6 neurons, there is no clear evidence that these neurons send collaterals to the TRN [50,51]. Depending on the cortical region, layer 5 and 6 CT projections from the same cortical area can either partially overlap within the thalamus (potentially even sending input to the same TC neurons) [52], send input to distinct subregions of the same thalamic nuclei [53], or send input to completely different thalamic nuclei [50]. A fourth

and final possibility is that intracortical plastic changes, initiated by sensory or motor experience, lead to subsequent changes in spindling via increased postsynaptic responses to TC input [54,55] or increased CT feedback to the thalamus (**Figure 2.1B, black arrow**) [56,57].

2.4 So…why spindle? The function of spindles in thalamocortical circuits

The phenomenon of local spindling has opened a window for better understanding relationships between spindle oscillations and brain function. There is abundant evidence that local increases in spindling following specific types of learning (*e.g.*, sensorimotor) may have important implications for subsequent cognitive function and performance. For example, training human subjects on a left-hand motor task leads to a subsequent, sleep-dependent improvement in task performance. This improvement is proportional to both EEG spindle density and lateralization of spindle power recorded at sites overlying right (contralateral) motor cortex (**Figure 2.1B**) [58]. Similarly, training on verbal and visuospatial memory tasks leads to overnight improvements that correlate with post-training NREM spindle numbers at left frontal and parietal EEG recording sites (areas associated with learning on these two tasks), respectively [59,60]. Analogous lateralized changes in spindle density and amplitude are seen in sleep during odor-based cueing of visual information presented to specific visual hemifields during prior waking experience - odors paired with images presented to the left hemifield in waking evoke spindles in right visual cortex when presented again during subsequent sleep, and vice versa [61]. Recently, it was shown using a combination of high-density EEG and fMRI during post-learning sleep that local spindles lead to selective reactivation of brain areas previously engaged by the learning task [62,63]. This reactivation included temporally coordinated increases in activity between the

hippocampus and specific cortical areas engaged by learning a particular task [62]. Cumulatively, it seems clear that local spindles may either directly promote adaptive, circuit-specific plasticity following learning, or be a highly reliable biomarker of such processes [55].

Understanding the function of spindle oscillations in brain plasticity has major implications for human performance. Many years after Loomis noted that spindle occurrence was highly variable between subjects [1,2], various spindle features have been found to correlate with general IQ measures in both children and adults [64-66]. As is true of any correlation, it remains unclear whether this indicates that spindle oscillations directly promote overall cognitive function, or rather whether optimal thalamocortical circuit function (and thus increased spindling) results from other processes that affect cognitive function. However, the numerous studies linking spindles to sleep-dependent improvement on new tasks suggests that the former relationship is plausible. A limited number of studies have found evidence that patterns of thalamocortical activity associated with spindles could lead to synaptic plasticity. One seminal study by Rosanova and Ulrich [67] used a pattern of neuronal activity recorded from rat somatosensory cortex during spindle oscillations *in vivo* to drive presynaptic activity in connected pairs of cortical pyramidal neurons (in layers 2/3 and 5, respectively). They found that this naturalistic activity pattern, repeated at intervals that mimicked the frequency at which spindles occur during NREM, could reliably evoke postsynaptic long-term potentiation (LTP). They also found that artificially-generated bursts, generated presynaptically at spindle frequency (*i.e.*, 10 Hz), evoked a similar form of LTP. Similarly, repetitive transcranial magnetic stimulation (rTMS) applied to the cat primary visual cortex (V1) at 10 Hz (but at not lower

frequencies) over a period of minutes could elicit potentiation of visually-evoked potentials [68]. Thus available data indicate that simple patterns of activity occurring at spindle frequency are sufficient to induce potentiation in cortical synapses *in vivo.*

Studies using *in vivo* paradigms in which synaptic plasticity is induced by novel waking experience (*e.g.*, novel sensory or motor experience) indicate a potential role for sleep spindles in promoting adaptive synaptic changes. Two recent examples come from the visual systems of cats and mice, in which novel visual experience leads to subsequent, sleep-dependent changes in thalamocortical circuit function. Both forms of plasticity are mediated by potentiation of glutamatergic synapses in the primary visual cortex (V1), leading to enhanced responsiveness to visual stimuli previously experienced in wakefulness. The first example, ocular dominance plasticity (ODP) in juvenile cat V1, is initiated by a very brief period (on the order of a few hours) of monocular visual experience. ODP takes the form of enhanced responsiveness to spared-eye visual stimulation in V1 neurons, and is significantly enhanced by sleep in the hours following this experience [69]. Sleep-dependent ODP enhancements were recently shown to be mediated by LTP-associated mechanisms in V1 [70], and were proportional to phase-locking of V1 neurons' firing with NREM spindle oscillations in the hours following experience [71]. The second form of plasticity, orientation-specific response potentiation (OSRP) in adult mouse V1, is initiated by brief exposure to a patterned visual stimulus such as an oriented grating [72]. It is expressed several hours after this experience, as a selectively enhanced visually-evoked response in V1 to stimuli of the same orientation. Available data suggests that OSRP is mediated by LTP-like changes at TC synapses in layer 4 [73], and data from our lab have shown that these changes occur during sleep in

the hours following visual experience [74,75]. Intriguingly, like sleep-dependent ODP, response changes during OSRP are also proportional to phase-locking of V1 neurons' firing with spindle oscillations in the hours following experience [74]. Taken together, these studies show that from the early development of sensory responses through adulthood, NREM spindles can support strengthening of cortical synapses in an adaptive manner, promoting enhanced neuronal responses to behaviorally-relevant sensory stimuli.

The cellular mechanisms by which spindle-frequency oscillations (vs. network oscillations at other frequencies) promote synaptic strengthening *in vivo* is still a matter of speculation [76,77]. However, the pattern of activity used to mimic spindle-associated activity *in vivo* (*i.e.*, bursts of presynaptic activity occurring at approximately 10 Hz) [67] is similar to theta-burst stimulation (TBS) protocols used to induce LTP at glutamatergic synapses [78]. A great deal is known about cellular mechanisms mediating TBS-induced LTP in the neocortex [79-81] and the hippocampus [82]. Intriguingly, 10 Hz stimulation in the form of single spikes (instead of bursts) has the opposite effect on glutamatergic synapses - inducing long term depression (LTD) [83]. Thus one possibility is that by generating 10 Hz inputs in a large population of thalamic inputs to the cortex, weak inputs (those generating only ≤ 1 spike/cycle) further weaken their connections with postsynaptic cortical targets, while stronger inputs (those generating bursts of spikes) strengthen connections with their postsynaptic partners. Thus it is possible that in certain conditions, spindles may also promote the preferential downscaling of weaker synapses during sleep [84].

Based on the available data, there appears to be a strong link between NREM spindles, plasticity in thalamocortical circuits, and cognition. How can this knowledge

inform our understanding of early nervous system development, plasticity through childhood and adolescence, and cognitive dysfunction and neurodegeneration in the aging brain? The remainder of our discussion will focus on these issues, emphasizing spindle phenomenology and potential function across the lifespan.

2.5 Sleep spindle "precursors" in the developing brain

Studies of sleep across the lifespan of humans and rodents [85,86] have demonstrated that sleep architecture changes dramatically across early postnatal development. In particular, both total sleep time and the relative proportion of REM to NREM sleep decrease dramatically between birth and adulthood. Because of the limitations of early EEG and behavioral techniques on which early studies in the field were based, until recently very little was known about pre- and peri-natal sleep architecture and brain activity. Thus almost nothing was known about how the activity patterns we associate with REM and NREM initially develop. However, recent studies using surface EEG in pre-term and full-term neonates have allowed new insights into how sleep features emerge at early stages of brain development.

EEG features termed "delta brushes" are the dominant pattern of activity seen in premature infants and *in utero* (**Figure 2.2**). They consist of spindle-like oscillations of 8-20 Hz, riding on top of delta (0.3-1.5 Hz) waves [87]. Prior to 28 gestational weeks, they are found exclusively at central areas, but from 28 weeks to term, they can be seen at central, occipital, and parietal areas [88]. These oscillations can occur during any stage (sleep or waking), however, as the brain matures they become restricted to sleep [89]. Topographically, they are relatively local events, and generally asymmetrical across hemispheres. Delta brushes diminish in voltage and density by 9 months gestation, and

thus are predominantly studied in premature human infants [89]. Little is known about how delta brushes are generated, although they can be triggered by sensory input in a manner similar to spindles in the adult brain [90]. This suggests that delta brushes can be initiated by sensory-evoked activity in the same circuits that generate spindles in the fully-developed brain.

To understand the mechanisms generating delta brushes and their potential function, many groups have examined an analogous oscillation in animal models - so-called “spindle bursts”. Spindle bursts occur during developmental periods comparable to that of delta brushes in humans [91,92], and comprise a similar oscillation frequency band (5-25 Hz). Spindle bursts, like delta brushes, occur locally and primarily during sleep [93]. They may also be initiated in a manner similar to both delta brushes and adult sleep spindles. Neonatal rats exhibit myoclonic twitches, after which spindle bursts occur in contralateral somatosensory cortex [93]. Spinal cord transection significantly decreases, but does not eliminate, spindle burst activity. Thus like delta brushes, spindle bursts can be elicited by sensory stimulation, although external input is not required for their initiation. The tight temporal relationship between spindle bursts and myoclonic twitches, and the fact that spindle bursts can be elicited by cutaneous stimulation, has led researchers to speculate that they may provide sensory feedback to the developing somatosensory and motor cortices [92-94]. Such feedback may serve an important function for proper topographic mapping of these cortices during development. While the precise cellular mechanisms mediating this process are still unknown, one possibility is that (through LTP-like mechanisms) spindle bursts lead to functional activation of silent thalamocortical synapses. In fact, from postnatal days 2-5 in rats, a significant portion of thalamocortical

synapses are silent. Isaac and colleagues [95] demonstrated that LTP could first be elicited at silent thalamocortical synapses in brain slices at postnatal days 3-7 (a period in which spindle bursts are frequent *in vivo*) but not at postnatal day 8 (when spindle bursts are rarely seen). Spindle bursts could also facilitate somatotopic mapping in other ways, for example, through plasticity of inputs to thalamic relays, or through plasticity of intracortical circuitry. It is tempting to speculate that, like spindle bursts, delta brushes may promote adaptive plasticity in synaptic connections. Delta brushes appear around the time that sensory-driven thalamocortical synapse formation is taking place, approximately 31-34 weeks of gestation [96]. At this developmental stage in humans *in utero*, generalized body movements begin to occur [97]. It is possible that delta brushes serve a similar purpose to topographically wire somatosensory cortex using sensory feedback following body movement. Consistent with this idea, Milh et al. [90] demonstrated that hand and foot movements in premature infants (31-33 weeks gestational age) preceded delta brush occurrence in developing somatosensory cortex; these brushes are local in nature, and occur predominantly contralateral to the movement. Hand and foot stimulation likewise elicited delta brushes in these cortical areas. Taken together, these findings support a role for delta brushes in the human brain *in utero* that is analogous to spindle bursts in animal models in early postnatal development; *i.e.*, in somatotopic cortical mapping [90,92]. Recent studies in both animals and humans have sought to understand the role of spindle bursts and delta brushes in the development of other sensory cortical areas. Spindle bursts occur either spontaneously or are evoked by stimulation in visual cortex in rats [87,98] and ferrets [99,100], as well as barrel cortex in rats [101]. Likewise, delta brushes may play a

role in human visual cortex development [102], and are seen in temporal areas following auditory stimulation [103].

How similar are these early oscillations to spindles in the mature brain? Spindle bursts in animal models and delta brushes and sleep spindles in humans are similar frequencies, although delta brushes are more likely to associate with delta frequency oscillations [89]. Furthermore, the topographies of delta brushes and sleep spindles throughout development are similar, each starting with a central distribution and spreading to other cortical areas as the brain matures [88,104]. Delta brushes are also believed to be thalamocortical in origin, similar to sleep spindles [103]. Recent work by Yang et al., indicate that a fraction of spindle bursts in barrel cortex are dependent on the ventral posterior medial (VPM) nucleus of the thalamus[105]. Finally, spindle bursts, delta brushes, and sleep spindles may all play a functional role in synaptic plasticity [67,71,74,92,10692-95]. Despite these similarities, it is unclear if spindle bursts or delta brushes can be called sleep spindle precursors in animal models and humans, respectively. After all, there is an unexplained two month gap between the disappearance of delta brushes and the appearance of the first sleep spindles in humans [89](see below). More work exploring the mechanistic underpinnings of these early oscillations is necessary before it can be said whether or not these oscillations are truly sleep spindle precursors. Despite these reservations, delta brushes in humans and spindle bursts in animal models may represent the earliest instances of “spindle-like” oscillations playing a role in, or serving as a reliable biomarker for, plastic changes in the brain.

2.6 Developmental onset and function of mature spindles

In contrast to delta brushes and spindle bursts, mature sleep spindles do not occur for several weeks following birth [89]. Available data suggest that between 6 weeks to 3 months of age, mature spindles appear and gradually increase in number and duration (**Figure 2.2**) [107-109]. The earliest spindles appear primarily around central leads (*i.e.*, over the central sulcus dividing primary motor and primary somatosensory cortices) of EEG recordings and are bilaterally synchronous [104]. By 4 months of age, there is greater distribution to frontotemporal regions, with higher levels of asynchrony in those areas; by 12 months, these spindles become more synchronous, possibly due to the increase in cerebral cortex white and gray matter by 88% during the first year of life [104,110]. In fact, synaptogenesis, apoptosis, and myelination, which are all crucial in the formation of functional neural circuits, continue from infancy through adolescence [111].

Childhood and adolescence are also periods of substantial change in spindle frequency, distribution, and power. Over the course of development, the occurrence of both slow and fast spindles increases [112]. During childhood and adolescent maturation of frontal gray and white matter, there are corresponding changes in spindle power in the slow (9-12 Hz) frequency band which predominates in adults in frontal regions [113]. Frontal (slow) spindles become more prominent with age, with a sudden increase in frequency during puberty, despite an overall decrease in power [114-116]. In contrast, there is very little age-dependent change in the power of centroparietal (fast) spindles across this same developmental period [115]. Topographically, spindle amplitude becomes greater in anterior regions, and decreases in posterior regions in children 7-11 years of age [117] (**Figure 2.2**).

In children and adolescents, spindle density and frequency also vary overnight as a function of time [117,118], with spindles becoming faster over successive NREM cycles [117].

Though these changes in spindle activity and topography have been well documented, until recently, there was a relative paucity of literature describing the role of spindles in postnatal cognitive development (*i.e.*, in children and adolescents). While studies in adults have found positive relationships between NREM spindle occurrence and IQ [66,119], findings have been less consistent in children. A recent study found a positive correlation between total spindle power in NREM and the nonverbal IQ in children aged 9-12 [65], however, this relationship seems to vary widely depending on the frequency band under study. “Fast” and “slow” sleep spindles correlate negatively and positively, respectively, with IQ measures. Faster spindle oscillations are negatively correlated with IQ [65], working memory, fine motor skills, planning ability [120], and perceptual reasoning [65] in children. In contrast, slow spindles show the opposite relationship to cognitive abilities. Doucette and colleagues examined younger (*i.e.*, preschool) children and found a positive relationship between simple reaction time task performance and slow spindle power [112]. Importantly, many of the above studies have focused on “fluid intelligence” rather than “crystallized intelligence” (*e.g.*, skill learning and episodic memory consolidation). The former appears to rely more on genetics than the latter, which seems to benefit substantially from both experience and sleep [121]. Based on this distinction, Gruber and colleagues have suggested that a common heritable factor may affect both the speed of spindle oscillations and measures of fluid intelligence [117].

More recently, experiments have begun to address the role of sleep spindles in building crystallized intelligence during development. Unlike adults, children under 5 sleep

in biphasic or polyphasic patterns, taking naps in addition to overnight sleep. Spindles are hypothesized to drive improvements in learning seen after a short nap in preschoolers [122]. These midday naps may be particularly important for preschool-aged children, since parietal and temporal cortices mature around this time and prefrontal cortex is beginning to undergo plasticity based on experience [123]. Kurdziel and colleagues found that sleep spindle density during a nap was positively correlated with sleep-dependent (*i.e.*, post-nap - pre-nap) improvements in children's performance on a visuospatial task [122].

A good understanding of the differences between spindles' role in children vs. adults is still lacking. What is clear is that spindles in children are particularly associated with intrinsic measures of intelligence, and often these correlations are negative. In adults, these correlations are frequency positive. One possibility to explain these differences is the need for refinement and pruning of synapses in children. Myelination, synaptogenesis, and apoptosis occur throughout childhood and adolescence. Chatburn and colleagues have speculated that negative correlations represent the immaturity of the thalamocortical network and intracortical connections [120]. Though studies examining spindle function in children are lacking, there are even fewer studies in adolescents. This represents a significant gap in the literature, as puberty and adolescence are times of significant change in both body and brain development, marking the transition from childhood to adulthood.

2.7 Sleep spindles and disorders of neurodevelopment

The relationship between spindles and brain development has been examined in patient populations where cognitive development is delayed or disrupted [124,125]. For example, in children with Down syndrome, there is a significant delay in the

developmental onset of identifiable spindle activity, spindle density is significantly reduced, and development of interhemispheric synchrony of spindles is delayed [124]. These differences are likely due to the numerous neurodevelopmental abnormalities associated with Down syndrome. For example, children with Down syndrome show decreased proliferation of neuronal progenitor cells during gestation, decreased mature neuronal numbers overall, decreased dendritic spine density, changes in LTP and LTD, and early-onset neurodegeneration when compared with typically-developing children [126-128]. Patients with cortical malformations, in which gray matter and (to a lesser extent) white matter do not develop properly, have decreases in bilaterally-occurring spindles relative to controls [129]. Spindle occurrence in these patients is less frequent in the hemisphere exhibiting the malformation, indicating disruption of thalamocortical pathways to generate spindles. Children with ASD also show significantly reduced spindle density during sleep [130,131]. Thus it seems that spindle density could serve as a generalizable biomarker for disorders of neurodevelopment.

Some disorders emerge only later in development, as children's brains mature; available data indicate that these disorders may also have features related to deficits in sleep behavior generally and sleep spindles in particular. For example, a substantial number of studies have described decreases in overall sleep time and disrupted sleep architecture in early-onset major depressive disorder (EO-MDD), which is highly prevalent in both children and adolescents [132]. Recently, Lopez et al [118] demonstrated that both children and adolescents diagnosed with EO-MDD, and those undiagnosed but at high risk for EO-MDD (based on a significant family history of MDD), showed reduced spindle density across the night compared to those with neither a diagnosis or a family history.

Because spindle reductions have been less consistently found in adult MDD patients [133,134], one possibility is that a reduction in spindles at this earlier developmental stage (*i.e.*, when the brain is more plastic) has a more pronounced effect on cognitive function (resulting in earlier symptom presentation).

Researchers have also known for some time that sleep disturbances are common in schizophrenia patients. Spindles are reduced in density, amplitude, and duration in schizophrenia patients who are either medicated [135-137] or drug-naïve [138]. It is still unclear how these changes relate to cognitive and behavioral dysfunction in schizophrenia. Since patients typically first present with symptoms of schizophrenia during adolescence [139], decreased spindling during adolescent development may be a diagnostic biomarker for these patients [138]. It is possible that decreased spindle density in schizophrenia patients is due to either structural or functional abnormalities in TC signaling, for example, due to changes in the number of TC neurons [140] or in the balance between intrathalamic excitatory and inhibitory signaling [141]. There evidence of both GABAergic signaling deficits [142] and abnormal glutamatergic signaling in the thalamus of schizophrenia patients [143,144]. Interestingly, decreases in thalamic volume in schizophrenia correlate with both decreases in NREM spindles and cognitive dysfunction [140]. One intriguing possibility is that treatments aimed at increasing sleep spindles in schizophrenic patients could have clinical value [138]. Recently, hypnotics which increase spindle numbers (such as eszopiclone) have been tested as a treatment for cognitive dysfunction in schizophrenia [138,145]. One study assessed overnight improvement on a motor sequence task in patients trained in the evening and subsequently treated with either eszopiclone or a placebo. Eszopiclone significantly increased NREM spindle counts, and while there was no

significant effect of treatment on overnight improvement on motor performance, spindle counts in both the placebo and eszopiclone groups correlated with overnight improvement on the task [145]. This strategy hold promise, particularly as a longer-term (*i.e.*, nightly vs. one-time) adjuvant treatment for cognitive dysfunction in schizophrenia.

2.8 Aging alters architecture: Sleep spindle changes in normal aging

Aging adults self-report sleep issues at a greater frequency than any other age group [146]. While the general population has an insomnia rate of up to 48%, the aging population reports a prevalence of up to 65% (reviewed in [147]). In aging, sleep is altered in multiple capacities including timing, duration, architecture, and quality. The elderly population experiences a circadian phase shift in which they wake up earlier and go to sleep earlier than younger adults, with decreased duration of sleep and increased napping [148]. The sleep aged adults do get is more fragmented, with increased arousals and more frequent transitions between sleep states [149]. Total time spent in both REM and deep slow wave sleep (SWS) decreases, while lighter NREM sleep increases in duration [150]. The density of both K complexes and sleep spindles decreases [151]. NREM spectral power decreases in alpha (relaxed wake), delta (deep sleep), theta (consciousness), and sigma (spindle) bands. Sleep macroarchitecture across the night also changes dramatically. In young adults, across the night, SWS decreases in duration and spindle occurrence decreases as the night goes on. This is thought to reflect homeostatic changes in NREM sleep after wakefulness, leading to greater SWS and spindle occurrence at sleep onset, and decreasing SWS and spindle amounts across the night. Aging alters this process, making SWS duration and spindle occurrence more homogeneous across the night [152,153].

Age-dependent changes in spindle density, amplitude, duration, and topography have been extensively characterized using EEG **(Figure 2.2**) [151,154,155]. All of the reported sleep spindle changes appear to be progressive with increasing age [156,157]. For example, spindle density progressively decreases (relative to density in young adults) across middle age and into old age [156]. Three features of age-dependent spindle decline are noteworthy, in that they may illustrate the neurobiological changes underlying this process. First, these changes are not homogenous across the cortex; rather, decreases in spindle density at older ages are most pronounced at frontal and occipital sites [158]. This progressive topographical change is actually the reverse of what appears to happen during development, in which density in these areas gradually increases relative to the rest of the cortex (**Figure 2.2**). This may relate to progressive neurodegenerative changes that preferentially affect these cortical areas with aging [159]. It also appears that slow and fast spindles are differentially affected with aging. There is general agreement that NREM spectral power in the fast spindle range (*i.e.*, between 13-15 Hz) gradually, but dramatically, decreases with age [153,160]. However, it is unclear whether slower-frequency (9-12 Hz) spindles are similarly affected. Finally, it is possible that global and local spindles are differentially affected with advanced age. A loss of local spindles may indicate either a selective age related change in the CT-TRN-TC circuitry mediating local spindles, or general decline in neuroplasticity with aging. Recently, a study by Huupponen and colleagues [161] found a (nonsignificant) trend of increasing prevalence of global vs. local spindles with increasing age. While the spatial resolution was limited in this study (only six EEG channels were used) future studies using higher density EEG and MEG

may clarify how aging affects the topology of spindle occurrence, and local spindles induced by prior learning are affected with aging.

Not everyone is equally affected by spindle changes with age. For example, in younger and middle aged subjects, there is a clear gender difference in spindling, with women having higher spindle density; in aging this difference decreases [151]. Across-the-night changes in spindle density are also altered in older subjects [153-155]. Even when differences in age and gender are accounted for, there is still high variability, with some adults being much less affected by age than others [162].

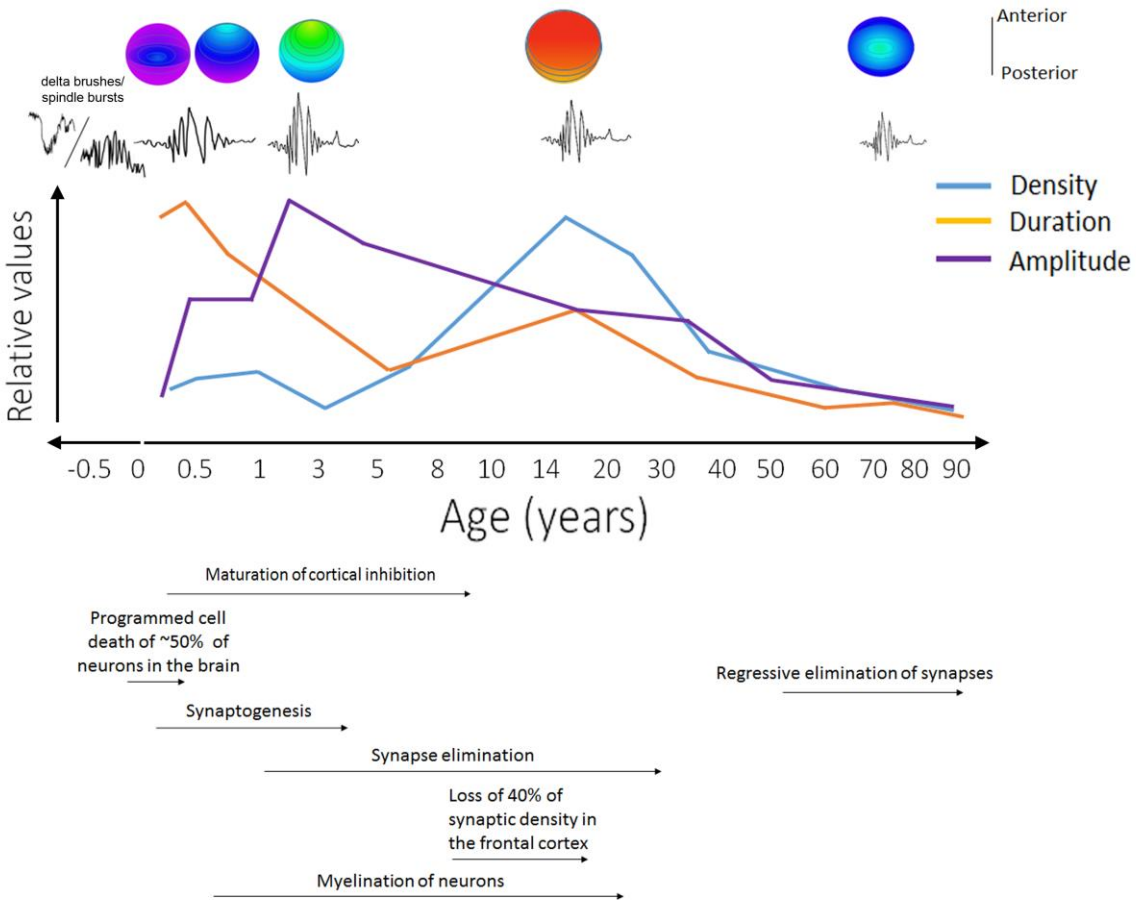

Figure 2.2 Changes in spindle form across the lifespan. Top - Heat maps depict topographical spindles density during early development, adolescence, and aging. Spindles are initially seen over central areas of the brain, and gradually develop over frontotemporal areas during the first year of life [104]. During adolescence, density reaches a relative maximum with equal distribution across frontal, central, and parietal leads. In aging, there is a return to the same pattern seen earlier in development, with highest density at central leads [158]. Below the heat maps are representations of spindle morphology at these ages. **Middle** - Sleep spindle density (**blue trace**) increases throughout early development, peaking during puberty and steadily declining from adolescence to old age [109,156]. Duration of sleep spindles (**orange trace**), on the other hand, peaks early in life, then generally declines over the lifespan. Spindle amplitude (**purple trace**) is relatively small early in development, increasing to maximum values over the first year of life, and then steadily declines until old age [151]. **Bottom** - Neurodevelopmental milestones.

2.9 What are the effects of spindle changes as we age?

There have been two main focuses for understanding the functional effects of age-related changes in sleep-spindles: 1) possible changes in sleep architecture, and 2) potential changes in cognition. In fact, the earliest study looking at the effects of spindle changes examined both. Guazzelli and colleagues found no correlation between spindle density and either the number or duration of bouts of wake after sleep onset in older subjects [154]. Similarly, Nicolas et al., found no interaction between sleep spindle characteristics and overall sleep efficiency in aging subjects [156]. In the same study, Guazzelli et al., also examined the potential relationship between spindle decrease and cognitive decline. They found no correlation between overall verbal or performance IQ and spindle changes with aging. However, studies using more specific cognitive measurements (*e.g.*, with tests of motor learning and episodic memory) found consistent correlations between preservation of spindles with increasing age and preservation of cognitive functioning [163,164].

Many age-related pathologies present with cognitive decline, including Alzheimer's and Parkinson's diseases. In these two syndromes, further decreases in spindle density (beyond that seen in normal aging) have been observed [165,166]. The most dramatic reductions - and even a complete loss of sleep spindles - have been reported in the most severe cases of dementia [167,168]. Alzheimer's disease patients who presented with greater mean intensity and number of fast spindles performed better in an episodic memory (story recall task) than patients who showed lower spindle numbers and intensity [165]. Similarly, a decrease in spindle density and amplitude has been observed in Parkinson's disease patients who experience dementia relative to those who do not. These decreases

occurred to a greater extent in posterior areas, with prominent decreases at central, parietal, and occipital derivations. The strength of the decrease in posterior areas was correlated with a decrease in visuospatial capabilities [166]. Interestingly, a similar spindle-cognition relationship has been observed in a premature aging syndrome (Mulvihill-Smith syndrome), with a complete loss of NREM spindles associated with cognitive deficits [169].

2.10 Why do we lose spindles as we age?

There is a large gap in our understanding of the neurophysiological changes that cause declines in spindling with age. However, some speculations can be made. Changes in brain anatomy with aging are often referred to under the umbrella of the "shrinking brain phenomenon": as senescence proceeds, cortical volume decreases [170]. This occurs in an anterior to posterior gradient, with both gray and white matter [171]. Decreases in gray matter are concentrated in prefrontal cortex, alongside the inferior frontal and insular regions, and the inferior parietal cortex [170,172,173]. White matter is most reduced with aging in medial frontal and medial lateral regions [174,175].These alterations may offer explanatory value for region-specific decreases in spindling with aging. In line with this, decrease in spindles in aging has been correlated with increased sulcal atrophy [154]. Additional age-related thalamocortical circuit changes may explain overall decreases in spindles. For example, the thalamus shows a significant decrease in volume in aging, and its connectivity with the cortex is altered (reviewed in [176]). This change parallels structural changes associated with reduced spindling in the brains of schizophrenia patients described above. Furthermore, T-type calcium channel (Cav 3.1) expression decreases as a function of age [177]. This latter change could translate into a fundamental deficit in the generation of spindle oscillations, independent of anatomical changes to TC

circuitry. Finally, given that melatonin signaling enhances activity in the 11-14 Hz frequency band [178-180], and melatonin levels decrease significantly with age [179] this may account for both the reduced occurrence of spindles and the upward shift in spindle frequency in aging.

2.11 Summary and future directions

Previous work clearly defined that spindles evolve across the lifespan and that changes in spindle activity are correlated with changes in cognition. However, a major gap in our knowledge remains with regard to causality. We currently do not know for certain whether (and how) network activity in wakefulness promotes local spindle activity. Neither do we know whether (and how) global and local spindles contribute to thalamocortical network plasticity and cognitive functions associated with this plasticity. The use of new tools, such as pharmacogenetics, optogenetics, or transcranial magnetic stimulation, to alter spindle generation or density should clarify our understanding of the relationship between spindle form and function.

A majority of the literature examining sleep spindle function in humans has focused on adult populations. However, broadening our understanding of these oscillations throughout the lifespan may illuminate spindle functions that are not apparent in healthy adults. Infancy, childhood, and adolescence are times of dramatic change in the brain, characterized by widespread synaptogenesis, myelination, and synaptic pruning. During these years, spindle amplitude, duration, density, frequency, and topology change. Understanding the relationship between spindle form and function during these transitions has implications for a variety of neurodevelopmental disorders in which spindle activity is altered.

With advancing age come dramatic alterations in brain architecture, cognition, and sleep patterns. Many of these are the reverse of changes seen during development. Both healthy age-related and pathological changes in the brain cause decreases in brain volume and synaptic connections. Decreases in sleep and sleep spindles during this time are likely caused by structural alterations in thalamocortical circuitry. However, augmentation of spindles may be useful for mitigating deficits seen with cognitive aging.

In conclusion, sleep spindles change over the course of a lifetime, in parallel with the multitude of changes in the developing and aging brain. Spindles may serve different functions throughout the lifespan. Future studies focused on age-specific brain anatomical and functional differences will ultimately help us understand these functions.

2.12 References

1 Loomis, A. L., Harvey, E. N. & Hobart, G. Potential Rhythms of the Cerebral Cortex during Sleep. *Science* **81**, 597-598 (1935).

2 Loomis, A. L., Harvey, E. N. & Hobart, G. Further Observations on the Potential Rhythms of the Cerebral Cortex during Sleep. *Science* **82**, 198-200 (1935).

3 Destexhe, A., Contreras, D., Sejnowski, T. J. & Steriade, M. Modeling the control of reticular thalamic oscillations by neuromodulators. *Neuroreport* **5** (1994).

4 Golshani, P., Liu, X. B. & Jones, E. G. Differences in quantal amplitude reflect GluR4- subunit number at corticothalamic synapses on two populations of thalamic neurons. *Proc Natl Acad Sci U S A* **98**, 4172-4177 (2001).

5 Astori, S. *et al.* The Ca(V)3.3 calcium channel is the major sleep spindle pacemaker in thalamus. *Proc Natl Acad Sci U S A* **108**, 13823-13828 (2011).

6 Luthi, A. Sleep spindles: where they come from, what they do. *The Neuroscientist* **20**, 243-256 (2014).

7 Espinosa, F., Torres-Vega, M. A., Marks, G. A. & Joho, R. H. Ablation of Kv3.1 and Kv3.3 potassium channels disrupts thalamocortical oscillations in vitro and in vivo. *J Neurosci* **28**, 5570-5581 (2008).

8 Long, M. A., Landisman, C. E. & Connors, B. W. Small clusters of electrically coupled neurons generate synchronous rhythms in the thalamic reticular nucleus. *J Neurosci* **24**, 341-349 (2004).

9 McCormick, D. A. & Bal, T. Sleep and arousal: thalamo-cortical mechanisms. *Annual Review of Neuroscience* **20**, 185-215 (1997).

10 Fuentealba, P. & Steriade, M. The reticular nucleus revisited: intrinsic and network properties of a thalamic pacemaker. *Prog Neurobiol* **75**, 125-121 (2005).

11 Fuentealba, P., Timofeev, I., Bazhenov, M., Sejnowski, T. J. & Steriade, M. Membrane bistability in thalamic reticular neurons during spindle oscillations. *J Neurophsiol* **93**, 294-304 (2005).

12 Kandel, A. & Buzsaki, G. Cellular-synaptic generation of sleep spindles, spike-and-wave discharges, and evoked thalamocortical responses in the neocortex of the rat. *J Neurosci* **17**, 6783-6797 (1997).

13 Bal, T. & McCormick, D. A. What stops synchronized thalamocortical oscillations? *Neuron* **17**, 297-308 (1996).

14 Luthi, A. & McCormick, D. A. Periodicity of thalamic synchronized oscillations: the role of Ca2+-mediated upregulation of Ih. *Neuron* **20**, 553-563 (1998).

15 Bartho, P. *et al.* Ongoing network state controls the length of sleep spindles via inhibitory activity. *Neuron* **82**, 1367-1379 (2014).

16 Sohal, V. S., Keist, R., Rudolph, U. & Huguenard, J. R. Dynamic GABA(A) receptor subtype-specific modulation of the synchrony and duration of thalamic oscillations. *J Neurosci* **23**, 3649-3657 (2003).

17 Zhang, L. & Jones, E. G. Corticothalamic inhibition in the thalamic reticular nucleus. *J Neurophysiol* **91**, 759-766 (2004).

18 Bonjean, M. *et al.* Corticothalamic feedback controls sleep spindle duration in vivo. *J Neurosci* **31**, 9124-9134 (2011).

19 Nir, Y. *et al.* Regional slow waves and spindles in human sleep. *Neuron* **70**, 153-169 (2011).

20 Andrillon, T. *et al.* Sleep spindles in humans: insights from intracranial EEG and unit recordings. *J Neurosci* **31**, 17821-17834 (2011).

21 Contreras, D., Destexhe, A., Sejnowski, T. J. & Steriade, M. Control of spatiotemporal coherence of a thalamic oscillation by corticothalamic feedback. *Science* **274**, 771-774 (1996).

22 Kim, D., Hwang, E., Lee, M., Sung, H. & Choi, J. H. Characterization of topographically specific sleep spindles in mice. *Sleep* **38**, 85-96 (2015).

23 Terrier, G. & Gottesmann, C. L. Study of cortical spindles during sleep in the rat. *Brain Res Bull* **3**, 701-706 (1978).

24 Peter-Derex, L., Comte, J. C., Mauguiere, F. & Salin, P. A. Density and frequency caudo-rostral gradients of sleep spindles recorded in the human cortex. *Sleep* **35**, 69-79 (2012).

25 Wrzosek, M. *et al.* Visual and quantitative electroencephalographic analysis of healthy young and adult cats under medetomidine sedation. *Vet J* **180**, 221-230 (2009).

26 Dehghani, N., Cash, S. S. & Halgren, E. Topographical frequency dynamics within EEG and MEG sleep spindles. *Clinical Neurophysiology* **122**, 229-235 (2011).

27 Wester, J. C. & Contreras, D. Columnar interactions determine horizontal propagation of recurrent network activity in neocortex. *J Neurosci* **32**, 5454-5471 (2012).

28 Stroh, A. *et al.* Making waves: initiation and propagation of corticothalamic Ca2+ waves in vivo. *Neuron* **77**, 1136-1150 (2013).

29 Theyel, B. B., Llano, D. A. & Sherman, S. M. The corticothalamic circuit drives higher-order cortex in the mouse. *Nat Neurosci* **13**, 84-88 (2010).

30 Hughes, J. R. *et al.* Relationship of the magnetoencephalogram to the electroencephalogram. Normal wake and sleep activity. *Electroenceph Clin Neurophysiol* **40**, 261-278 (1976).

31 Nakasato, N. *et al.* Magnetic detection of sleep spindles in normal subjects. *Encephalography and Clinical Neurophysiology* **76**, 123-130 (1990).

32 Dehghani, N., Cash, S. S. & Halgren, E. Emergence of synchronous EEG spindles from asynchronous MEG spindles. *Hum Brain Mapp* **32**, 2217-2227 (2011).

33 Dehghani, N., Cash, S. S., Rossetti, A. O., Chen, C. C. & Halgren, E. Magnetoencephalography demonstrates multiple asynchronous generators during human sleep spindles. *J Neurophsiol* **104**, 179-188 (2010).

34 Rubio-Garrido, P., Perez-de-Manzo, F., Porrero, C., Galazo, M. J. & Clasca, F. Thalamic input to distal apical dendrites in neocortical layer 1 is massive and highly convergent. *Cereb. Cortex* **19**, 2380-2395 (2009).

35 Bonjean, M. *et al.* Interactions between core and matrix thalamocortical projections in human sleep spindle synchronization. *J Neurosci* **32**, 5250-5263 (2012).

36 Dehghani, N. *et al.* Divergent cortical generators of MEG and EEG during human sleep spindles suggested by distributed source modeling. *PLoS ONE* **5**, e11454 (2010).

37 Kim, U., Thierry, B. & McCormick, D. A. Spindle waves are propagating synchronized oscillations in the ferret LGNd in vitro. *Journal of Neuroscience* **74**, 1301-1323 (1995).

38 Bal, T., Debay, D. & Destexhe, A. Cortical feedback controls the frequency and synchrony of oscillations in the visual thalamus. *J Neurosci* **20**, 7478-7488 (2000).

39 Ganes, T. & Anderson, P. Barbiturate spindle activity in functionally corresponding thalamic and cortical somato-sensory areas in the cat. *Brain Res* **98**, 457-472 (1975).

40 Stickgold, R., Whifbee, D., Schirmer, B., Patel, V. & Hobosn, J. A. Visual discrimination task improvement: a multi-step process occuring during sleep. *J.Cogn.Neuroscience* **12**, 246-254 (2000).

41 Gais, S., Plihal, W., Wagner, U. & Born, J. Early sleep triggers memory for early visual discrimination skills. *Nat.Neurosci.* **3**, 1335-1339 (2000).

42 Bang, J. W., Khalilzadeh, O., Hamalainen, M., Watanabe, T. & Sasaki, Y. Location specific sleep spindle activity in the early visual areas and perceptual learning. *Vision Research* **99**, 162-171 (2014).

43 Woody, C. D., Gruen, E. & Wang, X. F. Electrical properties affecting discharge of units of the mid and posterolateral thalamus of conscious cats. *Neuroscience* **122**, 531-539 (2003).

44 Fitzgibbon, T., Szmajda, B. A. & Martin, P. R. First order connections of the visual sector of the thalamic reticular nucleus in marmoset monkeys (Callithrix jacchus). *Vis Neurosci* **24**, 857-874 (2007).

45 Kimura, A., Imbe, H., Donishi, T. & Tamai, Y. Axonal projections of single auditory neurons in the thalamic reticular nucleus: implications for tonotopy-related gating function and cross-modal modulation. *Eur J Neurosci* **26**, 3524-3535 (2007).

46 Paz, J. T., Christian, C. A., Parada, I., Prince, D. A. & Huguenard, J. R. Focal cortical infarcts alter intrinsic excitability and synaptic excitation in the reticular thalamic nucleus. *J Neurosci* **30**, 5465-5479 (2010).

47 Jones, E. G. The thalamic matrix and thalamocortical synchrony. *Trends Neurosci* **24**, 595-601 (2001).

48 Castro-Alamancos, M. A. & Calcagnotto, M. E. Presynaptic long-term potentiation in corticothalamic synapses. *J Neurosci* **19**, 9090-9097 (1999).

49 Hsu, C. L., Yang, H. W., Yen, C. T. & Min, M. Y. Comparison of synaptic transmission and plasticity between sensory and cortical synapses on relay neurons in the ventrobasal nucleus of the rat thalamus. *J Physiol* **588**, 4347-4363 (2010).

50 Bourassa, J. & Deschenes, M. Corticothalamic projections from the primary visual cortex in rats: a single fiber study using biocytin as an anterograde tracer. *Neuroscience* **66**, 253-263 (1995).

51 Grant, E., Hoerder-Suabedissen, A. & Molnar, Z. Development of the corticothalamic projections. *Front Neurosci* **6**, 53 (2012).

52 Kakei, S., Na, K. & Shinoda, Y. Thalamic terminal morphology and distribution of single corticothalamic axons originating from layers 5 and 6 of the cat motor cortex. *J Comp Neurol* **437**, 170-185 (2001).

53 Ojima, H. Terminal morphology and distribution of corticothalamic fibers originating from layers 5 and 6 of cat primary auditory cortex. *Cereb. Cortex* **4**, 646-663 (1994).

54 Destexhe, A., Contreras, D. & Steriade, M. Cortically-induced coherence of a thalamic-generated oscillation. *Neuroscience* **92**, 427-443 (1999).

55 Werk, C. M., Harbour, V. L. & Chapman, C. A. Induction of long-term potentiation leads to increased reliability of evoked neocortical spindles in vivo. *Neuroscience* **131**, 793-800 (2005).

56 Petrus, E. *et al.* Developmental switch in the polarity of experience-dependent synaptic changes in layer 6 of mouse visual cortex. *J Neurophysiol* **106**, 2499-2505 (2011).

57 Chandrasekaran, S. *et al.* Unbiased, high-throughput electron microscopy analysis of experience-dependent synaptic changes in the neocortex. *J Neurosci* **35**, 16450-16462 (2015).

58 Nishida, M. & Walker, M. P. Daytime naps, motor memory consolidation and regionally specific sleep spindles. *PloS ONE* **2**, e341 (2007).

59 Clemens, Z., Fabo, D. & Halasz, P. Overnight verbal memory retention correlates with the number of sleep spindles. *Neuroscience* **132**, 529-535 (2005).

60 Clemens, Z., Fabo, D. & Halasz, P. Twenty-four hours retention of visuospatial memory correlates with the number of parietal sleep spindles. *Neurosci Lett* **403**, 52-56 (2006).

61 Cox, R., Hofman, W. F., de Boer, M. & Talamini, L. M. Local sleep spindle modulations in relation to specific memory cues. *NeuroImage* **99**, 103-110 (2014).

62 Bergmann, T. O., Molle, M., Diedrichs, J., Born, J. & Siebner, H. R. Sleep spindle-related reactivation of category-specific cortical regions after learning face-scene associations. *NeuroImage* **59**, 2733-2742 (2012).

63 Yotsumoto, Y. *et al.* Location-specific cortical activation changes during sleep after training for perceptual learning. *Current Biology* **19**, 1278-1282 (2009).

64 Hoedlmoser, K. *et al.* Slow sleep spindle activity, declarative memory, and general cognitive abilities in children. *Sleep* **37**, 1501-1512 (2014).

65 Geiger, A. *et al.* The Sleep EEG as a Marker of Intellectual Ability in School Age Children. *Sleep* **34**, 181-189 (2011).

66 Fogel, S. M., Nader, R., Cote, K. A. & Smith, C. T. Sleep spindles and learning potential. *Behav Neurosci* **121**, 1-10 (2007).

67 Rosanova, M. & Ulrich, D. Pattern-specific associative long-term potentiation induced by a sleep spindle-related spike train. *J Neurosci* **25**, 9398-9405 (2005).

68 Avdin-Abidin, S., Moliadze, V., Eysel, U. T. & Funke, K. Effects of repetitive TMS on visually evoked potentials and EEG in the anaesthetized cat: dependence on stimulus frequency and train duration. *J Physiol* **574**, 443-455 (2006).

69 Frank, M. G., Issa, N. P. & Stryker, M. P. Sleep enhances plasticity in the developing visual cortex. *Neuron* **30**, 275-287 (2001).

70 Aton, S. J. *et al.* Mechanisms of sleep-dependent consolidation of cortical plasticity. *Neuron* **61**, 454-466 (2009).

71 Aton, S. J. *et al.* Visual experience and subsequent sleep induce sequential plastic changes in putative inhibitory and excitatory cortical neurons. *Proc Natl Acad Sci U S A* **110**, 3101-3106 (2013).

72 Frenkel, M. Y. *et al.* Instructive effect of visual experience in mouse visual cortex. *Neuron* **51**, 339-349 (2006).

73 Cooke, S. F. & Bear, M. F. Visual experience induces long-term potentiation in the primary visual cortex. *J Neurosci* **30**, 16304-16313 (2010).

74 Aton, S. J., Suresh, A., Broussard, C. & Frank, M. G. Sleep promotes cortical response potentiation following visual experience. *Sleep* **37**, 1163-1170 (2014).

75 Durkin, J. & Aton, S. J. Sleep-Dependent Potentiation in the Visual System Is at Odds with the Synaptic Homeostasis Hypothesis. *Sleep* **39**, 155-159 (2016).

76 Aton, S. J. Set and setting: How behavioral state regulates sensory function and plasticity. *Neurobiol Learn Mem* **106**, 1-10 (2013).

77 Aton, S. J., Seibt, J. & Frank , M. G. in *Encyclopedia of Life Science* (John Wiley and Sons, Ltd., Chichester, 2009).

78 Capocchi, G., Zampolini, M. & Larson, J. Theta burst stimulation is optimal for induction of LTP at both apical and basal dendritic synapses on hippocampal CA1 neurons. *Brain Res* **591** (1992).

79 Kramár, E. A. *et al.* Synaptic evidence for the efficacy of spaced learning. *PNAS* **109**, 5121-5126 (2012).

80 Arami, M. K. *et al.* Reciprocal homosynaptic and heterosynaptic long-term plasticity of corticogeniculate projection neurons in layer VI of the mouse visual cortex. *J Neurosci* **33**, 7787-7798 (2013).

81 Shaffery, J. P., Sinton, C. M., Bissette, G., Roffwarg, H. P. & Marks, G. A. Rapid eye movement sleep deprivation modifies expression of long-term potentiation in visual cortex of immature rats. *Neuroscience* **110**, 431-443 (2002).

82 Cao, G. & Harris, K. M. Augmenting saturated LTP by broadly spaced episodes of theta-burst stimulation in hippocampal area CA1 of adult rats and mice. *J Neurophysiol* **112**, 1916-1924 (2014).

83 Goh, J. J. & Manahan-Vaughan, D. Synaptic depression in the CA1 region of freely behaving mice is highly dependent on afferent stimulation parameters. *Front Integr Neurosci* **7**, 1 (2013).

84 Tononi, G. & Cirelli, C. Sleep function and synaptic homeostasis. *Sleep Medicine Reviews* **10**, 49-62 (2006).

85 Roffwarg, H. P., Muzio, J. N. & Dement, W. C. Ontogenetic development of the human sleep-dream cycle. *Science*, 604-619 (1966).

86 Jouvet-Mounier, D., Astic, L. & Lacote, D. Ontogenesis of the states of sleep in rat, cat and guinea pig during the first postnatal month. *Developmental Psychobiology* **2**, 216-239 (1970).

87 Hanganu, I. L., Ben-Ari, Y. & Khazipov, R. Retinal waves trigger spindle bursts in the neonatal rat visual cortex. *J. Neurosci.* **26**, 6728-6736 (2006).

88 Anderson, C. M., Torres, F. & Faoro, A. The EEG of the early premature. *Electroenceph Clin Neurophysiol* **60**, 95-105 (1985).

89 Ellingson, R. J. Development of sleep spindle bursts during the first year of life. *Sleep* **5**, 39-46 (1982).

90 Milh, M. *et al.* Rapid cortical oscillations and early motor activity in premature human neonate. *Cereb. Cortex* **17**, 1582-1594 (2007).

91 Clancy, B., Darlington, R. B. & Finlay, B. L. Translating developmental time across mammalian species. *Neuroscience* **105**, 7-17 (2001).

92 Khazipov, R. & Luhmann, H. J. Early patterns of electrical activity in the developing cerebral cortex of humans and rodents. *Trends Neurosci* **29**, 414-418 (2006).

93 Khazipov, R. *et al.* Early motor activity drives spindle bursts in the developing somatosensory cortex. **432**, 758-761 (2004).

94 Blumberg, M. S. Developing sensorimotor systems in our sleep. *Curr Dir Psychol Sci* **24**, 32-37 (2015).

95 Isaac, J. T., Crair, M. C., Nicoll, R. A. & Malenka, R. C. Silent synapses during development of thalamocortical circuits. *Neuron* **18**, 269-280 (1997).

96 Kostovic, I. & Judas, M. The development of the subplate and thalamocortical connections in the human foetal brain. *Acta Paediatrica* **99**, 1119-1127 (2010).

97 Hadders-Algra, M. Putative neural substrate of normal and abnormal general movements. *Neurosci Biobehav Rev* **31**, 1181-1190 (2007).

98 Hanganu, I. L., Staiger, J. F., Ben-Ari, Y. & Khazipov, R. Cholinergic modulation of spindle bursts in the neonatal rat visual cortex in vivo. *J Neurosci* **27**, 5694-5705 (2007).

99 Chiu, C. & M., W. Spontaneous activity in developing ferret visual cortex in vivo. *Journal of Neuroscience* **21**, 8906-8914 (2001).

100 Chiu, C. & Weliky, M. Relationship of correlated spontaneous activity to functional ocular dominance columns in the developing visual cortex. *Neuron* **35**, 1123-1134 (2002).

101 Minlebaev, M., Ben-Ari, Y. & Khazipov, R. Network mechanisms of spindle-burst oscillations in the neonatal rat barrel cortex in vivo. *J Neurophsiol* **97**, 692-700 (2007).

102 Colonnese, M. T. *et al.* A conserved switch in sensory processing prepares developing neocortex for vision. *Neuron* **67**, 480-498 (2010).

103 Chipaux, M. *et al.* Auditory stimuli mimicking ambient sounds drive temporal "delta-brushes" in premature infants. *PLoS ONE* **8**, e79028 (2013).

104 Hagne, I. Development of the Sleep EEG in Normal Infants During the First Year of Life. *Acta Paediatrica* **61**, 25-53 (1972).

105 Yang, J. W. *et al.* Thalamic network oscillations synchronize ontogenetic columns in the newborn rat barrel cortex. *Cereb. Cortex* **23** (2013).

106 Steriade, M. & Timofeev, I. Neuronal plasticity in thalamocortical networks during sleep and waking oscillations. *Neuron* **37**, 563-576 (2003).

107 Ellingson, R. J. & Peters, J. F. Development of EEG and daytime sleep patterns in low risk premature infants during the first year of life: longitudinal observations. *Electroenceph Clin Neurophysiol* **50**, 165-171 (1980).

108 Metcalf, D. The Effect of Extrauterine Experience on the Ontogenesis of EEG Sleep Spindles. *Psychosomatic Medicine* **31**, 393-399 (1969).

109 Louis, J., Zhang, J. X., Revol, M., Debilly, G. & Challamel, M. J. Ontogenesis of nocturnal organization of sleep spindles: a longitudinal study during the first 6 months of life. *Electroenceph Clin Neurophysiol* **83**, 289-296 (1992).

110 Knickmeyer, R. C. *et al.* A structural MRI study of human brain development from birth to 2 years. *J Neurosci* **28**, 12176-12182 (2008).

111 Tau, G. Z. & Peterson, B. S. Normal development of brain circuits. *Neuropsychopharmacology* **35**, 147-168 (2010).

112 Doucette, M. R., Kurth, S., Chevalier, N., Munakata, Y. & LeBourgeois, M. K. Topography of Slow Sigma Power during Sleep is Associated with Processing Speed in Preschool Children.Brain Science. *Brain Science* **5**, 494-508 (2015).

113 Kurth, S. *et al.* Mapping of Cortical Activity in the First Two Decades of Life: A High-Density Sleep Electroencephalogram Study. *J Neurosci* **30**, 13211-13219 (2010).

114 Nagata, K., Shinomiya, S., Takahashi, K. & Masumura, T. Developmental characteristics of frontal spindle and centro-parietal spindle. *Brain and Development* **28**, 409 (1996).

115 Shinomiya, S., Nagata, K., Takahashi, K. & Masumura, T. Development of sleep spindles in young children and adolescents. *Clinical EEG and Neuroscience* **30**, 39-43 (1999).

116 De Gennaro, L. & Ferrara, M. Sleep spindles: an overview. *Sleep Med Rev* **7**, 423-440 (2003).

117 Gruber, R. *et al.* The association between sleep spindles and IQ in healthy school-age children. *In J Psychophysiol* **89**, 229-240 (2013).

118 Lopez, J., Hoffmann, R. & Armitage, R. Reduced sleep spindle activity in early-onset and elevated risk for depression. *J Am Acad Child Adolesc Psychiatry* **49**, 934-943 (2010).

119 Schabus, M. *et al.* Sleep spindle-related activity in the human EEG and its relation to general cognitive and learning abilities. *European Journal of Neuroscience* **23**, 1738-1746 (2006).

120 Chatburn, A. *et al.* Sleep Spindle Activity and Cognitive Performance in Healthy Children. *Sleep* **36**, 237-243 (2013).

121 Deary, I. J., Johnson, W. & Houlihan, L. M. Genetic foundations of human intelligence. *Hum Genet* **126**, 215-232 (2009).

122 Kurdziel, L., Duclos, K. & Spencer, R. M. Sleep spindles in midday naps enhance learning in preschool children. *PNAS* **110**, 17267-17272 (2013).

123 Casey, B. J., Galvan, A. & Hare, T. A. Changes in cerebral functional organization during cognitive development. *Curr Opin Neurobiol* **15**, 239-244 (2005).

124 Ellingson, R. J. & Peters, J. F. Development of EEG and daytime sleep patterns in trisomy-21 infants during the first year of life: Longitudinal observations. *Elec. Clin. Neurophysiol.* **50**, 457-466 (1980).

125 Feinberg, I., Braun, M. & Shulman, E. EEG sleep patterns in mental retardation. *Elec. Clin. Neurophysiol.* **27**, 128-141 (1969).

126 Contestabile, A., Behfenati, F. & Gasparini, L. Communication breaks-Down: from neurodevelopment defects to cognitive disabilities in Down syndrome. *Prog Neurobiol* **91**, 1-22 (2010).

127 Contestabile, A. *et al.* Cell cycle alteration and decreased cell proliferation in the hippocampal dentate gyrus and in the neocortical germinal matrix of fetuses with Down syndrome and in Ts65Dn mice. *Hippocampus* **17**, 665-678 (2007).

128 Guidi, S. *et al.* Neurogenesis impairment and increased cell death reduce total neuron number in the hippocampal region of fetuses with Down syndrome. *Brain Pathol* **18**, 180-197 (2008).

129 Selvitellia, M. F., Krishnamurthya, K. B., Herzog, A. G., Schomera, L. & Changa, B. S. Sleep spindle alterations in patients with malformations of cortical development. *Brain and Development* **31**, 163-168 (2009).

130 Godbout, R., Bergeron, C., Limoges, E., Stip, E. & Mottron, L. A laboratory study of sleep in Asperger's syndrome. *Neuroreport* **11**, 127-130 (2000).

131 Limoges, E., Mottron, L., Bolduc, C., Berthiaume, C. & Godbout, R. Atypical sleep architecture and the autism phenotype. *Brain* **128**, 1049-1061 (2005).

132 Augustinavicius, J. L., Zanjani, A., Zakzanis, K. K. & Shapiro, C. M. Polysomnographic features of early-onset depression: a meta-analysis. *J Affect Disord* **158**, 11-18 (2014).

133 de Maertelaer, V., Hoffman, G., Lemaire, M. & Mendlewicz, J. Sleep spindle activity changes in patients with affective disorders. *Sleep* **10**, 443-451 (1987).

134 Plante, D. T. *et al.* Topographic and sex-related differences in sleep spindles in major depressive disorder: a high-density EEG investigation. *J Affect Disord* **146**, 120-125 (2013).

135 Ferrarelli, F. *et al.* Reduced sleep spindle activity in schizophrenia patients. *American Journal of Psychiatry* **164**, 483-492 (2007).

136 Ferrarelli, F. *et al.* Thalamic dysfunction in schizophrenia suggested by whole-night deficits in slow and fast spindles. *American Journal of Psychiatry* **167**, 1339-1348 (2010).

137 Manoach, D. S. *et al.* Reduced overnight consolidation of procedural learning in chronic medicated schizophrenia is related to specific sleep stages. *Journal of Psychiatric Research* **44**, 112-120 (2010).

138 Manoach, D. S. *et al.* Sleep spindle deficits in antipsychotic-naïve early course schizophrenia and in non-psychotic first-degree relatives. *Front Hum Neurosci* **8** (2014).

139 Tesler, N. *et al.* Reduced sleep spindle density in early onset schizophrenia: a preliminary finding. *Schizophrenia Research* **166**, 355-357 (2015).

140 Buchmann, A. *et al.* Reduced mediodorsal thalamic volume and prefrontal cortical spindle activity in schizophrenia. *NeuroImage* **102**, 540-547 (2014).

141 Lewis, D. A. Cortical circuit dysfunction and cognitive deficits in schizophrenia–implications for preemptive interventions. . *Eur J Neurosci* **35**, 1871-1878 (2012).

142 Thompson, M., Weickert, C. S., Wyatt, E. & Webster, M. J. Decreased glutamic acid decarboxylase 67 mRNA expression in multiple brain areas of patients with schizophrenia and mood disorders. . *J Psychiatric Res* **43**, 970-977 (2009).

143 Ibrahim, H. M. *et al.* Ionotropic glutamate receptor binding and subunit mRNA expression in thalamic nuclei in schizophrenia. . *Am J Psychiatry* **157**, 1811-1823 (2000).

144 Smith, R. E., Haroutunian, V., Davis, K. L. & Meador-Woodruff, J. H. Expression of excitatory amino acid transporter transcripts in the thalamus of subjects with schizophrenia. . *Am J Psychiatry* **158**, 1393-1399 (2001).

145 Wamsley, E. J. *et al.* The effects of eszopiclone on sleep spindles and memory consolidation in schizophrenia: a randomized placebo-controlled trial. *Sleep* **36**, 1369-1376 (2013).

146 Foley, D. J. *et al.* Sleep complaints among elderly persons: an epidemiologic study of three communities. *Sleep* **18**, 425-432 (1995).

147 Ohayon, M. M. Epidemiology of insomnia: what we know and what we still need to learn. *Sleep Med Rev* **6**, 97-111 (2002).

148 Huang, Y. L. *et al.* Age-associated difference in circadian sleep-wake and rest-activity rhythms. *Physiol Behav* **76**, 597-603 (2002).

149 Bliwise, D. L. Sleep in normal aging and dementia. *Sleep* **16**, 40-81 (1993).

150 Van Cauter, E., Leproult, R. & Plat, L. Age-related changes in slow wave sleep and REM sleep and relationship with growth hormone and cortisol levels in healthy men. *JAMA* **284**, 861-868 (2000).

151 Crowley, K., Trinder, J., Kim, Y., Carrington, M. & Colrain, I. M. The effects of normal aging on sleep spindle and K-complex production. *Clin Neurophysiol* **113**, 1615-1622 (2002).

152 Carrier, J., Land, S., Buysse, D. J., Kupfer, D. J. & Monk, T. H. The effects of age and gender on sleep EEG power spectral density in the middle years of life (ages 20-60 years old). *Psychophysiology* **28**, 232-242 (2001).

153 Landolt, H. P., Dijk, D. J., Achermann, P. & Borbely, A. A. Effect of age on the sleep EEG: slow-wave activity and spindle frequency activity in young and middle-aged men. *Brain Res* **738**, 205-212 (1996).

154 Guazzelli, M. *et al.* Sleep spindles in normal elderly: comparison with young adult patterns and relation to nocturnal awakening, cognitive function and brain atrophy. *Elec. Clin. Neurophysiol.* **63**, 526-539 (1986).

155 Wei, H. G., Riel, E., Czeisler, C. A. & Dijk, D. J. Attenuated amplitude of circadian and sleep-dependent modulation of electroencephalographic sleep spindle characteristics in elderly human subjects. *Neurosci Lett* **260**, 29-32 (1999).

156 Nicolas, A., Petit, D., Rompre, S. & Montplaisir, J. Sleep spindle characteristics in healthy subjects of different age groups. *Clin Neurophysiol* **112**, 521-527 (2001).

157 Principe, J. C. & Smith, J. R. Sleep spindle characteristics as a function of age. *Sleep* **5**, 73-84 (1982).

158 Martin, N. *et al.* Topography of age-related changes in sleep spindles. *Neurobiol Aging* **34**, 468-476 (2013).

159 Nelson, P. T. *et al.* Alzheimer's-type neuropathology in the precuneus is not increased relative to other areas of neocortex across a range of cognitive impairment. *Neurosci Lett* **450**, 336-339 (2009).

160 Luca, G. *et al.* Age and gender variations of sleep in subjects without sleep disorders. *Ann Med* **47**, 482-491 (2015).

161 Huupponen, E. *et al.* A study on gender and age differences in sleep spindles. *Neuropsychobiology* **45**, 99-105 (2002).

162 Peters, K. R., Ray, L. B., Fogel, S., Smith, V. & Smith, C. T. Age differences in the variability and distribution of sleep spindle and rapid eye movement densities. *PLoS ONE* **9**, e91047 (2014).

163 Peters, K. R. *et al.* Neuropsychiatric symptom clusters and functional disability in cognitively-impaired-not-demented individuals. *Am J Geriatr Psychiatry* **16**, 136-144 (2007).

164 Mander, B. A. *et al.* Impaired prefrontal sleep spindle regulation of hippocampal-dependent learning in older adults. *Cereb. Cortex* **24**, 3301-3309 (2014).

165 Rauchs, G. *et al.* Is there a link between sleep changes and memory in Alzheimer's disease? *Neuroreport* **19**, 1159-1162 (2008).

166 Latreille, V. *et al.* Sleep spindles in Parkinson's disease may predict the development of dementia. *Neurobiol Aging* **36**, 1083-1090 (2015).

167 Allen, S. R., Stahelin, H. B., Seiler, W. O. & Spiegel, R. EEG and sleep in aged hospitalized patients with senile dementia: 24-h recordings. *Experientia* **39**, 249-255 (1983).

168 Prinz, P. N. *et al.* Sleep, EEG and mental function changes in senile dementia of the Alzheimer's type. *Neurobiol Aging* **3**, 361-370 (1982).

169 Yagihashi, T. *et al.* Case report: Adult phenotype of Mulvihill-Smith syndrome. *Am J Med Genet A* **149A**, 496-500 (2009).

170 Resnick, S. M., Pham, D. L., Kraut, M. A., Zonderman, A. B. & Davatzikos, C. Longitudinal magnetic resonance imaging studies of older adults: a shrinking brain. *J Neurosci* **23**, 3295-3301 (2003).

171 Thambisetty, M. *et al.* Longitudinal changes in cortical thickness associated with normal aging. *NeuroImage* **52**, 1215-1223 (2010).

172 Raz, N., Rodrigue, K. M., Kennedy, K. M. & Acker, J. D. Hormone replacement therapy and age-related brain shrinkage: regional effects. *Neuroreport* **15**, 2531-2541 (2004).

173 Raz, N. *et al.* Differential age-related changes in the regional metencephalic volumes in humans: a 5-year follow-up. *Neurosci Lett* **349**, 163-166 (2003).

174 Head, D. *et al.* Differential vulnerability of anterior white matter in nondemented aging with minimal acceleration in dementia of the Alzheimer type: evidence from diffusion tensor imaging. *Cereb. Cortex* **14**, 410-423 (2004).

175 Bartzokis, G. *et al.* White matter structural integrity in healthy aging adults and patients with Alzheimer disease: a magnetic resonance imaging study. *Arch Neurol* **60**, 393-398 (2003).

176 Fama, R. & Sullivan, E. V. Thalamic structures and associated cognitive functions: Relations with age and aging. *Neurosci Biobehav Rev* **54**, 29-37 (2015).

177 Rice, R. A., Berchtold, N. C., Cotman, C. W. & Green, K. N. Age-related downregulation of the CaV3.1 T-type calcium channel as a mediator of amyloid beta production. *Neurobiol Aging* **35**, 1002-1011 (2014).

178 Dijk, D. J. *et al.* Melatonin effect on daytime sleep in men: suppression of EEG low frequency activity and enhancement of spindle frequency activity. *Neurosci Lett* **201**, 13-16 (1995).

179 Cajochen, C., Munch, M., Knoblauch, V., Blatter, K. & Wirz-Justice, A. Age-related changes in the circadian and homeostatic regulation of human sleep. *Chronobiol Int* **23**, 461-474 (2006).

180 Knoblauch, V., Martens, W., Wirz-Justice, A., Krauchi, K. & Cajochen, C. Regional differences in the circadian modulation of human sleep spindle characteristics. *J Neurosci* **18**, 155-163 (2003).

CHAPTER III

Sleep promotes, and sleep loss inhibits, selective changes in firing rate, response properties, and functional connectivity of primary visual cortex neurons.

*This chapter includes the publication: **Clawson, B. C**., Durkin, J., Suresh, A. K., Pickup, E. J., Broussard, C., Aton, S. J. (2018). Sleep Promotes, and Sleep Loss Inhibits, Selective Changes in Firing Rate, Response Properties and Functional Connectivity of Primary Visual Cortex Neurons. Frontiers in Systems Neuroscience, 12: 40.*

3.1 Abstract

Recent studies suggest that sleep differentially alters the activity of cortical neurons based on firing rates during preceding wake - increasing the firing rates of sparsely firing neurons and decreasing those of faster firing neurons. Because sparsely firing cortical neurons may play a specialized role in sensory processing, sleep could facilitate sensory function via selective actions on sparsely firing neurons. To test this hypothesis, we analyzed longitudinal electrophysiological recordings of primary visual cortex (V1) neurons across a novel visual experience which induces V1 plasticity (or a control experience which does not), and a period of subsequent *ad lib* sleep or partial sleep deprivation. We find that across a day of *ad lib* sleep, spontaneous and visually-evoked firing rates are selectively augmented in sparsely firing V1 neurons. These sparsely firing neurons are more highly visually responsive, and show greater orientation selectivity than their high firing rate neighbors. They also tend to be “soloists” instead of “choristers” - showing relatively weak coupling of firing to V1 population activity. These population-specific changes in firing rate are blocked by sleep disruption either early or late in the day, and appear to be brought about by increases in neuronal firing rates across

bouts of REM sleep. Following a patterned visual experience that induces orientation-selective response potentiation (OSRP) in V1, sparsely firing and weakly population-coupled neurons show the highest level of sleep-dependent response plasticity. Across a day of *ad lib* sleep, population coupling strength increases selectively for sparsely firing neurons - this effect is also disrupted by sleep deprivation. Together, these data suggest that sleep may optimize sensory function by augmenting the functional connectivity and firing rate of highly responsive and stimulus-selective cortical neurons, while simultaneously reducing noise in the network by decreasing the activity of less selective, faster-firing neurons.

3.2 Introduction

Sleep is hypothesized to play a critical role in learning and memory, by facilitating long-lasting plastic changes in the strength of synapses and across networks.[4,5,9,15,29,42] Among the mechanisms by which sleep may promote information storage in the brain, general synaptic downscaling has been proposed as a possible mediator. In theory, widespread synaptic downscaling is proposed as a homeostatic response by which network excitability could be constrained and signal-to-noise ratios for neuronal firing could be improved following widespread synaptic potentiation associated with waking experience.[36,37] This idea is supported by biochemical and transcriptomic studies in rodents, demonstrating that cellular markers of neuronal activity and synaptic strengthening are increased in the forebrain after a period of wake, and decreased after a period of sleep.[10,24,39] However, recent studies suggest that these effects may vary between brain areas[14,35] and as a function of experience.[4,30,31,34,38] Thus it is unclear whether downscaling is a phenomenon associated with experience-dependent plasticity

in neuronal circuits, such as are initiated by learning. In addition, it is unclear whether downscaling occurs during rapid eye movement (REM) or non-REM (NREM) sleep. For example, studies of cortical neurons have attributed decreases in firing to slow wave activity in NREM,[40] while studies of hippocampal neurons have shown firing increases across bouts of NREM, and rapid decreases across REM sleep.[20] Moreover, it is unclear whether, or how, sleep-dependent downscaling would affect the response properties and information-processing capabilities of individual neurons. Recent data suggest that sleep-associated decreases in synaptic strength and neuronal excitability are heterogeneous, even within a given brain region. For example, only a subset of synaptic structures appear to be reduced in size in the cortex across sleep,[13] and only a subset of cortical neurons show significant decreases in firing rate after sleep.[40] The idea that these changes are not uniform, but may preferentially affect a specific subpopulation of network neurons, is supported by recent studies of firing rate changes in rodent frontal cortex and hippocampus across bouts of sleep and wake behavior. For example, Watson et al found that while most rat cortical neurons show firing decreases across bouts of REM sleep, only those neurons that have the fastest baseline firing rates show firing decreases in NREM sleep. Overall changes in firing across sleep periods (containing REM, NREM, and microarousals) are opposite between higher firing neurons (which show net firing decreases) and sparsely firing neurons (which show net firing increases). Thus instead of uniformly decreasing firing rates, sleep seems to narrow the distribution of firing rates among cortical neurons.[41] In contrast to what is seen in frontal cortex, firing rates among both interneurons and principal neurons in hippocampal area CA1 generally increase across bouts of NREM, and dramatically decrease across bouts of REM.[20] Available data

suggests that as is true for cortical neurons, these changes in firing across sleep differentially affect higher-firing and lower-firing neurons.[25]

Recent studies have also characterized neurons in sensory cortical areas based on how coupled their firing is to that of the population.[7,28] So-called “choristers” fire in a manner which is tightly linked to spontaneous population-level activity, while “soloists” tend to fire independently from the population. In sensory areas, fast-spiking interneurons, and bursting pyramidal neurons, tend to fire as choristers, while non-bursting pyramidal neurons fire as soloists.[28] Bachatene et al. also demonstrated that population-coupling strength of neurons in sensory cortex varies as a function of firing rate.[7] Thus, the neurons on the lower end of the firing rate distribution appear to be comprised of soloists, while high-firing neurons are likely choristers.[7] Critically, the relationship between neurons’ population coupling strength, their sensory response characteristics, and their information-carrying capacity remains a matter of speculation.[7,28] While soloists may be able to respond very selectively and precisely to sensory stimuli, choristers’ firing appears to carry additional information regarding an animal’s behavioral state and other non-sensory factors.[28] Thus two important unanswered questions are how sleep and wake states affect soloist and chorister populations, and how this might be relate to sleep-dependent plasticity in neural circuits.

Recent work from our lab has shown that mean firing rates are differentially affected by sleep in mouse primary visual cortex (V1), depending on prior visual experience. For example, we have shown that when mice are presented with a single oriented grating over a prolonged period (several minutes to an hour), neurons in V1, show an enhanced firing rate response to grating stimuli of the same orientation, but only

after a period of sleep.[6,16,17] After a visual experience that induces OSRP, firing rates for V1 neurons increase across bouts of sleep, particularly across REM sleep.[17] Thus state-dependent changes in V1 neurons' firing rates are functionally linked to sensory plasticity and may vary as a function of prior sensory experience.

Here we aim to address how brain state-dependent changes in different neuronal populations may affect the basic function and information-processing capabilities of sensory cortex.[2] We first assess how both spontaneous and visually-evoked firing rates of sparse- or fast-firing V1 neurons are affected by visual experience, across a period of subsequent *ad lib* sleep, or across a similar period with partial sleep deprivation. We then assess how these parameters are affected in neurons which fire in a manner that is either weakly or strongly coupled to V1 population activity. We also determine which neurons' orientation preferences are most altered in the context of OSRP.

3.3 Materials and Methods

In vivo neurophysiology

All mouse procedures were approved by the University of Michigan Institutional Animal Care and Use Committee. For chronic recordings, male and female C57BL/6J mice (Jackson) aged 1-3 months (an age range where OSRP is induced robustly by visual experience)[6,16,19] were implanted with custom-built drivable headstages (EIB-36 Neuralynx) under isoflurane anesthesia, using previously described techniques.[6] For each mouse, two 200 µm-diameter bundles of seven stereotrodes each (25 µm nichrome wire, California Fine Wire; Grover Beach, CA) were placed in right hemisphere V1 (0.5-1 mm apart), reference and ground electrodes were placed in left hemisphere V1 and

cerebellum, respectively, and three electromyography (EMG) electrodes were placed in nuchal muscle.

Following surgical procedures, mice were individually housed in standard caging with beneficial environmental enrichment (nesting material, toys, and treats) throughout all subsequent experiments. With the exception of OSRP or blank screen experimental days, during which room lights were kept off, lights were maintained on a 12-h:12-h light:dark cycle (lights on at 8 AM, lights off at 8 PM). Food and water were provided *ad lib* throughout all procedures. After 1-2 weeks of post-operative recovery, mice were prepared for chronic stereotrode recording in their home cage, which was placed inside a sound-attenuated recording chamber (Med Associates). Mice were tethered using a lightweight cable for neural recording, and were habituated to daily handling, restraint, and head fixation over a period of 5 days. During this time, electrodes were gradually lowered into V1 until stable neuronal recordings were obtained. Recording stability was defined by the continuous presence of spike waveforms on individual electrodes for at least 24 h prior to the onset of baseline recording. Signals from each electrode were split and differentially filtered to obtain spike data (200 Hz-8 kHz) and local field potential (LFP)/EMG activity (0.5-200 Hz). Data were amplified at 20 ×, digitized, further digitally amplified at 20-100 ×, and recorded using Plexon Omniplex software and hardware (Plexon Inc.; Dallas, TX). For all chronic recordings, single-unit data was referenced locally to a recording channel without single-unit activity, to eliminate low-frequency noise.

Visual stimuli, OSRP induction, and assessment of visual response properties.

A continuous 24-h baseline recording was carried out for each mouse, starting at lights-on (8 AM; CT0 – Circadian Time 0). The following day at CT0, mice were head-

fixed. To assess baseline (AM) visual response properties in V1 neurons, phase-reversing oriented gratings (spatial frequency 0.05 cycles/degree, 100% contrast, reversal frequency 1.0 Hz) of 4 orientations (0, 45, 90, and 135 degrees from horizontal) and a blank (dark) screen (to assess spontaneous activity) were presented to the left (contralateral) visual field. Each of these stimuli was presented 8 times (10 s for each presentation) in a random, interleaved fashion. Neuronal firing rate responses were quantified and averaged for each stimulus orientation (and blank [dark] screen) across total presentation time (i.e., 10 s × 8 repetitions). Immediately following this baseline (8 AM; CT 0) test, either a single grating stimulus (of a randomly-selected orientation) or a blank [dark] screen was continuously presented over a 30-min period to induce OSRP. Mice were then returned to their home cage and recordings continued until CT12 in complete darkness (with far-infrared illumination only, to prevent additional visual experience), at which time mice were again head-fixed for a second (PM) test of visual response properties. Between 30-min grating (or blank screen) presentation and PM testing, mice were either allowed to sleep *ad lib* (Vis Stim + Sleep: n = 14 mice, Blank Screen + Sleep: n = 7 mice), or were kept awake over the first 6 h (Vis Stim + early sleep deprivation [ESD]: n = 11 mice) or last 6 h (Vis Stim + late sleep deprivation [LSD]: n = 13 mice), using gentle handling procedures.[6] Briefly, when mice were observed (under far-infrared illumination) taking stereotyped sleep postures and LFP data indicated transitioning from wake to NREM sleep, cages were tapped gently to awaken the mice. Later in the procedure (typically within the last 1-2 hours), disturbance of the nest or lightly brushing the mouse with a cotton-tipped applicator was used to prevent sleep.

For each stably-recorded neuron (i.e., those with consistent spike waveforms on the two stereotrode channels across 24-h baseline recording, and across the 12-h experiment; see below for details of single-unit identification), a number of visual response properties were assessed during CT0 (i.e., the time of expected lights-on; “AM”) and CT12 (i.e., the time of expected lights-off; “PM”) tests (at 8 AM and 8 PM, respectively), using previously-described metrics.[3,4,6] Mean firing rates (in Hz) were averaged across all repetitions of the same visual stimulus (or blank [i.e., dark] screen). Mean blank screen firing (in Hz) was used as a metric of each neuron’s spontaneous activity. Mean firing at each neuron’s preferred stimulus orientation (i.e., that which evoked maximal firing rate response) was used as a metric of maximal visually-evoked firing rate. An orientation selectivity index (OSI45; used to indicate the strength of orientation tuning, regardless of orientation preference) was calculated for each neuron, as 1 - [(average firing rate at ± 45° from preferred orientation)/(average firing rate at the preferred stimulus orientation)]. Thus OSI45 values for individual neurons range from 0 (minimal selectivity for the preferred stimulus orientation) to 1 (maximal selectivity for the preferred stimulus orientation). Neuronal visual responsiveness (to any visual stimulus) was assessed as a responsiveness index (RI), calculated as 1 - [(average firing rate at blank screen presentation)/(average firing rate at the preferred stimulus orientation)]. RI values for individual V1 neurons typically range from 0 (not visually responsive) to 1 (maximally responsive), although negative values are possible for non-responsive neurons). Changes in these values between AM and PM tests (i.e., during the inactive phase of the rest-activity cycle; from CT 0 to CT12) were assessed in non-sleep deprived and sleep deprived mice. For mice presented with a visual stimulus to induce OSRP,

initial preference for the presented stimulus orientation was quantified as the ratio of mean firing rate responses for the presented orientation (X°) to that of the orthogonal to presented stimulus (X+90°) as described previously. Changes in this measure (and in other visual response properties) were quantified by subtracting CT0 baseline (AM) (X°/X+90°) ratio from CT12 (PM) (X°/X+90°) ratio; this difference was then expressed as a percent change from the baseline value.

Histology

At the conclusion of each recording, mice were deeply anesthetized with barbiturate injection, and an electrolytic lesion was made at each electrode site (2 mA, 3 s per electrode). Mice were then perfused with formalin and euthanized. Brains were post-fixed, cryosectioned at 50 µm, and stained with DAPI (Fluoromount-G; Southern Biotech) to verify electrode placement in V1.

Single unit identification and data analysis

Single-neuron data were discriminated offline using standard principle component-based procedures as described previously.[3,6,16,17,26,27] To ensure stable tracking of single-neuron activity across time, all data analyses were carried out on spike data that was continuously acquired throughout the experiment. Example data are shown for pair of neurons stably recorded on the same V1 stereotrode, from a freely-behaving mouse, in **Fig. 3.1**. As shown in **Fig. 3.1**, spikes from individual neurons were discriminated based on consistent spike waveform shape and width, relative spike amplitude on the two stereotrode wires, and relative positioning of waveform clusters in three-dimensional principal component space. Single-neuron isolation was verified quantitatively using standard techniques.[21] Clusters with interspike interval (ISI)-based absolute refractory

period violations were eliminated from analysis. Waveform cluster separation (for channels with more than one discriminated single unit) was validated using MANOVA on the first 3 principal components ($p < 0.05$ for all sorted clusters), and the Davies-Bouldin (DB) validity index,[33] as described previously.[16,27]

Only neurons that 1) met the criteria described above and 2) were reliably discriminated and continuously recorded throughout each experiment (*i.e.*, across both 24-h baseline and 12-h experimental condition) were included in firing rate analyses. For analysis of firing rate changes across the population of recorded V1 neurons (e.g., in **Figs. 3.3-3.8**), spontaneous and maximal visually-evoked firing rates (calculated as described above) were $\log_{(10)}$-transformed. For ANOVA analyses of visual response properties and firing rate changes, all recorded neurons in a given experimental group were grouped into sextiles, based on either their spontaneous firing rate, maximal visually-evoked firing rate, or population coupling strength (see below) at baseline. Sextiling of data allowed statistical comparisons between changes seen in the highest and lowest firing neurons, and direct comparisons of our results with those of other labs.[41] Changes in firing rate across the day were expressed as a fold change.

Intracortical LFP and nuchal EMG signals were used to categorize recorded data into REM, NREM, and wake states over 10-s intervals of recording using custom software. Firing rates were calculated separately within REM, NREM, and wake using NeuroExplorer software (Plexon). To assess neuronal firing rate changes across individual bouts of these states, we used a calculation similar to that described previously.[17] Briefly, firing rates across time were $\log_{(10)}$-transformed, and mean firing rates across the first and last 30 s of each state bout were calculated. Changes in firing

rate were calculated using custom software, by subtracting the mean firing rate in the first 30 from the mean firing rate in the last 30 s. Bouts with less than 60 s duration, and neurons with a firing rate of 0 Hz in either the first or last 30 s of a particular bout, were excluded from the analysis. Mean rate changes were averaged for all the bouts of a given state (i.e., REM, NREM, or wake) occurring across the entire *ad lib* sleep portion of the experiment for each animal. Thus for Vis Stim + Sleep and Blank Screen + Sleep mice, data were averaged over the CT0 to CT12 *ad lib* sleep recording period; for Vis Stim + ESD mice, data were averaged over the last 6 h of recording; for Vis Stim + LSD mice, data were averaged over the first 6 h of recording.

To assess population coupling, neurons were cross-correlated with the population rate activity during the AM test using a cross-correlogram (CCG) algorithm. Population rate time series were first constructed from the firing of all single units and multi-unit activity across the AM test, with the neuron of interest's spike times removed; this was done separately for each neuron. Each neuron's spike train was then cross-correlated with the population rate in 1 ms bins, with counts per bin normalized to the number of reference events as probabilities to account for differences in firing rate. A 95% confidence interval was applied to each CCG. CCGs were corrected using a shift-predictor procedure during the AM and PM tests to correct for coincident firing due to common visually-driven input (similar to methods described in (Bachatene et al., 2015)) and CCGs were smoothed with a Gaussian filter with a 3 bin width. Peaks in the corrected CCGs were used as measures of population coupling; these peaks were compared between AM and PM tests to assess changes in population coupling across the day.

Results

3.4 Visual response plasticity among V1 neurons relies on both visual experience and sleep.

To characterize effects of visual experience and brain states on visual response properties and firing rates, we first quantified V1 neuronal firing in recordings from C57BL/6J mice. An example showing the stability of our V1 neuronal recordings (from a representative mouse) is shown in **Fig. 3.1**. Mice underwent continuous recording across a 24-h baseline period (to verify stability of neuronal recordings), a baseline (AM) visual response assessment (at lights-on; CT0), a 30-min presentation of a single oriented flickering grating (or, as a negative control, a blank screen), and a 12-h post-stimulus period in complete darkness (to prevent additional visual experience). During this post-stimulus period, mice were either allowed *ad lib* sleep, or were sleep deprived by gentle handling over the first or last 6 h (early sleep deprivation [ESD] or late sleep deprivation [LSD]). At CT12, response properties were reassessed to quantify OSRP and other changes in visual responses (**Fig. 3.2A**). As we have shown previously (Aton et al., 2014; Durkin et al., 2017; Durkin and Aton, 2016), oriented grating presentation resulted in an increase among V1 neurons' firing rate responses to the presented stimulus orientation. Consistent with our prior findings, both ESD and LSD disrupted OSRP. This was true for

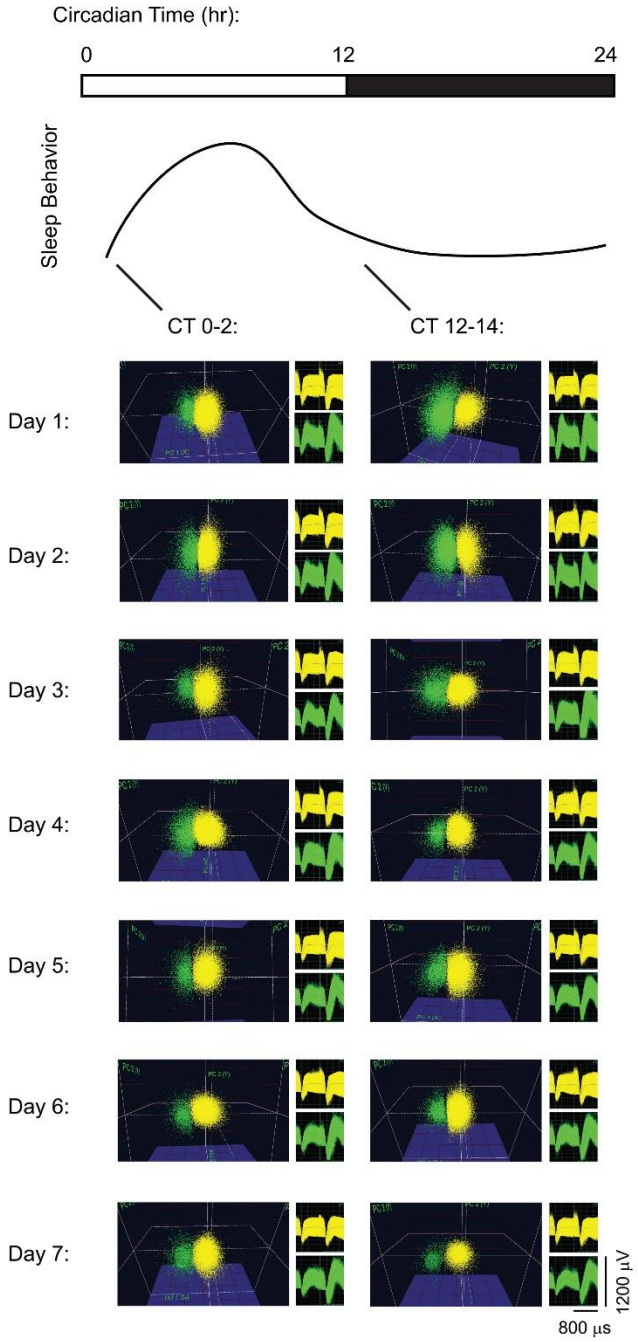

Figure 3.1. Long-term recordings of V1 neurons. Spike data are shown from two representative neurons on a V1 stereotrode across 7 days of continuous recording. For display purposes (i.e., to show stability of spike waveforms over time) neuronal spike data are shown over 2-h intervals of recording time at lights-on (CT0-2) and at lights-off (CT12-14) each day, clustered in three-dimensional principal component (PCA) space. Waveforms for the spikes in the two clusters are shown to the right of PCA plots.

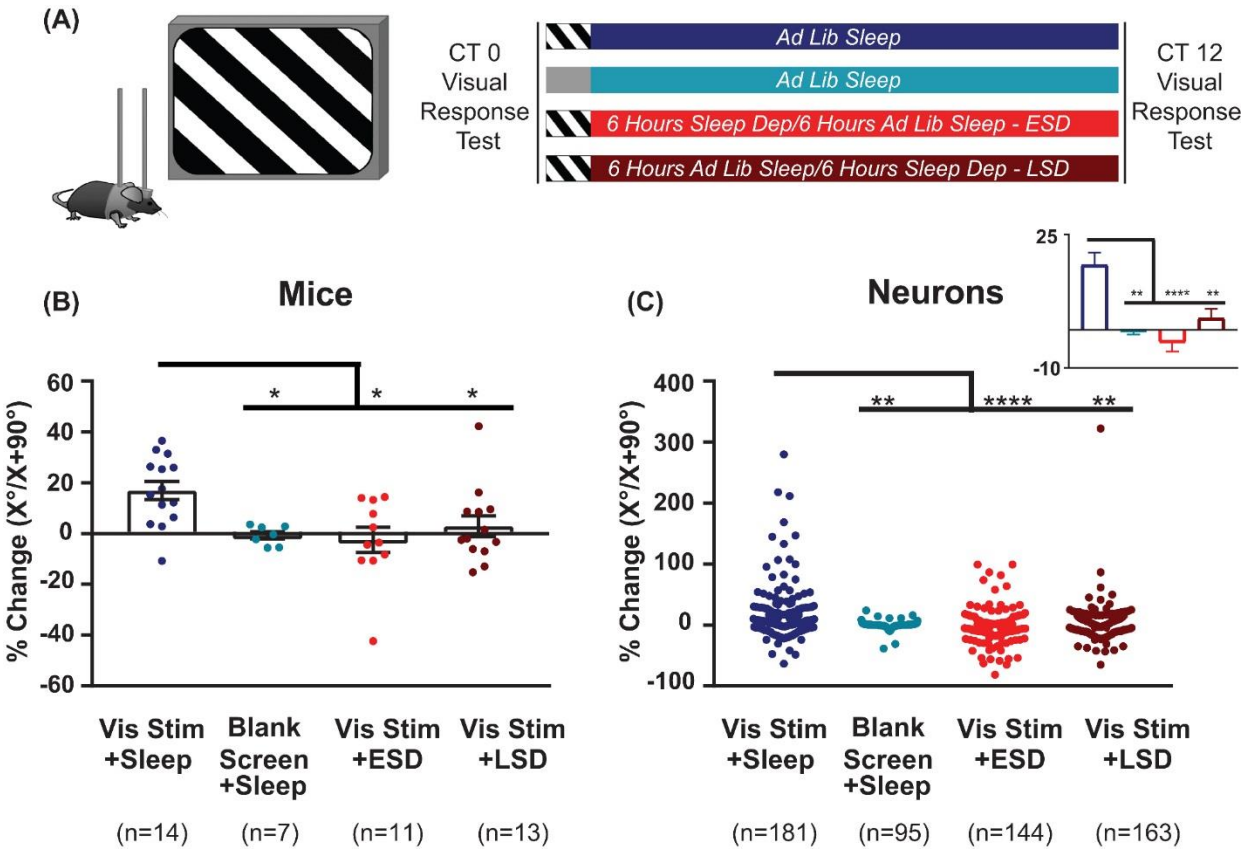

Figure 3.2. OSRP is induced in V1 by visual experience and dependent on subsequent sleep. (A) Experimental design. Mice were implanted with stereotrodes to record V1 neurons' firing across baseline (AM) visual response testing (at lights-on; CT0), 30-minute oriented grating stimulus presentation (to induce OSRP) or blank screen presentation, 12 h of subsequent ad lib sleep, early sleep deprivation (ESD) or late sleep deprivation (LSD), and a final (PM) visual response test at CT12. Mice were kept in complete darkness (under far-infrared illumination) across CT0-12, to avoid additional visual experience after stimulus presentation. **(B)** OSRP data, showing per-mouse average % changes in neurons' responses to the presented visual stimulus orientation (X°) vs. the orthogonal orientation (X + 90°) ($p = 0.007$, Kruskal-Wallis one-way ANOVA on ranks). Bar graphs show mean ±SEM. Numbers of mice are indicated for each group. **(C)** Neuron by neuron data, as in B ($p < 0.0001$, Kruskal-Wallis one-way ANOVA on ranks). For all panels, * indicates $p < 0.05$, ** indicates $p < 0.01$, *** indicates $p < 0.001$, and **** indicates $p < 0.0001$, Dunn's post hoc test.

both the average OSRP of each mouse (i.e., measured across all neurons recorded from each mouse; **Fig. 3.2B**) and for all neurons recorded in a given condition (**Fig. 3.2C**). As we have shown previously, there were no significant differences between OSRP measurements for male vs. female mice,[16] different neuronal subclasses (i.e., principal neurons vs. fast-spiking interneurons),[6] or differential timing of sleep deprivation.[6]

3.5 Spontaneous and visually-evoked firing among V1 neurons approximates a lognormal distribution

Watson et al. recently demonstrated that mean firing rates of frontal cortical neurons show a roughly lognormal distribution.[41] For our V1 recordings, we calculated the baseline (AM) spontaneous firing rate during blank screen presentation. We found that, as is true in frontal cortex, the distribution of spontaneous firing rates shows a clearly non-normal distribution ($p < 0.0001$ for all experimental groups, D'Agostino-Pearson normality test – **Fig. 3.3A**). As shown in **Fig. 3.3B**, when neuronal firing rates are $\log_{(10)}$-transformed, although most groups' distributions remain statistically non-normal, each is a closer approximation of normality (Vis Stim + Sleep: $p = 0.002$, Blank Screen + Sleep: $p = 0.004$, Vis Stim + ESD: $p = 0.15$, Vis Stim + LSD: $p = 0.017$, D'Agostino-Pearson normality test). A similar pattern was seen for distributions of maximal visually-evoked firing rates (i.e., for responses to each neuron's preferred stimulus orientation; **Fig. 3.3C-D**). Thus spontaneous and visually-evoked firing rate data were $\log_{(10)}$-transformed for all subsequent analyses.

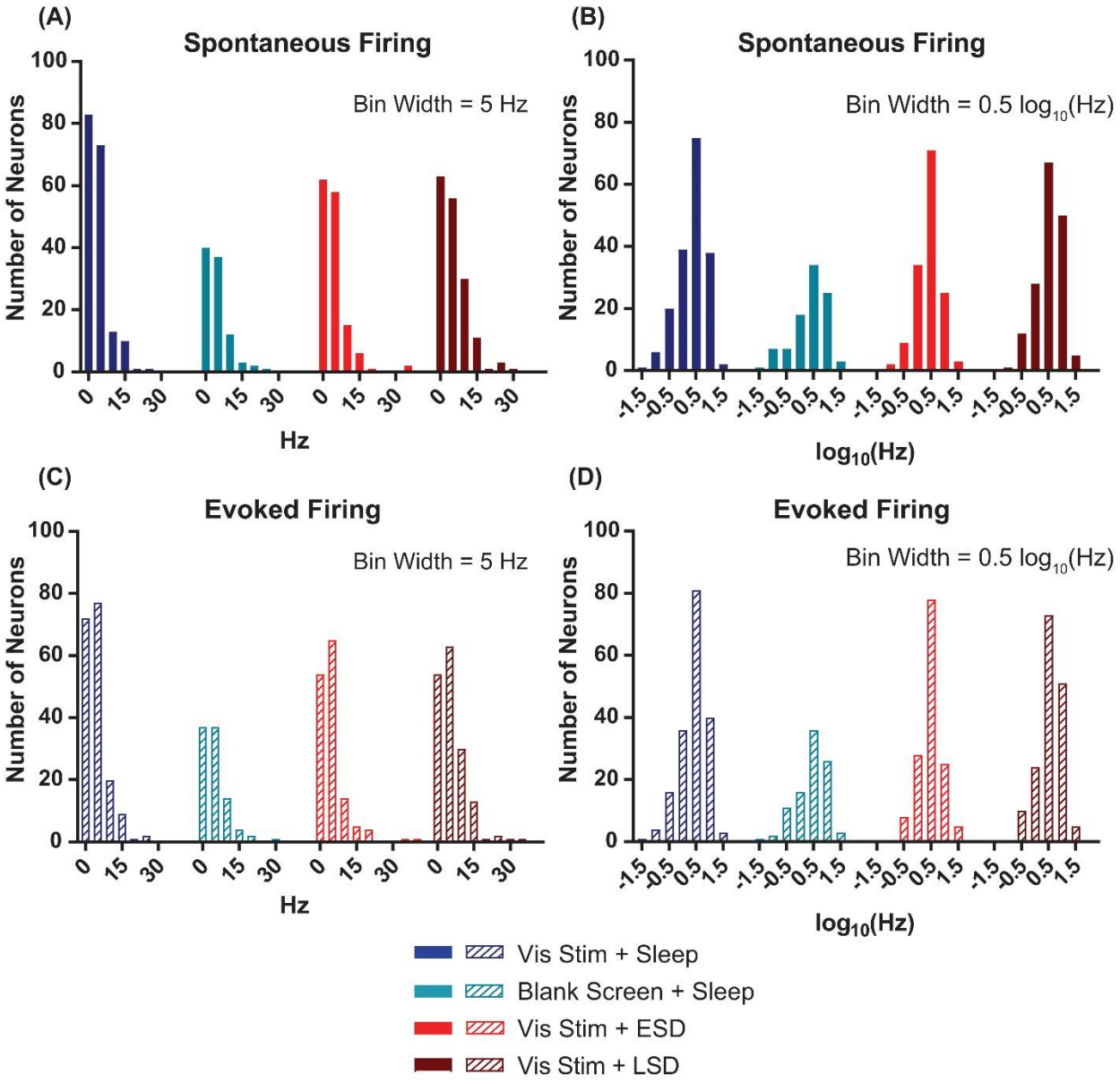

Figure 3.3. V1 neurons' spontaneous and evoked firing rates follow a log-normal distribution. (A) Distributions of baseline (AM) spontaneous firing rates of the neurons recorded from each of the treatment groups were non-normal ($p < 0.0001$, D'Agostino-Pearson normality test). **(B)** $\log_{(10)}$-transformed spontaneous firing rates' distributions approximated normality ($p = 0.002$, 0.004, 0.15, and 0.02, respectively, for Vis Stim + Sleep, Blank Screen + Sleep, Vis Stim + ESD, and Vis Stim + LSD, D'Agostino-Pearson normality test). **(C)** Distributions of baseline (AM) maximal evoked firing rates (i.e., for each neuron's preferred-orientation stimulus) of the neurons recorded from each of the treatment groups were non-normal ($p < 0.0001$, D'Agostino-Pearson normality test). **(D)** $\log_{(10)}$-transformed evoked firing rate data approximated normality ($p = 0.001$, 0.02, 0.55, and 0.05, respectively, for Vis Stim + Sleep, Blank Screen + Sleep, Vis Stim + ESD, and Vis Stim + LSD, D'Agostino-Pearson normality test).

3.6 Sleep promotes, and sleep deprivation impairs, re-distributions of firing rates among V1 neurons

We next assessed how sleep changes firing rates across the V1 neuronal population. As shown in **Fig. 3.4**, neurons recorded in both *ad lib* sleep conditions (following either visual stimulus or blank screen presentation) showed a re-distribution of both spontaneous (**Fig. 3.4A**) and maximal visually-evoked (**Fig. 3.4B**) firing rates across the day. This re-distribution was systematic, in that (as is true for firing changes across sleep in frontal cortex)[41], the lowest firing neurons showed increases in firing rate, and the highest firing neurons showed decreases in firing rate. This is illustrated by taking the regression of ($\log_{(10)}$-transformed) baseline (AM) spontaneous firing compared with the fold change in firing across the day. In the absence of systematic firing changes across the baseline V1 firing rate distribution, one would expect the slope of this regression to be zero. We find that firing rate changes among neurons in both *ad lib* sleep conditions (i.e., regardless of the type of visual experience) show negative relationships to baseline spontaneous firing, which are significantly different from zero (Vis Stim + Sleep: $p = 0.003$, Blank Screen + Sleep: $p < 0.001$ Spearman rank order, F-test $p < 0.001$). In contrast to what is seen in V1 of non-sleep deprived mice, V1 neurons recorded across both early and late sleep deprivation (ESD and LSD) conditions showed no systematic firing rate changes (for either spontaneous or visually-evoked firing rates). This is shown in **Fig. 3.4A-B**, where for ESD and LSD, the regressions of neurons' firing rate changes vs. their baseline firing rates do not differ from zero (*N.S.*, F-test).

Recent work[41] assessed sleep-dependent firing rate changes among neurons that had been grouped into sextiles based on their mean firing rates. We carried out a similar analysis on V1 neurons' firing rate changes. As shown in **Fig. 3.4C-J,** in mice from both

sleeping conditions, across-the-day firing rate changes varied in V1 depending on baseline firing rate sextile. For both spontaneous (**Fig. 3.4C-D**) and maximal visually-evoked (**Fig. 3.4G-H**) firing, the lowest-firing sextile of V1 neurons from the two sleeping conditions (regardless of visual experience) showed firing rate increases relative to the highest-firing sextile, where neurons tended to have firing rate reductions across the day. This effect was not present in either of the two sleep deprived groups (ESD and LSD), where both spontaneous (**Fig. 3.4E-F**) and visually-evoked (**Fig. 3.4I-J**) firing rate changes across the day did not vary as a function of baseline firing rate. Together, these analyses suggest that firing rates in V1 neurons are altered across a day of *ad lib* sleep, as a function of their baseline firing rate, and that sleep deprivation (at any time of day) disrupts this process.

3.7 V1 neurons' visual response properties vary as a function of baseline firing rate

Our analyses of firing rates suggest that specific subpopulations of V1 neurons (those with the lowest and highest baseline firing rates) undergo the largest sleep-dependent alterations in firing (increases and decreases in firing rate respectively). One question, in light of the well-described effects of sleep on visual response plasticity,[3,4,6,16,17,18] is how visual response properties vary between sparsely firing and higher firing neurons. We assessed how visual responses varied at baseline (i.e., during the AM visual response test at CT0) as a function of firing rate. As shown in **Fig. 3.5** (where baseline [AM] data from the four experimental groups are aggregated), we found that both visual responsiveness (**Fig. 3.5A**) and orientation selectivity (**Fig. 3.5B**) are

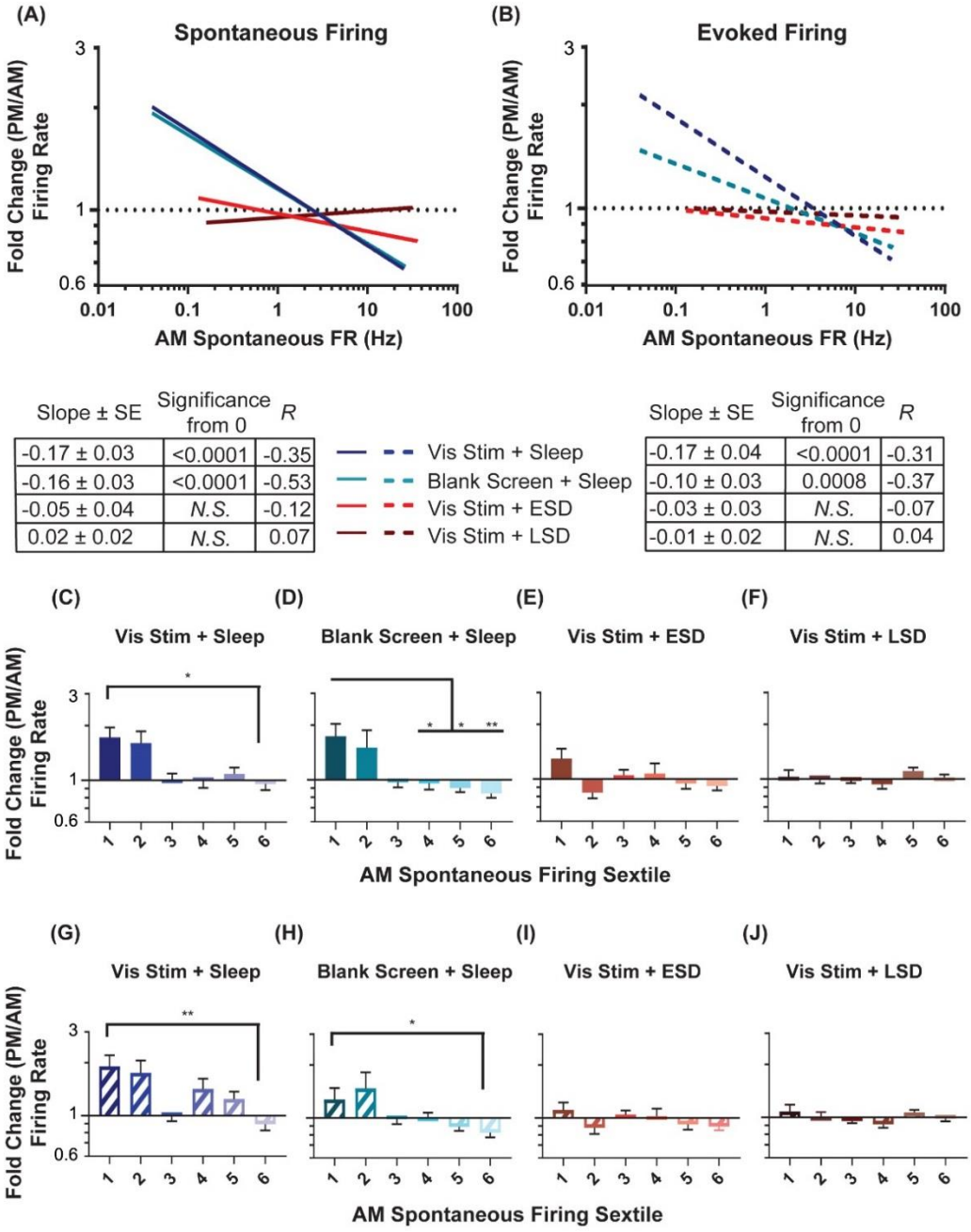

Figure 3.4. Sleep deprivation impairs neuronal firing rate homeostasis. (A-B). Linear fits of data for the change in spontaneous firing rate (A) and maximal visually-evoked firing rate (i.e., at each neuron's preferred stimulus orientation; B) across the day (expressed as a fold change and plotted on a $\log_{(10)}$ scale) vs the AM spontaneous firing rate of the cell (plotted on a $\log_{(10)}$ scale). In both groups with ad lib sleep, sparsely-firing neurons' firing rates increased (i.e., showed a fold change > 1) while highly active neurons' firing decreased (i.e., showed a fold change < 1). In (A) the lines for the visual stimulus and blank screen regressions closely overlap. The table below shows, for each experimental group, the regression slope and SE, Spearman R-value, and Bonferroni-corrected F test p-value. **(C-F)** Sextiles of the change in spontaneous firing rate, based on AM spontaneous firing rate, which is shown in (A) (p = 0.0015 for panel D, respectively, all others N.S., Kruskal-Wallis one-way ANOVA on ranks). **(G-J)** Sextiles of the change in evoked firing rate, based on AM spontaneous firing rate, which is shown in (B) (p = 0.0356, 0.0087 for panels G-H respectively, all others N.S., Kruskal-Wallis one-way ANOVA on ranks). Error bars indicate mean ± SEM for log changes in firing rate; * indicates p < 0.05, ** indicates p < 0.01, *** indicates p < 0.001, and **** indicates p < 0.0001, Dunn's post hoc test.

highest for sparsely firing neurons, and show a significant negative relationship with spontaneous firing rate. This relationship was statistically significant ($p < 0.0001$, Spearman rank order) and regressions were significantly different from 0 ($p < 0.0001$, F-test) across all four experimental groups (when examined separately). A similar relationship between spontaneous firing rate and visual response properties was seen during the CT12 (PM) test ($p < 0.0001$, Spearman rank order; $p < 0.0001$ for slope significance from 0, F Test). **Fig. 3.5C** and **D**, show that these properties vary significantly by firing rate sextile. Together, this suggests that those V1 neurons that show sleep-associated increases in firing (*i.e*., the lowest-firing neurons) are highly visually responsive and sharply orientation-tuned, and thus encode highly specific visual information. Conversely, V1 neurons that show sleep-associated firing decreases (*i.e.*, the highest-firing neurons) are less visually responsive and less orientation selective.

3.8 V1 neurons' visual response properties vary with population-coupling strength

Recent studies have categorized populations of neurons in sensory cortex, not based on firing rate, but rather on how strongly coupled their firing is to population activity.[7,28] Okun et al. and Bachetene et al. classified cortical neurons into 'choristers' (i.e., strongly coupled) and 'soloists' (i.e., weakly coupled) based on how correlated their firing was with population activity during both visual stimulation and spontaneous activity.[7,28] We similarly calculated coupling values for each neuron as the peak of the cross-correlogram (CCG) between each spike train and the population rate summed from all other neurons recorded simultaneously (**Fig. 3.6A-B**). Similar to results seen by Bachetene et al., there was a significant relationship between spontaneous firing rate and population coupling (**Fig. 3.6C**), where highly-coupled neurons ("choristers") exhibited

higher spontaneous firing rates ($p < 0.0001$, Spearman rank order).[7] We next examined how baseline visual response properties varied as a function of how strongly coupled neuronal firing is to V1 population activity. We found that across all groups, coupling strength showed a significant negative relationship to both visual responsiveness and orientation selectivity at baseline (**Fig. 3.6D-E**). These findings are consistent with previous literature demonstrating that weakly coupled neurons tend to encode more specific visual information, while strongly coupled neurons do not.[7,28] However, we also found that this relationship was likely mediated by differences in baseline spontaneous firing rates among neurons (p = 1e-8 and p = 3e-5, respectively, Sobel tests for mediation of the relationships between population coupling and visual responsiveness and between population coupling and orientation selectivity).

3.9 OSRP varies across the V1 population, as a function of both baseline firing rate and population coupling

To characterize how experience- and sleep-dependent plasticity varies across the population of V1 neurons, we next characterized changes in orientation preference across the day based on neurons' initial firing rate and population coupling. As shown in **Fig. 3.7**, we found that among neurons recorded from non-sleep deprived mice, OSRP was greatest among neurons with the lowest baseline firing rates. The magnitude of OSRP was negatively correlated with baseline firing rate in mice allowed *ad lib* post-stimulus sleep (Vis Stim + Sleep; p = 0.0375, Spearman rank order), but critically, showed no relationship to baseline firing rate in Blank Screen + Sleep, Vis Stim + ESD, or Vis Stim

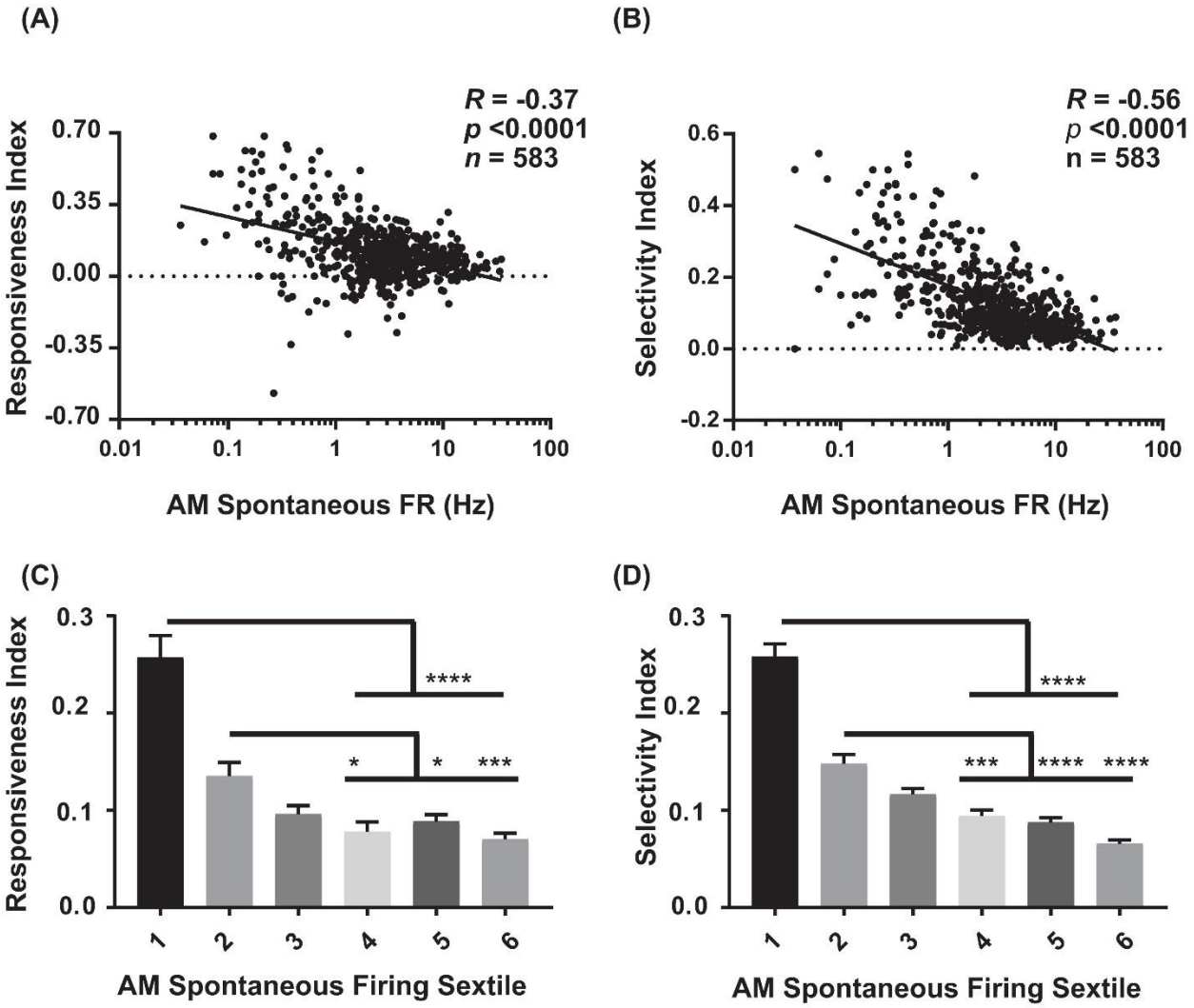

Figure 3.5. Visual response properties vary across the V1 population as a function of firing rate. (A) For baseline (AM) data aggregated across the four experimental groups, there is a significant negative relationship between neurons' spontaneous firing rate and the responsiveness index (RI) (Spearman rank order R- and p-values shown). **(B)** A similar negative relationship was seen between AM spontaneous firing rate and neurons' selectivity index (OSI45; Spearman rank order). **(C) and (D)** The aggregated data was sextiled based on AM spontaneous firing rate. Responsiveness index (RI; C) and selectivity index (OSI45; D) varied significantly across sextiles ($p < 0.0001$, Kruskal-Wallis one-way ANOVA on ranks), with sparsely firing neurons showing higher RI and OSI45 values than faster firing neurons. For panels C-D, * indicates $p < 0.05$, ** indicates $p < 0.01$, *** indicates $p < 0.001$, and **** indicates $p < 0.0001$, Dunn's post hoc test.

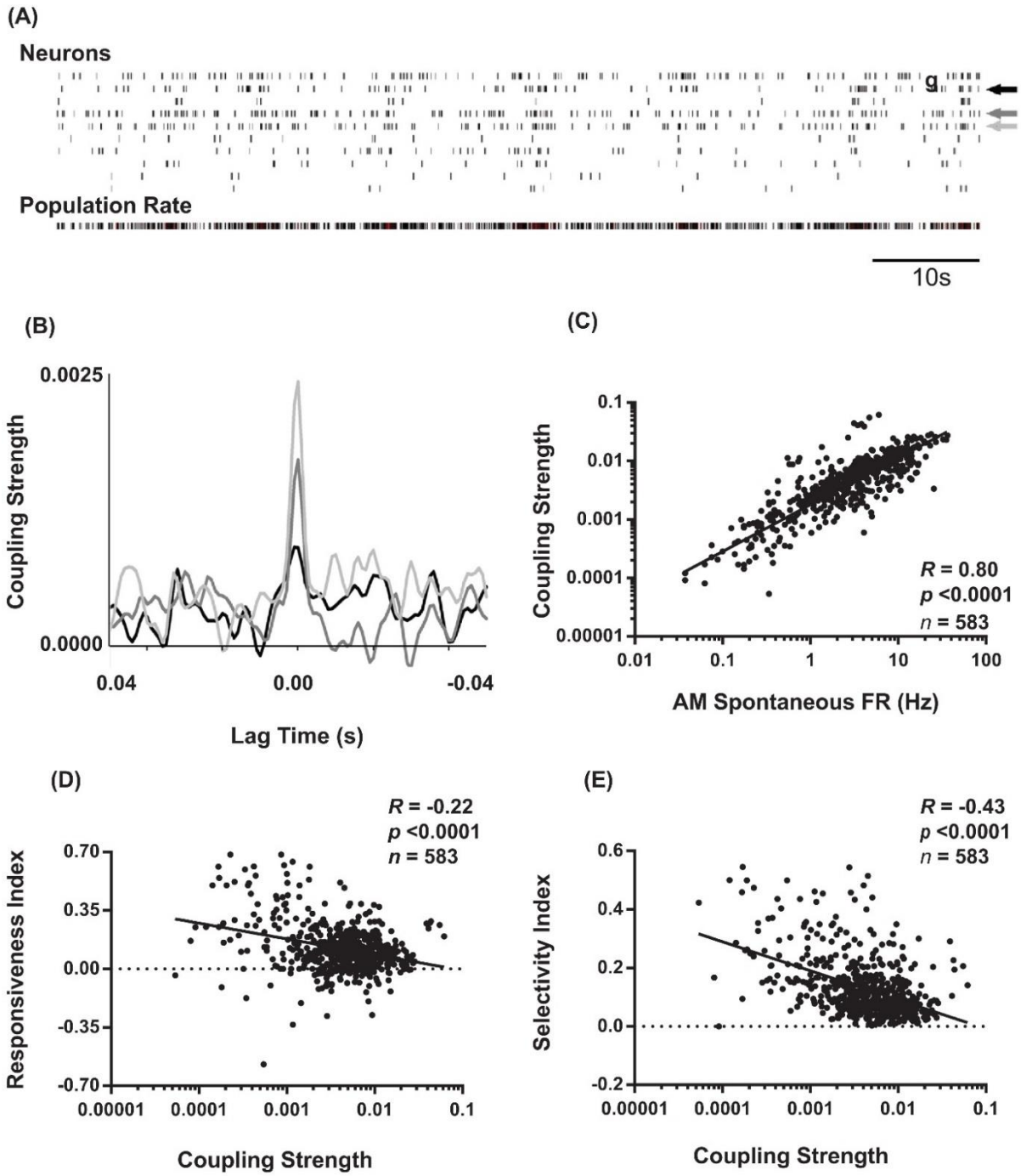

Figure 3.6. Coupling of V1 neurons' firing to population activity is negatively correlated with visual responsiveness and orientation selectivity. (A) Schematic representation of coupling strength calculation. Across AM visual response testing, spike times for individual neurons (indicated by arrows) were cross-correlated with population activity from all other simultaneously recorded neurons (i.e., with the reference neuron's activity subtracted from total firing; shown in bottom raster). **(B)** Superimposed cross-correlograms of spiking from the neurons indicated with arrows in the raster plot are shown, following subtraction of the shift-predictor described in Materials and Methods. Coupling strength for each neuron was calculated as the value of the cross-correlation at 0 lag time. **(C)** For baseline (AM) data aggregated from the four experimental groups, coupling strength and spontaneous firing rate show a strong positive correlation. In contrast, at baseline, coupling strength is negatively correlated with both RI **(D)** and OSI45 **(E)**. Spearman rank order R- and p-values shown.

+ LSD mice (*N.S.*, Spearman rank order; **Fig. 3.7A**). When neurons' spontaneous AM firing rates were grouped into sextiles (**Fig. 3.7C-F**), the lowest-firing sextile showed significantly greater OSRP than neurons in the highest-firing sextiles for mice allowed *ad lib* sleep. However, OSRP was similar in magnitude across baseline firing sextiles in both sleep deprived groups. Similarly, the baseline coupling of firing to population activity tended to be a good predictor of the magnitude of OSRP across the day in neurons recorded from Vis Stim + Sleep mice and Vis Stim + ESD mice (where weakly-coupled neurons showed significantly greater OSRP than strongly-coupled neurons), but not from Blank Screen + Sleep and Vis Stim + LSD mice (**Fig. 3.7B, Fig. 3.7G-J**). The relationship between population coupling and OSRP appeared to be mediated in part by baseline firing rate among neurons recorded from the Vis Stim + Sleep group (p = 1e-6, Sobel test).. However, the same was not true for neurons recorded from Vis Stim + ESD mice, where firing rates did not predict OSRP. These data show that experience-dependent plasticity is not expressed uniformly across the V1 population, but is greatest among sparsely firing and weakly population-coupled neurons after a period of subsequent sleep.

3.10 V1 neurons' population-coupling strength is altered by visual experience and sleep

Because population coupling could itself be altered as a function of circuit plasticity, we next assessed how the strength of population coupling changes across the day for different neuronal populations. AM and PM population coupling were highly correlated across all groups (R = 0.82, 0.94, 0.85, 0.64 for Vis Stim + Sleep, Blank Screen + Sleep, Vis Stim + ESD, and Vis Stim + LSD, respectively; all $p < 0.000001$, Spearman rank order). However, there was a significant increase in coupling from AM to PM time points in the Vis Stim + Sleep condition (p = 0.014; Wilcoxon signed rank test) and

significant decrease in coupling from AM to PM in the Vis Stim + ESD condition (p = 0.001; Wilcoxon signed rank test). These changes were not uniform, but instead varied across the distribution of both V1 neurons' baseline (AM) spontaneous firing rates (**Fig. 3.8A**) and their baseline (AM) population coupling strength (**Fig. 3.8B**). Spontaneous firing rates were predictive of across-the-day coupling strength changes for neurons recorded from both sleeping groups ($p < 0.003$ and $p < 0.005$ for Vis Stim + Sleep and Blank Screen + Sleep respectively, Spearman rank order, **Fig. 3.8A**), with lower-firing neurons showing the greatest increase in coupling strength across the day (**Fig. 3.8C-D**). There was no relationship between baseline firing rate and coupling strength changes for neurons recorded from Vis Stim + ESD and Vis Stim + LSD mice (**Fig. 3.8A, E-F**). Baseline population-coupling strength was predictive of coupling strength changes in three of the four experimental groups following visual stimulus presentation (Vis Stim + Sleep, Blank Screen + Sleep, and Vis Stim + ESD; all $p < 0.005$; Vis Stim + LSD *N.S.*, Spearman rank order, F-test), with neurons with the lowest coupling strength at baseline showing the largest increases in coupling strength across the day (**Fig. 3.8B**). In spite of the maintained correlation in the Vis Stim + ESD group, the net change in coupling is negative, in contrast to the range of changes in the sleep conditions (**Fig. 3.8G-J**).

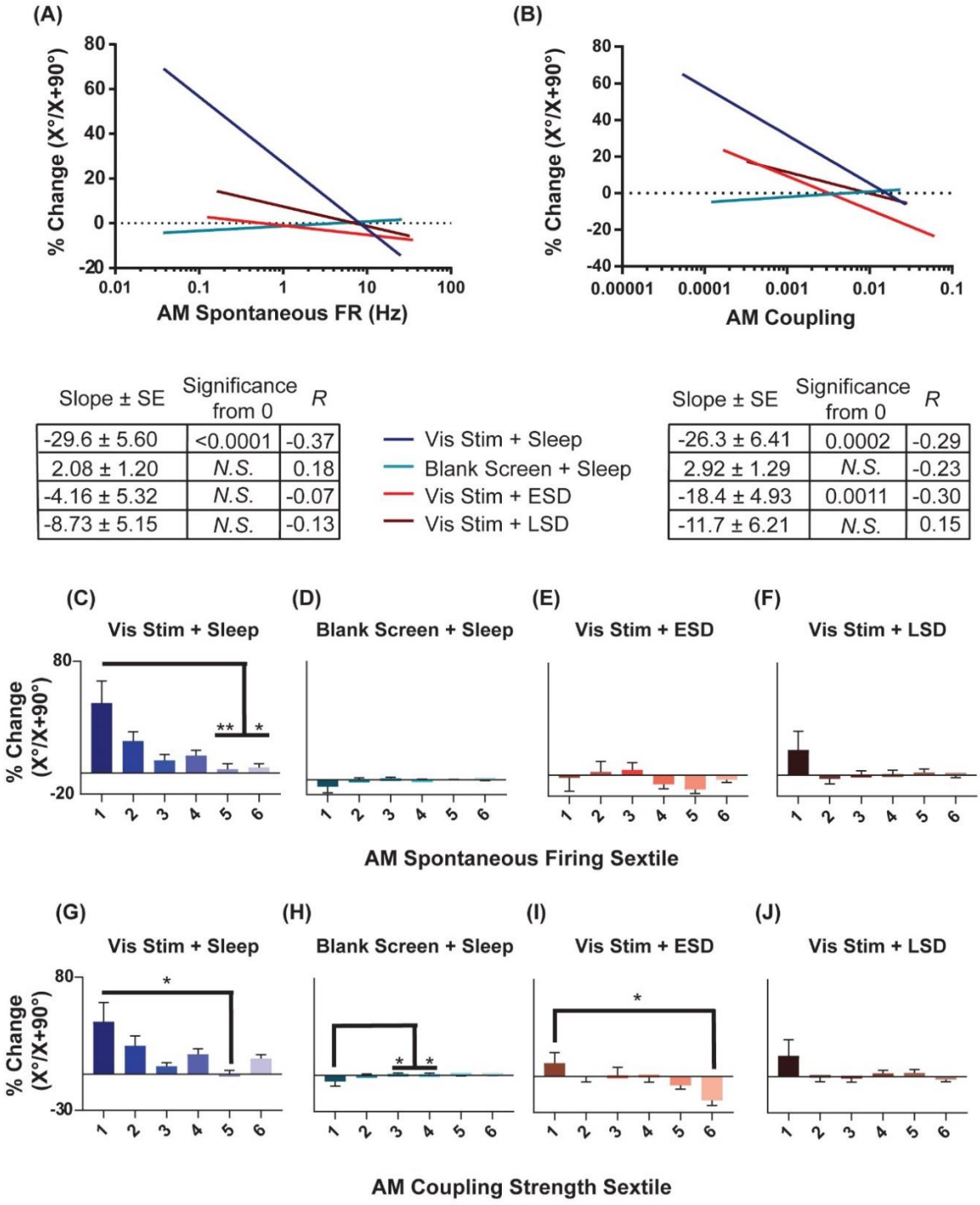

Slope ± SE	Significance from 0	*R*
-29.6 ± 5.60	<0.0001	-0.37
2.08 ± 1.20	*N.S.*	0.18
-4.16 ± 5.32	*N.S.*	-0.07
-8.73 ± 5.15	*N.S.*	-0.13

Slope ± SE	Significance from 0	*R*
-26.3 ± 6.41	0.0002	-0.29
2.92 ± 1.29	*N.S.*	-0.23
-18.4 ± 4.93	0.0011	-0.30
-11.7 ± 6.21	*N.S.*	0.15

Figure 3.7. OSRP is greatest in sparsely firing V1 neurons with weak population coupling. (A) and (B) Linear regressions of the relationship between OSRP (expressed as % changes in neurons' responses to the presented visual stimulus orientation [X°] vs. the orthogonal orientation [X + 90°] across the day, as in Figure 2) and AM spontaneous firing rate. The table below shows, for each experimental group, the regression slope and SE, Spearman R-value, and Bonferroni-corrected F test p-value. **(C-F)** Sextiles of the data, based on AM spontaneous firing rate, which is shown in (A) ($p = 0.0179$ for panel C, all others N.S., Kruskal-Wallis one-way ANOVA on ranks). **(G-J)** Sextiles of the data, based on AM coupling strength, which is shown in (B) ($p = 0.0011$, 0.0203 for panels H-I respectively, all others N.S., Kruskal-Wallis one-way ANOVA on ranks). Error bars indicate mean ± SEM for % changes in orientation preference; * indicates $p < 0.05$, and ** indicates $p < 0.01$, Dunn's post hoc test.

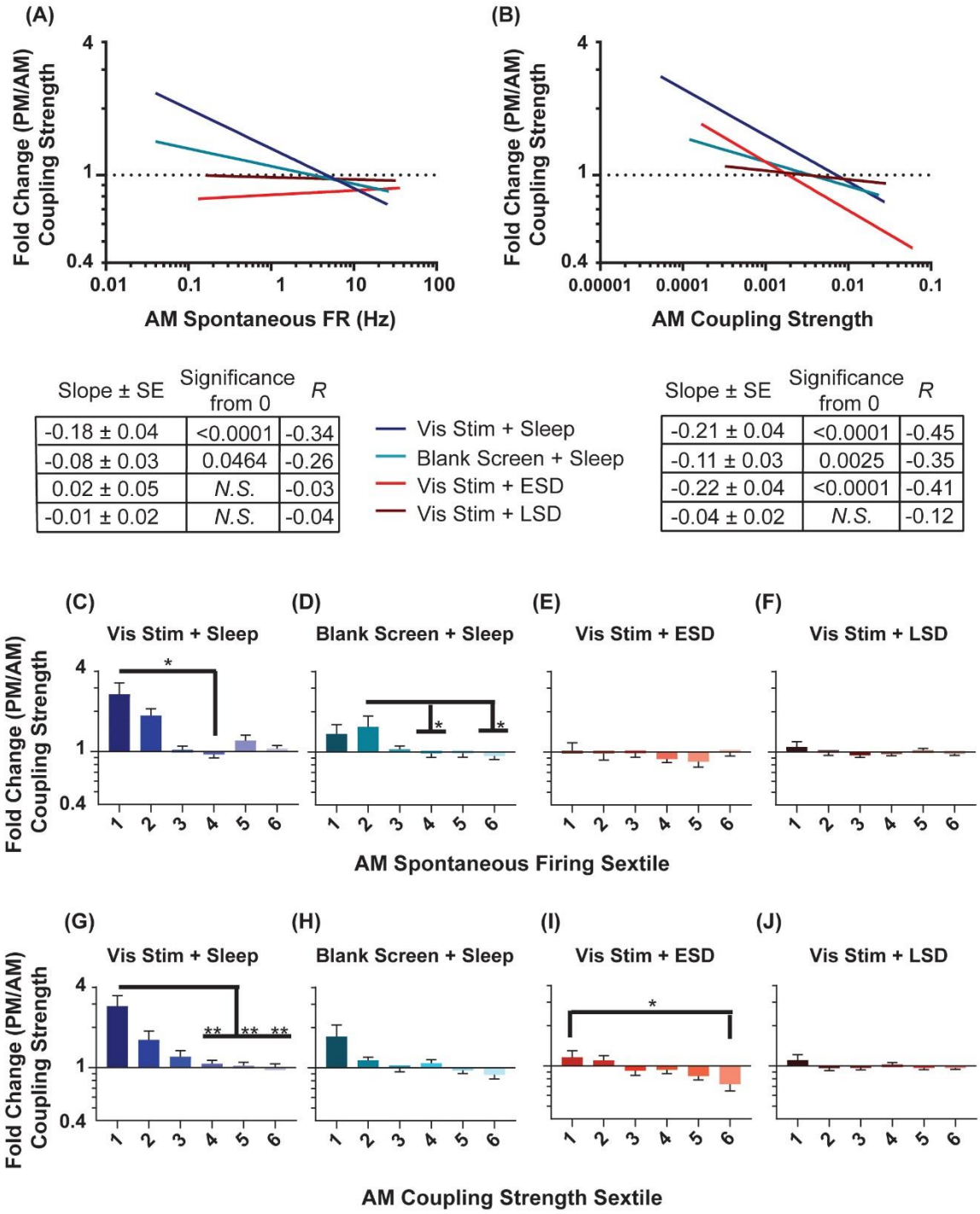

Slope ± SE	Significance from 0	*R*
-0.18 ± 0.04	<0.0001	-0.34
-0.08 ± 0.03	0.0464	-0.26
0.02 ± 0.05	*N.S.*	-0.03
-0.01 ± 0.02	*N.S.*	-0.04

Slope ± SE	Significance from 0	*R*
-0.21 ± 0.04	<0.0001	-0.45
-0.11 ± 0.03	0.0025	-0.35
-0.22 ± 0.04	<0.0001	-0.41
-0.04 ± 0.02	*N.S.*	-0.12

Figure 3.8. Changes in population coupling strength across the day vary as a function of neurons' baseline coupling and firing rate, visual experience, and sleep. (A-B). Linear fits of data for the fold change in coupling strength across the day as a function of AM spontaneous firing rate (A) and AM coupling strength (B). The table below shows, for each experimental group, the regression slope and SE, Spearman R-value, and Bonferroni-corrected F test p-value. **(C-F)** Sextiles of the data, based on AM spontaneous firing rate, which is shown in (A) (p = 0.0043, 0.0391 for panels C-D respectively, all others N.S., Kruskal-Wallis one-way ANOVA on ranks). **(G-J)** Sextiles of the data, based on AM coupling strength, which is shown in (B) (p = 0.0052, 0.0304 for panels G and I respectively, all others N.S., Kruskal-Wallis one-way ANOVA on ranks). Error bars indicate mean ± SEM for log changes in firing rate. * indicates p < 0.05, ** indicates p < 0.01, *** indicates p < 0.001, and **** indicates p < 0.0001, Dunn's post hoc test.

3.11 Firing rates of V1 neurons are differentially altered across bouts of NREM, REM, and wake

We next examined how firing rates among V1 neurons are altered across individual bouts of NREM, REM, and wake. Across groups, we found V1 firing changed little across NREM or wake bouts. In contrast, in both Vis Stim + Sleep and Blank Screen + Sleep mice, neurons showed an apparent increase in firing across bouts of REM (**Fig. 3.9**).

In Vis Stim + Sleep mice, as was true for firing increases across the day in these mice, this effect of REM was not uniform, but preferentially affected neurons with lower baseline firing rates (**Fig. 3.9A**). There was a similar trend across REM for neurons in Blank Screen + Sleep mice, although this did not reach statistical significance (**Fig. 3.9B**). There were no significant differences between sextiles in either sleep deprivation condition (**Fig. 3.9C-D**). When overall changes in firing rates across REM sleep were compared between groups, Vis Stim + Sleep and Blank Screen + Sleep showed larger total changes in firing rates than either sleep deprivation group ($p < 0.0001$, Kruskal-Wallis one-way ANOVA on ranks; Vis Stim + Sleep or Blank Screen + Sleep vs. Vis Stim + ESD, $p \leq 0.001$; Vis Stim + Sleep or Blank Screen + Sleep vs. Vis Stim + LSD, $p < 0.0001$, Dunn's post hoc test). A regression of sextile averages across two hour time blocks between CT0 and CT12 showed no significant modulation of firing changes during REM bouts by time of day in the Vis Stim + Sleep group. This suggests that REM bout-associated firing increases may be similar in magnitude across the entire rest phase following visual experience.

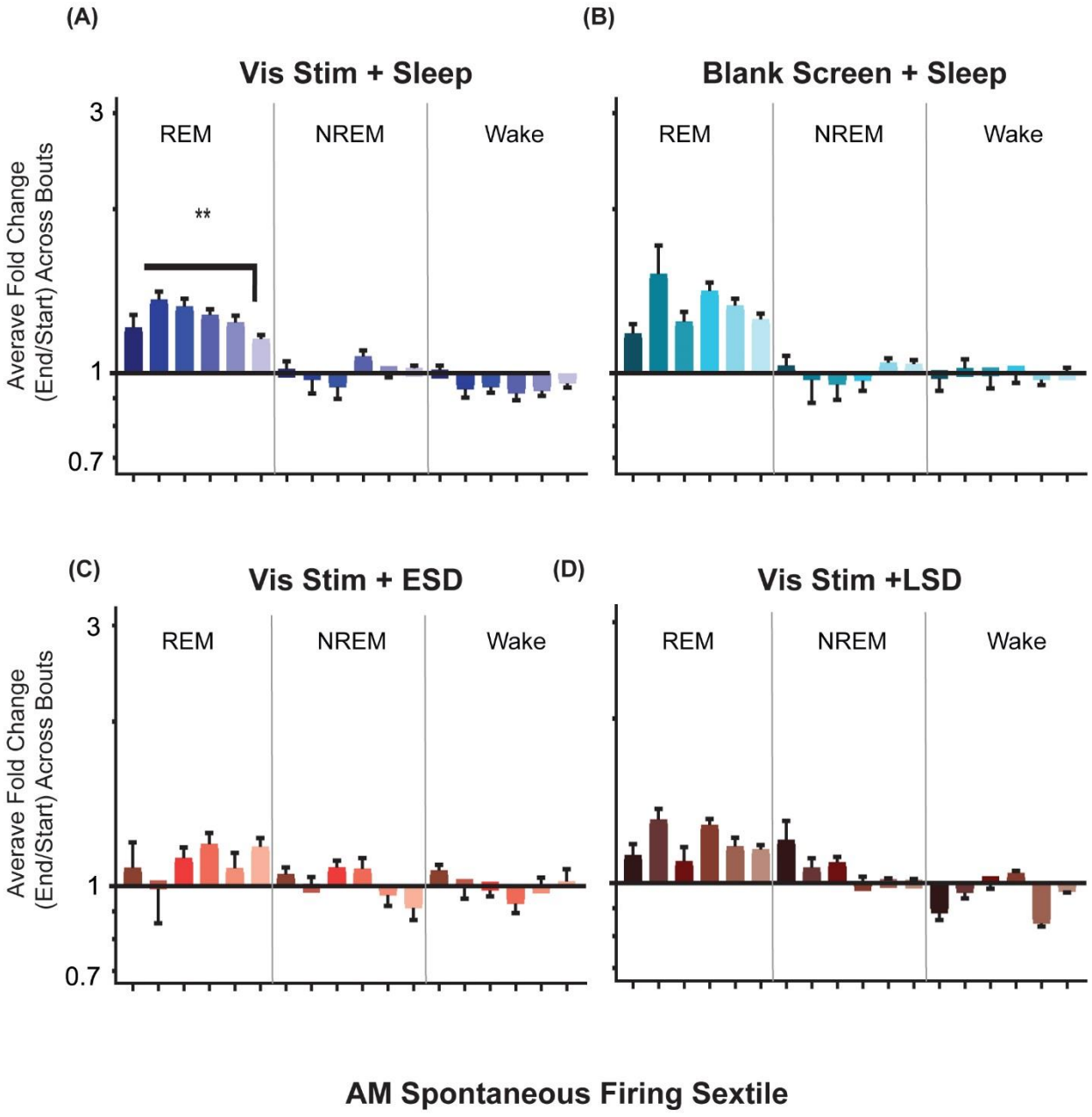

Figure 3.9. Firing rates of V1 neurons increase across bouts of REM sleep. (A-D) Neuronal firing rates were averaged over the first and last 30 s of each REM sleep, NREM sleep, or wake bout, and average firing rate changes across the portion of the day corresponding to ad lib sleep were calculated for each neuron (see Materials and Methods). Values indicate mean ± SEM for state specific changes in firing for each sextile of baseline (AM) spontaneous firing rate (sextile colors as in Figures 4 and 7). While firing rates were minimally affected across periods of NREM and wake, in the Vis Stim + Sleep group (A), increases in firing across post-stimulus REM bouts varied as a function of baseline (AM) spontaneous firing rate ($p = 0.0069$, Kruskal-Wallis one-way ANOVA on ranks). ** indicates $p < 0.01$, Dunn's post hoc test. While a similar trend was seen for Blank Screen + Sleep (B), there was no statistically significant effect of baseline firing rate. Changes in firing across REM were not statistically significant during the 6 h of recovery sleep in Vis Stim + ESD mice (C), or over the first 6 h of ad lib sleep in Vis Stim + LSD mice (D).

3.12 Discussion:

We have previously shown that, following a period of patterned visual experience, sleep facilitates visual response changes (OSRP) among mouse V1 neurons.[6,16,17] While visual responses are not altered across waking exposure to an oriented grating, after a 12-h period of subsequent sleep, firing rate responses to gratings of the same orientation are selectively enhanced.[17] This selective enhancement of firing rate responses is disrupted by post-stimulus sleep deprivation.[6,16,17] The underlying mechanisms for OSRP expression appear to involve thalamocortical long-term potentiation (LTP), as OSRP and LTP are mutually occluding *in vivo*[12] and rely on similar intracellular signaling pathways.[19] This suggests that information content regarding prior visual experience (i.e., orientation-specific information) is relayed from thalamus to cortex during post-stimulus sleep (a hypothesis we address more in **Chapter 4**). Here, we aimed to clarify how this information is distributed among neurons in the sensory cortex, and how this relates to what is known about the heterogeneity of neuronal firing rates, population coupling, and sleep-dependent changes in firing.[7,28,41] We find that sleep-dependent OSRP is not uniform across the population of V1 neurons. Rather, it is expressed preferentially among sparsely firing V1 neurons. These neurons are weakly coupled to V1 population activity (i.e., they are “soloists” rather than “choristers”), are more visually responsive than other V1 neurons, and have greater orientation selectivity than neighboring neurons. These neurons also selectively show firing increases across sleep - a process that (like OSRP itself)[6] is disrupted by partial sleep deprivation. Intriguingly, this same population of neurons also becomes more strongly coupled to population activity across a period of sleep.

Our present data suggest that for sensory cortical areas, the heterogeneous firing rate changes previously reported in frontal cortex across sleep (i.e., increases in firing among sparsely firing neurons, and simultaneous reductions in firing among high firing neurons)[41] may have special functional significance. By preferentially augmenting firing in neurons that show the highest responsiveness and selectivity, sleep may function generally to increase the signal-to-noise ratio of sensory responses. This is particularly relevant after an experience that induces response plasticity in the cortex, such as after visual experience that induces OSRP in V1. This idea is reminiscent of predictions of the "synaptic homeostasis hypothesis" (SHY), which proposes that sleep may improve signal-to-noise ratios in the spiking of neural circuits through firing reductions caused by general synaptic downscaling.[11,22,36] While our present findings do not address the synaptic basis of these changes, we find that improvements in sensory signal-to-noise ratios may be caused by simultaneous increases and decreases in the firing of distinct neuronal populations during sleep.

The fact that these firing rate changes are disrupted by sleep deprivation (either ESD or LSD) suggest that the mechanism underlying these heterogeneous changes in neuronal firing rate is distinctly sleep-dependent. This is supported by our analysis of firing rate changes across bouts of REM, NREM, and wake, where we find increases in firing rates, which are greatest in more sparsely firing neurons, occurring preferentially across periods of REM. This is in line with our prior work, showing firing rate increases in V1 neurons across REM bouts in the hours after visual stimulus presentation, but not after presentation of a blank screen.[17] The fact that we also see increases across REM bouts in our blank screen condition in this study is likely due to the fact that we are assessing

firing rate changes across the entire day (not over the first few hours following visual experience, as in the prior study). Because REM preferentially affects the activity of sparsely firing V1 neurons, this brain state may account for the firing increase seen across the day in this population. Intriguingly, this phenomenon seems to be exactly the opposite of changes in firing seen across REM in the hippocampus,[20,25] and frontal cortex,[41] where neuronal firing decreases across the population.

An unanswered question is what mechanism could mediate differential changes in the firing rates of sparsely firing and high firing neuronal populations across a period of sleep. A number of potential physiological mechanisms, regulated by activity patterns present in thalamocortical circuits during sleep, may explain these apparent simultaneous reductions and enhancements of firing in different neuronal populations.[29,32] One prominent hypothesis proposes that neurons activated by waking experience are preferentially re-activated during subsequent sleep, in the context of sleep-associated oscillations.[1,2,8,23] Thus it is possible that lower-firing neurons are preferentially re-activated during sleep, while higher-firing neurons are not. This could lead to differential activity-dependent plasticity (and thus firing changes) in sparsely firing and higher firing populations across a period of sleep. While our present analyses do not specifically test this mechanism, our previous studies of OSRP have shown that V1 neurons that exhibit the most coherent firing during NREM oscillations show the most dramatic changes in responsiveness to the presented stimulus orientation.[6,16] Another possibility is that, because high-firing neurons in this study likely include fast-spiking interneurons, the firing decreases seen after sleep among higher-firing neurons are due to differential effects of sleep on excitatory and inhibitory neuronal populations. This would be not be an

unprecedented finding - in previous recordings of rat cortical neurons, Vyazovskiy et al. reported significant firing rate decreases across sleep only in physiologically-defined fast spiking interneurons.[40] We and others have speculated previously that suppression of activity in the fast-spiking interneuron population may serve as a critical mechanism for some forms of sleep-dependent plasticity.[3,29] One intriguing possibility, worthy of future study, is that firing rate increases seen across a period of sleep in sparsely-firing neurons are the direct result of disinhibition.

Regardless of the mechanisms underlying the heterogeneous changes we observe in V1 neurons' firing rate and population coupling, the nature of these changes is likely to be highly informative for promoting visual response plasticity. We find that after a period of uninterrupted sleep, the most highly visually-responsive and orientation-selective neurons show increased firing, while less responsive and more poorly-tuned neurons show decreased firing. Moreover, we find that following patterned visual experience (which induces response plasticity), these highly responsive and selective neurons preferentially increase the coupling of their firing to population activity. Together, these data suggest that in the context of sleep-dependent sensory plasticity, neurons which carry highly specific visual information have an increased capacity to influence population activity in V1.

Author Contributions: BC, JD and SA designed research and wrote the article. AS and SA performed research. CB contributed new analytic tools. BC, JD, EP and SA analyzed data.

3.13 References

1. Antony, J., Piloto, L., Wang, M., Pacheco, P., Norman, K., and Paller, K. (2018). Sleep Spindle Refractoriness Segregates Periods of Memory Reactivation. Curr Biol S0960-9822, 30448-30442.

2. Aton, S.J. (2013). Set and setting: How behavioral state regulates sensory function and plasticity. Neurobiol Learn Mem 106, 1-10.

3. Aton, S.J., Broussard, C., Dumoulin, M., Seibt, J., Watson, A., Coleman, T., and Frank , M.G. (2013). Visual experience and subsequent sleep induce sequential plastic changes in putative inhibitory and excitatory cortical neurons. Proc Natl Acad Sci U S A 110, 3101-3106.

4. Aton, S.J., Seibt, J., Dumoulin, M., Jha, S.K., Steinmetz, N., Coleman, T., Naidoo, N., and Frank, M.G. (2009a). Mechanisms of sleep-dependent consolidation of cortical plasticity. Neuron 61, 454-466.

5. Aton, S.J., Seibt, J., and Frank , M.G. (2009b). Sleep and memory. In Encyclopedia of Life Science (Chichester, John Wiley and Sons, Ltd.).

6. Aton, S.J., Suresh, A., Broussard, C., and Frank, M.G. (2014). Sleep promotes cortical response potentiation following visual experience. Sleep 37, 1163-1170.

7. Bachatene, L., Bharmauria, V., Cattan, S., Chanauria, N., Rouat, J., and Molotchnikoff, S. (2015). Electrophysiological and firing properties of neurons: Categorizing soloists and choristers in primary visual cortex. Neurosci Lett 604, 103-108.

8. Batterink, L., Creery, J., and Paller, K. (2016). Phase of Spontaneous Slow Oscillations during Sleep Influences Memory-Related Processing of Auditory Cues. J Neurosci 36, 1401-1409.

9. Chauvette, S., Seigneur, J., and Timofeev, I. (2012). Sleep oscillations in the thalamocortical system induce long-term plasticity. Neuron 75, 1105-1113.

10. Cirelli, C., Gutierrez, C.M., and Tononi, G. (2004). Extensive and divergent effects of sleep and wakefulness on brain gene expression. Neuron 41, 35-43.

11. Cirelli, C., and Tononi, G. (2014). Sleep and synaptic homeostasis. Sleep 38, 161-162.

12. Cooke, S.F., and Bear, M.F. (2010). Visual experience induces long-term potentiation in the primary visual cortex. J Neurosci 30, 16304-16313.

13. de Vivo, L., Bellesi, M., Marshall, W., Bushong, E.A., Ellisman, H., Tononi, G., and Cirelli, C. (2017). Ultrastructural evidence for synaptic scaling across the wake/sleep cycle. Science 355, 507-510.

14. Delorme, J., Kodoth, V., and Aton, S.J. (2018). Sleep loss disrupts Arc expression in dentate gyrus neurons. Neurobiol Learn Mem Epub ahead of print.

15. Diekelmann, S., and Born, J. (2010). The memory function of sleep. Nat Rev Neurosci 11, 114-126.

16. Durkin, J., Suresh, A.K., Colbath, J., Broussard, C., Wu, J., Zochowski, M., and Aton, S.J. (2017). Cortically coordinated NREM thalamocortical oscillations play an essential, instructive role in visual system plasticity. Proceedings National Academy of Sciences 114, 10485-10490.

17. Durkin, J.M., and Aton, S.J. (2016). Sleep-dependent potentiation in the visual system is at odds with the Synaptic Homeostasis Hypothesis. Sleep.

18. Frank, M.G., Issa, N.P., and Stryker, M.P. (2001). Sleep enhances plasticity in the developing visual cortex. Neuron 30, 275-287.

19. Frenkel, M.Y., Sawtell, N.B., Diogo, A.C., Yoon, B., Neve, R.L., and Bear, M.F. (2006). Instructive effect of visual experience in mouse visual cortex. Neuron 51, 339-349.

20. Grosmark, A.D., Mizuseki, K., Pastalkova, E., Diba, K., and Buzsaki, G. (2012). REM sleep reorganizes hippocampal excitability. Neuron 75, 1001-1007.

21. Hill, D.N., Mehta, S.B., and Kleinfeld, D. (2011). Quality metrics to accompany spike sorting of extracellular signals. J Neurosci 31, 8699-8705.

22. Hill, S., and Tononi, G. (2005). Modeling sleep and wakefulness in the thalamocortical system. J Neurophysiol 93, 1671-1698.

23. Huber, R., Ghilardi, M.F., Massimini, M., and Tononi, G. (2004). Local sleep and learning. Nature 430, 78-81.

24. Mackiewicz, M., Shockley, K.R., Romer, M.A., Galante, R.J., Zimmerman, J.E., Naidoo, N., Baldwin, D.A., Jensen, S.T., Churchill, G.A., and Pack, A.I. (2007). Macromolecule biosynthesis - a key function of sleep. Physiol Genomics 31, 441-457.

25. Miyawaki, H., and Diba, K. (2016). Regulation of Hippocampal Firing by Network Oscillations during Sleep. Curr Biol 26, 893-902.

26. Ognjanovski, N., Maruyama, D., Lashner, N., Zochowski, M., and Aton, S.J. (2014). CA1 hippocampal network activity changes during sleep-dependent memory consolidation. Front Syst Neurosci 8, 61.

27. Ognjanovski, N., Schaeffer, S., Mofakham, S., Wu, J., Maruyama, D., Zochowski, M., and Aton, S.J. (2017). Parvalbumin-expressing interneurons coordinate hippocampal network dynamics required for memory consolidation. Nature Communications 8, 15039.

28. Okun, M., Steinmetz, N.A., Cossell, L., Iacaruso, M.F., Ko, H., Bartho, P., Moore, T., Hoefer, S.B., Mrsic-Flogel, T.D., Carandini, M., et al. (2015). Diverse coupling of neurons to populations in sensory cortex. Nature 521, 511-515.

29. Puentes-Mestril, C., and Aton, S.J. (2017). Linking network activity to synaptic plasticity during sleep: hypotheses and recent data. Frontiers in Neural Circuits 11, doi: 10.3389/fncir.2017.00061.

30. Ribeiro, S., Goyal, V., Mello, C.V., and Pavlides, C. (1999). Brain gene expression during REM sleep depends on prior waking experience. Learn Mem 6, 500-508.

31. Ribeiro, S., Mello, C.V., Velho, T., Gardner, T.J., Jarvis, E.D., and Pavlides, C. (2002). Induction of hippocampal long-term potentiation during waking leads to increased extrahippocampal zif-268 expression during ensuing rapid-eye-movement sleep. JNeurosci 22, 10914-10923.

32. Roach, J.P., Pidde, A., Katz, E., Wu, J., Ognjanovski, N., Aton, S.J., and Zochowski, M.R. (2018). Resonance with sub-treshold oscillatory drive organizes activity and optimizes learning in neural networks. Proc Natl Acad Sci U S A In Press.

33. Sato, T., Suzuki, T., and Mabuchi, K. (2007). Fast automatic template matching for spike sorting based on Davies-Bouldin validation indices. Conf Proc IEEE Eng Med Biol Soc, 3200-3203.

34. Seibt, J., Dumoulin, M., Aton, S.J., Coleman, T., Watson, A., Naidoo, N., and Frank, M.G. (2012). Protein synthesis during sleep consolidates cortical plasticity in vivo. Curr Biol 22, 676-682.

35. Thompson, C.L., Wisor, J.P., Lee, C.-K., Pathak, S.D., Gerashchenko, D., Smith, K.A., Fischer, S.R., Kuan, C.L., Sunkin, S.M., Ng, L.L., et al. (2010). Molecular and Anatomical Signatures of Sleep Deprivation in the Mouse Brain. Front Neurosci 4.

36. Tononi, G., and Cirelli, C. (2003). Sleep and synaptic homeostasis: a hypothesis. Brain Res Bull 62, 143-150.

37. Tononi, G., and Cirelli, C. (2014). Sleep and the price of plasticity: From synaptic and cellular homeostasis to memory consolidation and integration. Neuron 81, 12-34.

38. Ulloor, J., and Datta, S. (2005). Spatio-temporal activation of cyclic AMP response element-binding protein, activity-regulated cytoskeletal-associated protein and brain-derived nerve growth factor: a mechanism for pontine-wave generator activation-dependent two-way active-avoidance memory processing in the rat. Journal of Neurochemistry 95, 418-428.

39. Vyazovskiy, V.V., Cirelli, C., Pfister-Genskow, M., Faraguna, U., and Tononi, G. (2008). Molecular and electrophysiological evidence for net synaptic potentiation in wake and depression in sleep. advanced online publication.

40. Vyazovskiy, V.V., Olscese, U., Lazimy, Y.M., Faraguna, U., Esser, S.K., Williams, J.C., Cirelli, C., and Tononi, G. (2009). Cortical firing and sleep homeostasis. Neuron 63, 865-878.

41. Watson, B.O., Levenstein, D., Green, J.P., Gelinas, J.N., and Buzsaki, G. (2016). Network homeostasis and state dynamics of neocortical sleep. Neuron 90, 839-852.

42. Yang, G., Lai, C.S., Cichon, J., Ma, L., Li, W., and Gan, W.B. (2014). Sleep promotes branch-specific formation of dendritic spines after learning. Science 344, 1173-1178.

CHAPTER IV

Sleep-specific reactivation of the visual engram is necessary for the consolidation of visually-cued fear conditioning

Currently in review as Clawson *et al* 2020 for Nature Neuroscience

4.1 Abstract

Extensive work has elucidated the time scale, patterning, and oscillatory signatures associated with memory reactivation during sleep; however, the necessity of reactivation for sleep-dependent consolidation has not been directly tested. We combined visually-cued conditioning to oriented gratings with engram labelling to create a tractable system for manipulating a specific memory during sleep. We show that the TRAP (targeted recombination in active populations) engram mouse line can be used to drive transgene expression in a specific oriented grating ensemble in primary visual cortex. We then inhibit this ensemble during post-conditioning sleep causing impaired consolidation. This was done in a content specific way without sleep architecture or oscillations - indicating that reactivation itself is necessary for sleep dependent memory consolidation.

4.2 Introduction

Experiences during wake influence neural activity during subsequent sleep. For example, hippocampal place cells activated in a specific environment during wake displayed higher firing rates during subsequent sleep (reactivation)[1], and those that are activated sequentially during spatial exploration are reactivated sequentially during sleep (replay)[2–8]. Sleep-associated reactivation and replay have been observed in multiple species following a wide range of waking experiences, and across multiple brain regions-

including sensory cortices (Grenier 2001)[9–19]. This suggests that these phenomena could constitute an instructive mechanism by which sleep promotes memory consolidation[20]. However, establishing a causal relationship between sleep-dependent reactivation/replay and memory storage (and the synaptic plasticity thought to underlie memory storage) has proven difficult.

Two issues have hindered experimental progress toward testing whether sleep replay or reactivation are necessary for memory consolidation. First, this test requires selective disruption of sleep-associated activity patterns in sparse populations of neurons activated during experience. Recent studies have taken advantage of new genetic tools to target gene expression to neurons activated by experience[21]. These studies have established the role of so-called “engram neurons” in memory encoding and recall[22–24]. To date however, no studies have applied this technology to the question of sleep-dependent memory consolidation. Rather, studies investigating the role of sleep and memory consolidation have used transient disruption of large-scale network activity during specific sleep oscillations[25–28] or disruption of activity in whole populations of genetically-defined cell types across specific bouts of specific sleep states[29,30].

A second roadblock to testing the hypothesis that sleep reactivation drives memory consolidation is a lack of temporal resolution - with few memory tasks used in rodent models showing consolidation across a single post-learning sleep interval. Here we describe a form of visually-cued fear memory which is encoded by single trial conditioning, drives behavioral discrimination between conditioned and neutral visual cues, and is consolidated during post-conditioning sleep. By pairing visual presentation of a grating stimulus of a specific orientation with an aversive foot shock, mice form a

selective fear memory for gratings of the same orientation. This visually-cued memory is disrupted by post-conditioning sleep disruption. Using this paradigm, we take advantage of recently developed genetic tools to selectively manipulate orientation-selective (i.e., cue-activated) primary visual cortex (V1) neurons. We find that these cue-activated visual engram neurons are selectively reactivated during sleep in the hours following visually-cued fear conditioning. Optogenetic stimulation of these neurons in awake behaving mice generates a percept of the fear cue, which is sufficient to drive fear learning and recall. A period of rhythmic optogenetic activation of these neurons is sufficient to increase representation of the cue orientation in surrounding V1 neurons, and their optogenetic inhibition reduces cue orientation preference in V1. Finally, we show that selective sleep-targeted inhibition of cue-activated V1 neurons during post-conditioning sleep is sufficient to disrupt consolidation of visually-cued fear memory. Based on these findings, we conclude that neurons that are selectively activated in sensory cortical areas during learning play an instructive role in subsequent sleep-dependent memory consolidation.

4.3 Materials and Methods

Animal handling and husbandry

All animal procedures were approved by the University of Michigan Institutional Animal Care and Use Committee. With the exception of constant dark following tamoxifen administration, mice were kept on a 12 h:12 h light:dark (LD) cycle and were given food and water *ad lib* throughout the entirety of the study. Following surgical procedures, and during habituation prior to cued conditioning, mice were individually housed in standard caging with beneficial environmental enrichment (nesting material, manipulanda, and/or novel foods).

Visually-cued fear conditioning

For 3 days prior to conditioning, mice were habituated to 5 min/day of gentle handling. Following the habituation period, at ZT0, mice underwent visually-cued fear conditioning in a novel arena (context A). They were allowed 2 minutes to acclimate to the arena. They then experienced 3 pairings of a 30-s visual stimulus co-terminating with a 2-s 0.75 mA foot shock. These pairings were divided with a 60-s intertrial interval. Each visual stimulus consisted of a 1 Hz phase-reversing oriented grating (X°) with a spatial frequency of 0.05 cycles/degree and contrast of 100%.

Following conditioning, C57BL/6J mice (Jackson) used for experiments outlined in **Figure 4.1** were returned to their home cage and were either allowed 12 hr *ad lib* sleep, or were sleep deprived (SD) using gentle handling (i.e., cage tapping, nest disturbance, and light touch with a cotton-tipped applicator to cause arousal from sleep) for 6 h, after which they were allowed 6 hr *ad lib* sleep. All transgenic mice (see below) with data shown in **Figures 4.2**, **4.3**, and **4.7** were allowed *ad lib* sleep in their home cage following conditioning.

At ZT12 (i.e., 12 hours following conditioning) mice were placed in a dissimilar novel context B for cued fear memory testing. Context B differed from context A (used during conditioning), with the two arenas having a unique odor, shape, size, floor texture, and lighting condition. During testing, mice were exposed to two distinct oriented grating stimuli (X° and Y°) to assess cue discrimination. At the start of each test, mice were allowed 3 min to acclimate to the arena, after which an oriented grating either the same as the shock cue (X°) or distinct (Y°) was presented for 3 min followed by 1 min of post

stimulus arena exploration. A minimum of thirty minutes were left between the presentations of the tests.

Freezing responses were quantified for each grating stimulus using criteria described in Curzon et al 2009[31]. For each test, two scorers blinded to behavioral condition quantified periods of immobility during presentation of grating stimuli that included fear features such as hyperventilation and rigid posture. Freezing during presentation of the two gratings was compared to calculate a discrimination index: (percent freezing during shock [X°] simulus)/(percent freezing during shock [X°] stimulus + percent freezing during neutral [Y°] stimulus). To test for time-of-day effects on visually-cued fear memory recall (**Supplemental Figure 4.S2**), additional cohorts of mice were trained at ZT0 as described above, and tested at 12, 24, or 36 hrs later.

Genetic tagging of orientation-selective V1 neurons

Prior to all procedures for targeted recombination in “visual engram” neurons, mice were habituated for 3 days to gentle handling procedures. After habituation, at ZT0, the mice were placed in this square arena surrounded by 4 LED monitors. Each monitor presented a single-orientation (X°) phase-reversing grating stimulus (1 Hz, 0.05 cycles/degree, 100% contrast) for 30 min (or, for negative controls shown in **Figure 4.2**, a dark screen). Immediately after stimulus or dark screen presentation, mice received an i.p. injection of tamoxifen (100mg/kg in 95% corn oil/ 5% ethanol), and were placed in complete darkness for the next 3 d to prevent further visually-driven recombination in V1. Following 3 d of constant dark housing, mice were returned to a normal 12 h:12 h LD cycle for 7 d prior to further experiments. cfos-CRE^{ER} mice (Guenthner et al 2013; B6.129(Cg)-*Fos*$^{tm1.1(cre/ERT2)Luo}$/J; Jackson) crossed to either B6.Cg-

Gt(ROSA)26Sor$^{tm9(CAG\text{-}tdTomato)Hze}$/J, B6.Cg-*Gt(ROSA)26Sor*$^{tm32(CAG\text{-}COP4*H134R/EYFP)Hze}$/J, or B6.Cg-*Gt(ROSA)26Sor*$^{tm40.1(CAG\text{-}aop3/EGFP)Hze}$/J (Jackson) mice to induce CRE recombinase-mediated expression of tdTomato, ChR2, or ArchT.

Histology and immunohistochemistry

At the conclusion of each experiment, mice were deeply anesthetized with pentobarbital, and transcardially perfused with saline and 4% paraformaldehyde. Brains were dissected, post-fixed, cryoprotected in 30% sucrose, and cryosectioned at 50 µm. Transgene expression in V1 was verified for all experiments using CRE-dependent transgenic lines prior to subsequent data analysis. For electrophysiological recordings in V1, electrode placement was verified prior to data analysis. Immunohistochemistry for cFos was carried out using rabbit-anti-cfos 1:1000 (Abcam; ab190289) and secondary donkey-anti-rabbit conjugated to Alexa Fluor 405 (1:200; Abcam; ab175651); coronal sections containing V1 were mounted using Fluoromount-G (Southern Biotech). Co-labeling of tdTomato and anti-cFos was quantified using Image J software in 6 sections containing V1 from each mouse, average co-labeling values for each mouse are reported in **Figures 4.2** and **4.4**.

V1 visual response recordings, optogenetic manipulations, and data analysis

For anesthetized recordings of V1 neurons' visual responses and firing, mice were anesthetized using a combination of isoflurane (0.5-0.8%) and 1 mg/kg chlorprothixene (Sigma). Data was acquired using a 32-channel Plexon Omniplex recording system, using previously-described methods[29,32]. A 2-shank, linear silicon probe (250 µm spacing between shanks) with 25 µm inter-electrode spacing (16 electrodes/shank; Cambridge Neurotech) was slowly advanced into V1 until stable recordings (with consistent spike

waveforms continuously present for at least 30 min prior to baseline recording) were obtained. Orientation tuning curves for recorded neurons were generated by presenting a series of 8 full-field phase-reversing oriented gratings (0, 22.5, 45, 67.5, 90, 112.5, 135, or 157.5 degrees from horizontal, 1 Hz, 0.05 cycles/degree, 100% contrast, 10 s duration) and a blank screen (to evaluate spontaneous activity) presented repeatedly (4-8 times each) in an interleaved manner.

For recordings during rhythmic optogenetic activation of TRAPed neurons in ChR2-expressing mice (**Figure 4.5**) tuning curves were generated: 1) at baseline, 2) after a 20-30 min period without optogenetic manipulation, and 3) after a 20-30 min period of 1 Hz optogenetic stimulation. Optogenetic stimulation consisted of blue light pulses (10 ms, 473 nm, 10 mW power) delivered at 1 Hz. Only neurons stably recorded throughout all phases of the experiment (shown in **Figure 4.5A**) were included in firing and visual response analysis.

To assess effects of optogenetic inhibition of TRAPed V1 neurons in ArchT-expressing mice (**Figure 4.6**) recordings consisted of a 30-min spontaneous activity recording with no manipulation, a 30-min recording with periodic inhibition (532 nm green light, 15 mW, delivered in cycles of 5 s on, followed by a 500 ms offramp and a 1-s off period). Following these recordings, two orientation tuning curves were generated for all recorded neurons: 1) a baseline without inhibition, and 2) with inhibition of TRAPed V1 neurons occurring during 10-s presentations of oriented grating stimuli. Only neurons stably recorded throughout all phases of the experiment (shown in **Figure 4.6A**) were included in firing and visual response analysis.

For all recordings, stable single units were isolated using PCA-based analysis and MANOVA-based cluster separation, implemented using Plexon Offline Sorter software and previously-described methods[29,32]. Units that could not be reliably discriminated, or had refractory period violations in their spiking patterns, were eliminated from subsequent analyses. Changes in orientation tuning were assessed relative to the orientation of the TRAPed ensemble (X°), based on neurons mean firing rate responses to gratings of different orientations. For each tuning curve, an orientation preference index (OPI) was calculated for X° and the orthogonal stimulus orientation (X°/ X+90°), as described previously[29,33,34]. % changes in OPI (across optogenetic stimulation or control conditions) were calculated as $[(OPI^{pre}-OPI^{post})/OPI^{pre}] *100$. Firing responses of neurons during rhythmic optogenetic stimulation in ChR2-expressing mice was assessed from Z-scored perievent rasters centered on blue light onset; significance of time-locked excitation or inhibition was calculated based on positive or negative Z-score deviations beyond the 99% confidence interval (Neuralynx; Plexon). Changes in firing during optogenetic inhibition in ArchT-expressing mice were calculated for each neuron within the inhibition recording period, by comparing mean firing rate during the last 1.5 s of each green light delivery period with mean firing rate during the subsequent 500 ms offramps and 1-s off period.

Power spectral density for local field potentials was detrended using NeuroExplorer software (Plexon) with a single taper Hann Windowing Function with 50% window overlap. These were averaged across all active electrodes on each silicon probe shank. Distributions of power (between 0 and 20 Hz) were compared statistically using KS tests.

Surgical procedures

For V1 optical fiber implantation, mice were anesthetized using 1-2% isoflurane. Optical fibers (0.5 NA, 300 um core, ThorLabs) were positioned bilaterally at the surface of V1 at a 80 degree angle relative to the cortical surface (2.9 mm posterior, 2.7 mm lateral). Implants were secured to the skull with an anchor screw positioned anterior to bregma, using Loctite adhesive. For EEG/EMG recordings to differentiate sleep states, in addition to bilateral V1 optical fibers, mice received an EEG screw over V1 (2.9 mm posterior, 2.3 mm lateral), a reference screw over the cerebellum, and an additional EMG electrode in nuchal muscle. Mice were allowed 10 days of postoperative recovery before procedures to induce transgene expression in V1.

Optogenetic manipulations in behaving animals

Two cohorts of implanted mice, expressing ChR2 in the TRAPed ensemble, were used to test perception of optogenetic activation of this cell population. Prior to behavioral training and testing, these mice were habituated to handling and tethering (for light delivery to V1) procedures for 3 days. The first cohort underwent cued fear conditioning as described above in context A at ZT0, with 30-s blocks of rhythmic light delivery to V1 (1 Hz, 10 mW, 10 ms pulses) serving as a proxy shock cue (i.e., substituting for visual oriented grating presentation). Following 3 optogenetic stimulation-shock pairings, these mice were returned to their home cages and allowed *ad lib* sleep until ZT12. At ZT 12, they were placed in context B and freezing responses were assessed for visual presentation of both the same orientation as the TRAPed ensemble (X°) and an alternate orientation (Y°), as described above. A second cohort of mice underwent visually-cued fear conditioning to the same angle as the TRAPed ensemble (X°) in context A at ZT0.

After conditioning, they were returned to their home cage for *ad lib* sleep. At ZT12, they were tested in context B, where freezing behavior was assessed before, during, and after a period of 1 Hz light delivery to V1 (3 min before, 3 min during, and 1 min after).

To assess effects of sleep-targeted inhibition of visual engram neurons, 10 days after EEG/EMG and optical fiber implantation, mice underwent procedures to induce expression of ArchT in the TRAPed orientation-specific ensemble. Following 3 days of habituation to handling and tethering (for light delivery to V1 and EEG/EMG recording), these mice underwent 12 h sleep/wake baseline recordings, starting at ZT0. The next day, mice underwent visually-cued fear conditioning at ZT0, using either the same orientation as the TRAPed ensemble (X°) or an alternate orientation (Y°) as a cue for foot shock. They were then returned to their home cage for *ad lib* sleep. For the first 6 h post-conditioning, a subset of mice expressing ArchT underwent periodic optogenetic inhibition targeted to both NREM and REM sleep. The state targeting was based on EEG signals, EMG signals, and the animal's behavior. A control group of mice underwent the same procedures; however, they were not expressing ArchT. At ZT12, all mice were placed in context B to assess freezing responses to both X° and Y° oriented gratings, as described above.

EEG and EMG signals were used offline to classify each 10-s interval of baseline and post-conditioning recording periods as either wake, NREM, or REM sleep, using custom MATLAB software (Ognjanovski 2017; Durkin 2017). Additionally microarousals (periods of non-oscillatory activity between periods of NREM) as small as 5 s were identified as wake. Mean power spectral density was calculated separately within REM, NREM, and wake for each phase of recording, and within and outside of periods of light

delivery to V1, as described previously (Durkin 2017). The power spectra were calculated as percent of the total power spectral density.

Statistical Methods

All statistical analyses were done using GraphPad Prism. Prior to making comparisons across values, the normality of distributions was tested using the D'Agostino-Pearson ominbus k2 test. If the distribution was non normal or if the n value was too low to test normality, nonparametric statistical tests were chosen. If the data involved multiple measures of the same information from one animal (e.g. multiple images taken from the same animal for immunohistochemistry), nested statistics were used. All statistical tests were two-tailed. For each specific data set the statistical tests used are listed in the **Results** section. P values are represented as * p≤0.05, ** p≤0.01, *** p≤0.001, ****p≤0.0001

4.4 Visually cued fear memory consolidation is disrupted by sleep deprivation

We first tested the role of sleep in consolidation of a fear memory associated with a specific visual cue. At ZT0, wild-type mice underwent cued fear conditioning in a novel arena (context A), in which 3 presentations of a 30-s phase-reversing grating (of a specific orientation X°) co-terminated with a 2-s foot shock. Mice were then returned to their home cage and were either allowed *ad lib* sleep for the next 12 h, or were sleep deprived (SD) for 6 h and then permitted 6 h of *ad lib* recovery sleep. At ZT12, fear memory associated with cued grating was assessed in a second novel context B. During testing, mice were exposed to flickering gratings of the shock cue (X°) and a different orientation (Y°) (**Figure 4.1A**). As shown in **Figure 4.1B**, mice allowed *ad lib* sleep showed significantly higher freezing responses to the shock cue than the neutral cue (two-way

RM ANOVA, effect of sleep condition: $p = 0.014$, effect of cue orientation: $p < 0.001$, sleep condition × orientation interaction: $p = 0.047$). Both sleeping and SD mice discriminated between the shock and neutral cue ($p < 0.0001$ for sleep, $p = 0.03$ for SD, Holm-Sidak *post hoc* test), however, SD mice displayed significantly less freezing to the shock cue than mice allowed *ad lib* sleep ($p = 0.002$, Holm-Sidak *post hoc* test). To compare discrimination between cues, a discrimination index was calculated. Both freely sleeping and SD mice showed discrimination that differed from chance values; however, this effect was far clearer in mice allowed *ad lib* sleep (Wilcoxon signed rank test; Sleep: $p = 0.0003$, SD: $p = 0.049$). **Figure 4.1** shows data for both female and male mice (males - filled symbols, females - open symbols; a breakdown by sex is provided in **Figure 4.S1**). Both sexes displayed discrimination between shock and neutral cues when allowed *ad lib* sleep ($p = 0.001$ and $p = 0.007$ for males and females respectively, Holm-Sidak *post hoc* test) and impairment when sleep deprived (*N.S.* for shock vs. neutral, Holm-Sidak *post hoc* test). Both sexes showed significant discrimination from random chance only when sleep was allowed (p=0.0156 for both male and female sleep, *N.S.* for male and female SD, Wilcoxan signed rank test). Thus, for subsequent analysis, both sexes were used.

The circuitry in the primary visual cortex (V1) underlying visually-cued fear conditioning could be specifically amenable to alteration by sleep[29,33–35]. However, prior studies using tone-cued fear conditioning have provided conflicting results on the sleep-dependence of cued fear memory consolidation[36–39]. We hypothesized that these discrepancies are due to differences in the timing of either training or testing (or both) between studies. We performed a time course of fear memory testing for mice trained at ZT0 - and found that mice showed different visual cue discrimination performance when

tested 12, 24, and 36 hours after visually-cued fear conditioning - with better discrimination seen at the two ZT12 time points (ZT 12 and 36; **Figure 4.S2**).

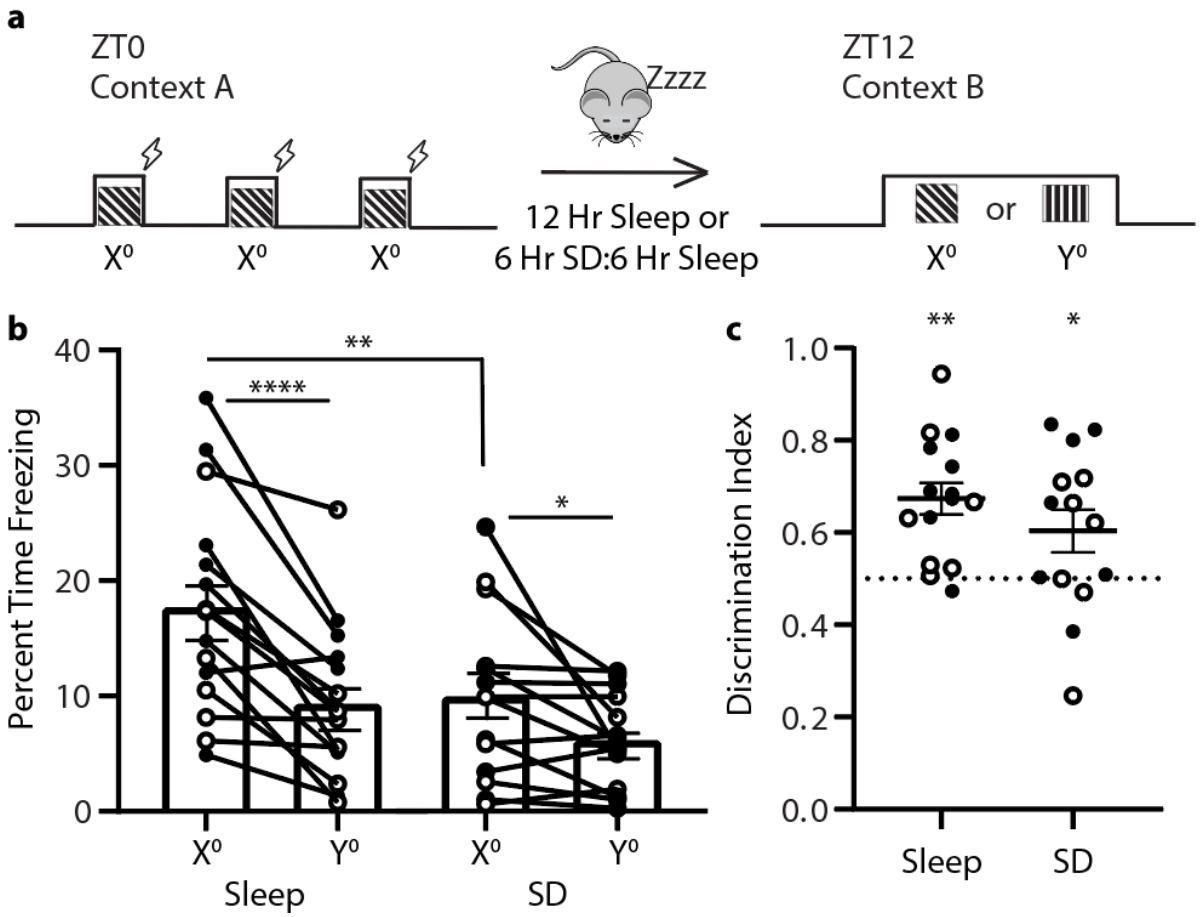

Figure 4.1. Consolidation of visually-cued fear memory is enhanced by post-conditioning sleep. ***(a)*** At ZT0, mice underwent three stimulus-shock pairings in context A. After either 12 h of *ad lib* sleep or 6 h sleep deprivation (SD) followed by 6 h *ad lib* sleep, mice were exposed to the shock cue (X° grating) and a neutral cue (Y° grating) in context B. **(b)** Freezing behavior of the mice during the ZT12 test (Sleep: *n* = 15 - sleep, SD: *n* =14; males - solid symbols, females - open symbols). Mice allowed to sleep froze significantly more to the shock cue than mice who were sleep deprived (** indicates *p*=0.002 t=3.29 df=54 ,Holm-Sidak *post hoc* test). Both the sleep and SD mice showed higher freezing the the shock cue (**** indicates *p*<0.0001 t=5.255 df=27, * indicates p=0.028 t=2.3 df=27, Holm-Sidak *post hoc* test). Sleep x orientation interaction was significant (*p*=0.047 F=4.365 df=1, Two-way RM ANOVA). **(c)** Freezing behavior quantified a discrimination index [X°/(X°+Y)] for each mouse and compared to chance performance (* indicates *p* =0.0494, ** indicates *p* = 0.0003, Wilcoxon signed rank test vs. chance).

4.5 Genetic targeting of orientation-selective neuronal populations in V1

In order to characterize and manipulate activity in neuronal populations selectively activated by a specific oriented grating in primary visual cortex (V1) (i.e., putative visual engram neurons), we used previously described techniques for transient recombination in activated populations (TRAP)[21]. For the following studies, cfos-CRE^{ER} mice were crossed to mice expressing tdTomato in a cre-dependent manner (*cfos::tdTom*), and presented with either an oriented grating (X°) or a dark screen (**Figure 4.2A**). Immediately following the visual stimulus presentation, we administered tamoxifen, and the mice were housed in complete darkness for the next 3 days to prevent additional visually-driven recombination in V1. 11 days later, visually-driven V1 tdTomato expression was quantified. The dark screen presentation induced very low V1 labelling; in contrast, oriented grating presentation led to higher levels of labelling (**Figure 4.2B-C**; nested t-test, p=0.0001).

To test the orientation-specificity of the TRAPed ensemble, mice were either presented with the same oriented grating (X°) or an alternate oriented grating (Y°) prior to sacrifice (**Figure 4.2D**). cFos protein expression was evaluated after the second presentation (**Figure 4.2E**). The TRAPed ensemble shows a significantly higher percent of cells reactivated after re-exposure to the same orientation (X°; average 32%, SEM 3%) than a different orientation (Y°; average 21%, SEM 2%) (**Figure 2E-F**). This level and specificity of cFos overlap is comparable to what has been reported for auditory sensory stimuli[21]. Together these data suggest that TRAP provides genetic access to orientation-specific ensembles.

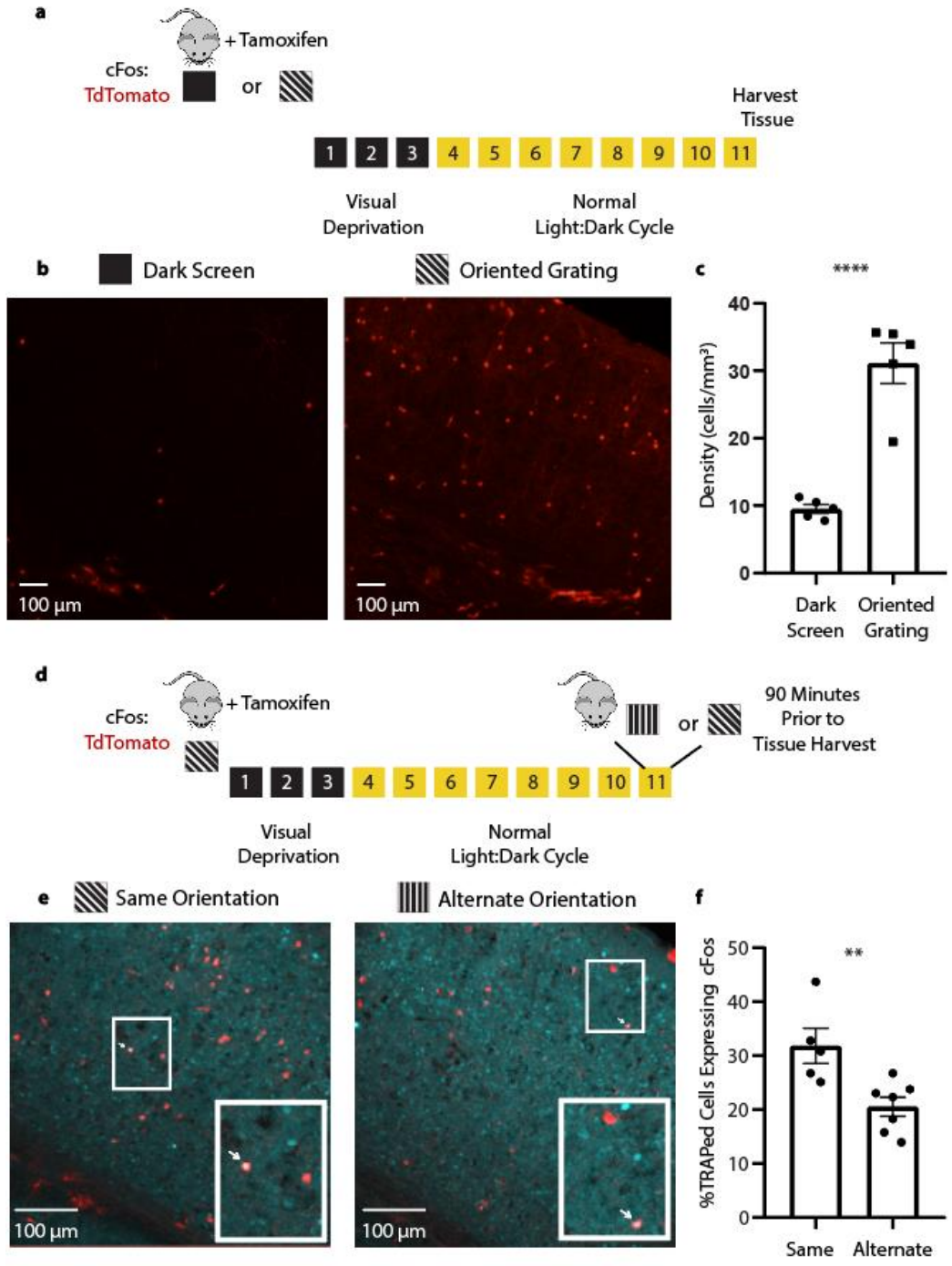

Figure 4.2. TRAP labels orientation-selective V1 ensembles. (a) *cFos::tdTom* mice were presented with either a dark screen or an oriented grating (X°) and were then injected with tamoxifen prior to 3 d of housing in complete darkness. **(b-c)** Representative V1 tdTomato labelling quantified 11 d after tamoxifen administration. **** indicates p =0.0001 t=7.068 df=8 for dark screen vs. X°, nested t-test (n = 5 mice/condition) **(d)** Prior to tissue harvest, mice were either re-exposed to gratings of the same orientation (X°) or an alternate orientation (Y°). **(e-f)** Representative images showing overlap of tdTomato (red) and cFos protein (cyan). An example of colocalization (quantified in **f**) is indicated with a white arrow for each image in the inset. ** indicates p=0.0092 t=3.219 df=10 nested t-test (n = 5 mice for X°, n = 6 mice for Y°).

4.6 Optogenetic activation of orientation-selective V1 neurons generates an orientation-specific percept

To further test the orientation selectivity of the TRAPed ensemble alongside evaluating the behavioral significance of this population, we used TRAP to drive expression of channelrhodopsin2 (*cfos::ChR2*). As shown in **Figure 4.3A**, cFos:ChR2 mice were implanted with bilateral V1 optic fibers and recombination was induced to a single orientation (X°). 11 days later, two variants of visually-cued fear conditioning were performed. In the first variant, the footshock was paired with optogenetic stimulation of the TRAPed ensemble (1 Hz light delivery) rather than visual stimulation (**Figure 4.3B**). During subsequent visual testing, the mice showed significantly higher freezing to the TRAPed angle (X°) than an alternate orientation (Y°) (ratio paired t-test, $p = 0.0081$) - showing discrimination between the gratings (Wilcoxon signed rank test vs. chance, $p = 0.0195$) (**Figure 4.3C**).

In the second variant, mice underwent visually-cued fear conditioning to the same orientation as the TRAPed ensemble. During subsequent testing, they received bilateral 1 Hz light delivery to V1 instead of a visual stimulus. These mice showed significantly greater freezing behavior during optogenetic stimulation than before and after stimulation (**Figure 4.3E**; $p = 0.0028$ for each Holm-Sidak *post hoc* test). Both of these results indicate that optogenetic activation of the TRAPed ensemble is sufficient to generate a percept of the oriented grating stimulus, consistent with recent data[40]. Moreover, these data demonstrate that the TRAPed ensemble can substitute behaviorally as a cue for either encoding or recalling fear memory.

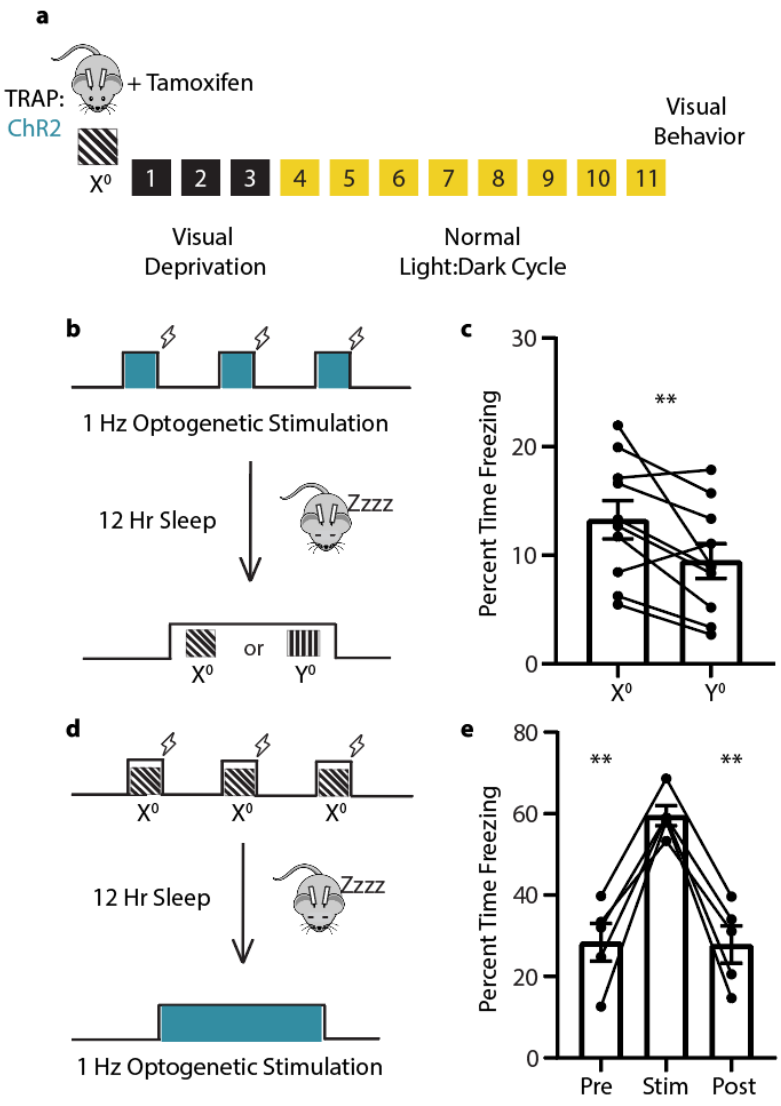

Figure 4.3. Optogenetic stimulation of TRAPed V1 neurons mimics visual experience. (a) *cFos::ChR2* mice with bilateral V1 fiber optics had recombination induced to a specific angle (X°). 11 days later, visual behavior was run. **(b-c)** At ZT 0, the mice received bilateral V1 optogenetic stimulation paired with foot shocks in lieu of the oriented grating visual stimuli used for cued conditioning in **Figure 1**. At ZT 12, the mice were presented with the same oriented grating used for TRAP (X°) and an alternate orientation (Y°). Optogenetically-cued conditioning resulted in higher subsequent cued freezing responses to X° relative to Y° (n = 10 mice; p = 0.0081, t =3.384, df = 9, ratio paired t-test). **(d-e)** At ZT0, a second cohort of mice underwent visually-cued fear conditioning to the same orientation as the TRAPed ensemble. At ZT12, the mice received optogenetic stimulation in place of a visual test. Freezing behavior was higher during optogenetic stimulation than before or after stimulation (n = 5 mice; Pre vs Stim - p = 0.0028 t = 7.300 df=4, Stim vs Post - p=0.0028 t=7.851 df=4; Holm-Sidak post hoc test, RM one-way ANOVA).

4.7 Orientation-selective V1 ensembles are reactivated during sleep-dependent consolidation of visually-cued fear memory.

Since sleep facilitates consolidation of visually-cued fear memory and activation of the TRAPed ensemble can provide cue-selective information, we next evaluated whether TRAPed population is selectively activated during sleep after visually-cued fear conditioning. As shown in **Figure 4.4A,** we used *cfos::tdTom* mice to TRAP the ensemble for a specific oriented grating (X°). 11 days later the mice underwent cued conditioning to either the same angle (X°) or an alternate angle (Y°). They were then returned to their home cage and allowed *ad lib* sleep over the next 4.5 h, after which they were sacrificed for V1 cFos immunostaining. When the cued orientation was the same as the orientation of the TRAPed ensemble (X°), 34 +/- 2% of tdTomato-expressing V1 neurons showed expression of cFos after subsequent sleep (**Figure4.4B**) - a level similar to that seen after same-orientation grating exposure (**Figure 4.2E**). When the cued orientation differed from the TRAPed ensemble, the percent overlap was significantly lower (26 +/- 1%). These results are in accordance prior work that have seen memory reactivation in the visual cortex during post learning sleep (Ji and Wilson 2007). These data suggest that V1 ensemble reactivation could serve as a plausible substrate underlying sleep benefits for visually-cued fear memory consolidation.

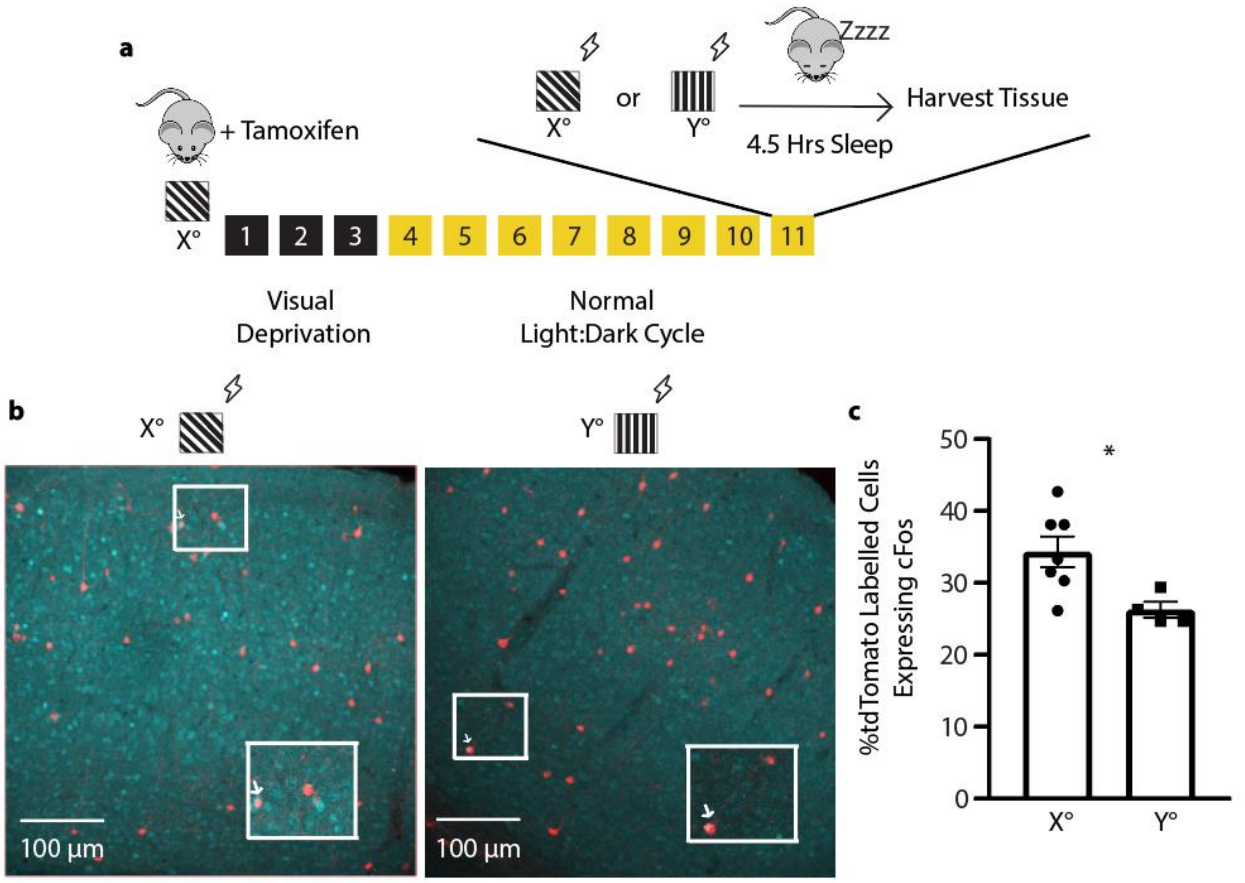

Figure 4.4. TRAPed V1 neurons selective for the conditioned stimulus are reactivated in post-conditioning sleep. (a) *cFos::tdTom* mice had recombination induced to a specific angle (X°). 11 days later, they were cue conditioned to either the same angle as induction (X°; *n* = 7 mice) or an alternate angle (Y°; *n* = 4 mice). All mice were allowed 4.5 h of post-conditioning *ad lib* sleep prior to tissue harvest. **(b-c)** Representative images showing overlap of cFos expression (cyan) with tdTomato (red). The boxed region is magnified as an inset with an arrow indicating an overlapping neuron. Expression of cFos in tdTomato-labelled cells was greater for mice conditioned to the same orientation used for TRAP labelling (* indicates *p*=0.0250 t=2.685 df=9, nested t-test).

4.8 Rhythmic offline reactivation of orientation-selective V1 ensembles induces plasticity and alters representation of orientation in V1.

To test whether sleep-associated reactivation of orientation-selective neurons could impact the representation of orientation in V1, we examined how rhythmic optogenetic activation of the TRAPed ensemble affected V1 neurons' response properties. We recorded neuronal firing responses in V1 from anesthetized *cfos::ChR2* mice with recombination induced to a specific oriented grating (X°). Using high density silicon probes, we recorded firing patterns and visual responses before, during and after a period of rhythmic (1 Hz) light delivery. We first generated tuning curves to assess orientation preference for each V1 neuron, measuring firing rate responses to a series of 8 different oriented gratings. This orientation preference test was followed by a 20-30 min period without optogenetic stimulation, a second orientation preference test, a 20-30 min period of 1 Hz optogenetic stimulation, and then a final orientation preference assessment (**Figure 4.5A**).

V1 neurons showed heterogeneous firing responses during rhythmic optogenetic stimulation of the TRAPed ensemble (**Figure 4.5B**). A small fraction of the recorded neurons (4%) fired selectively during the 10-ms light pulses, 1% were significantly inhibited, and 1% showed only long-latency (more than 200 ms) excitatory responses. The remaining recorded neurons were either unaffected by optogenetic stimulation (44%) or showed consistent firing 20-50 ms after light pulses (49%). These neurons firing within the 20-50 ms post-pulse window may be receiving excitatory input from the TRAPed population (**Figure 4.5C**). Rhythmic activation of the TRAPed ensemble did not

significantly alter the V1 local field potential (LFP) power spectrum (**Figure 4.5D**, N.S., K-S test).

To assess how optogenetic reactivation of the TRAPed population affects response properties in surrounding V1 neurons, orientation tuning curves for well-isolated and stably-recorded neurons were compared before vs. after optogenetic stimulation. While orientation preference for X° (vs. X+90°) was stable across 20-30 min period without optogenetic stimulation, a similar period of 1 Hz light delivery caused a selective shift in orientation preference across V1 toward the orientation of the TRAPed population. Shifts in orientation preference towards the orientation of the TRAPed ensemble (X°) were greater for those neurons that showed consistent excitatory responses 20-50 ms following light pulses, relative to neurons that did not show these responses (*N.S.* - not activated neurons, p = 0.0017 - activated neurons, nested t-test; **Figure 4.5e,f**). Critically, this shift is similar to that seen in V1 after presentation of oriented gratings, followed by a subsequent period of *ad lib* sleep [29,33,34]

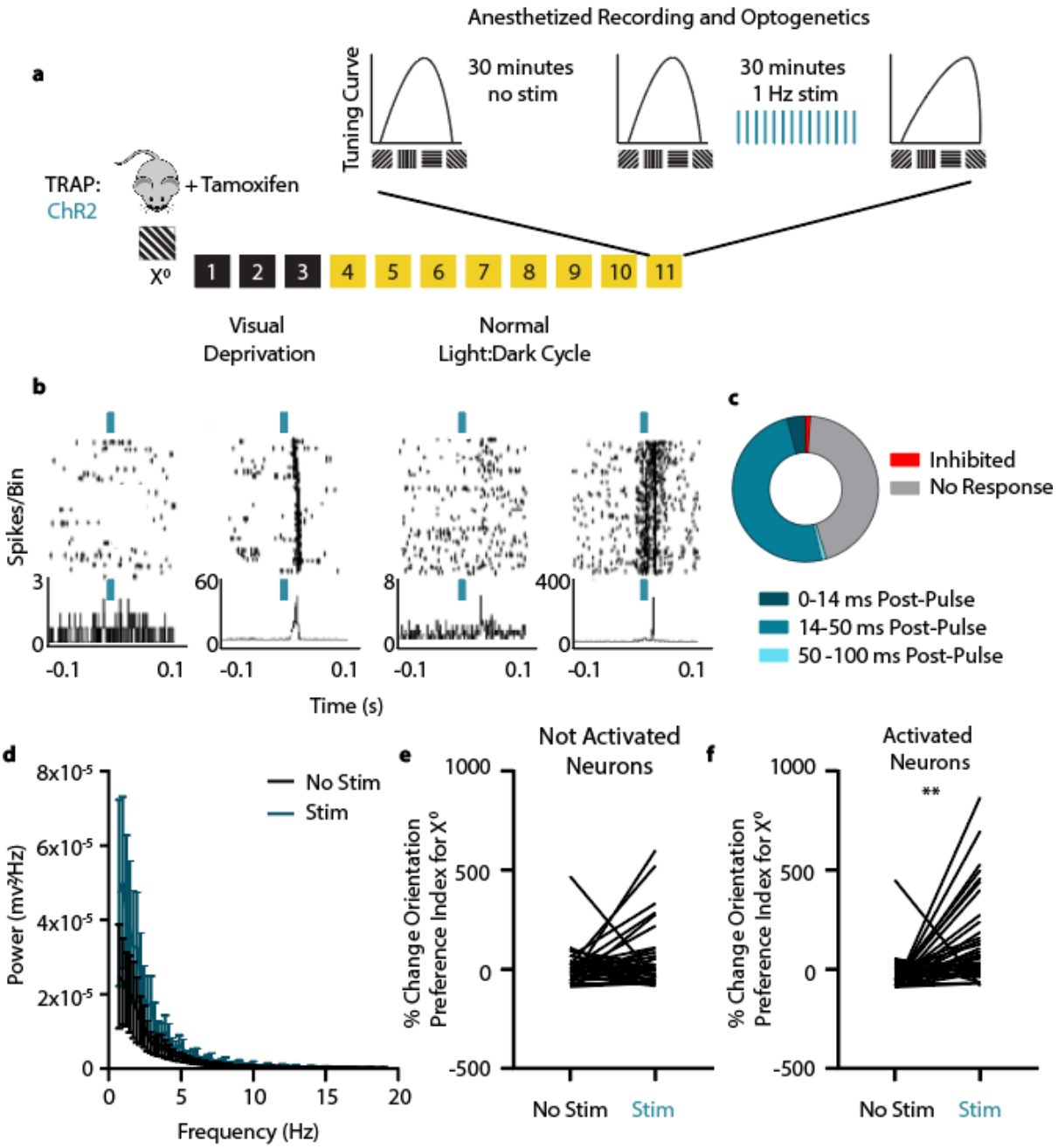

Figure 4.5. **Offline reactivation of orientation-selective TRAPed V1 neurons changes orientation representations in V1**. **(a)** *cFos::ChR2 mice* were presented with an oriented grating (X°) for TRAP. 11 days later, orientation tuning was measured repeatedly for V1 neurons recorded from anesthetized mice: at baseline, after a 20-30 min period without optogenetic stimulation, and after a 20-30 min period with 1 Hz light delivery. **(b)** Representative rasters and perievent histograms for 4 simultaneously-recorded neurons, showing diverse firing responses during optogenetic stimulation. **(c)** The majority of stably-recorded V1 neurons were reliably activated following light pulses, with variable lag times. A small proportion were inhibited by light delivery, and the remaining neurons were not affected (n=5 mice, n=62 neurons). **(d)** Power spectra for V1 LFPs showed no significant effect on ongoing rhythmic activity (*N.S.,*K-S test, n=5 mice) **(e-f)** After optogenetic stimulation, neurons that were not activated following light pulses showed no change in orientation preference (*N.S.*, nested t-test, n=5 mice, n=32 neurons). In contrast, activated neurons showed increased firing rate responses for gratings of the same orientation (X°) used for TRAP. (** indicates p=0.0017 t=3.272 df = 62, nested t-test, n=5 mice, n=30 neurons).

4.9 Sleep-associated reactivation of orientation-selective V1 neurons is necessary for consolidation of visually-cued fear memory

Since reactivation of orientation-selective populations occurs during post-conditioning sleep, and rhythmic reactivation of this population is sufficient to induce changes in orientation representations in V1, we next tested the necessity of sleep-associated ensemble reactivation for consolidation of visually-cued fear memory. To assess how inhibition of the TRAPed population affects firing in surrounding V1 neurons, we used TRAP to drive expression of ArchT (*cfos::ArchT*). We recorded spontaneous activity and visually responses in V1 neurons using high density silicon probes, before and during a period of optogenetic inhibition (**Figure 4.6A**).

Periodic inhibition (cycles of 5 s light delivery, followed by a 0.5 s ramp off, and 1 s off) led to heterogeneous changes in spontaneous firing (**Figure 4.6B-C**), with 34% showing no response (± 0-5% change in firing rate), 21% activated (> 5% increase in firing rate) and 34%, 9%, and 2%, respectively, inhibited slightly (6-33% decrease in firing rate), moderately (34-66% decrease), or strongly (67-100% decrease). Inhibition did not affect power spectral in the V1 LFP (**Figure 4.6D**, N.S., K-S test). Inhibition during presentation of oriented gratings led to a significant decrease in orientation preference for X° in inhibited neurons (**Figure 4.6f**, p =0.0065, nested t-test). There was no significant shift in non-inhibited neurons (**Figure 4.6e,** N.S., nested t-test). There was no significant shift in non-inhibited neurons. Together, these data indicate that inhibition of the TRAPed ensemble leads to changes in orientation representation across the population, without grossly disrupting network activity across V1.

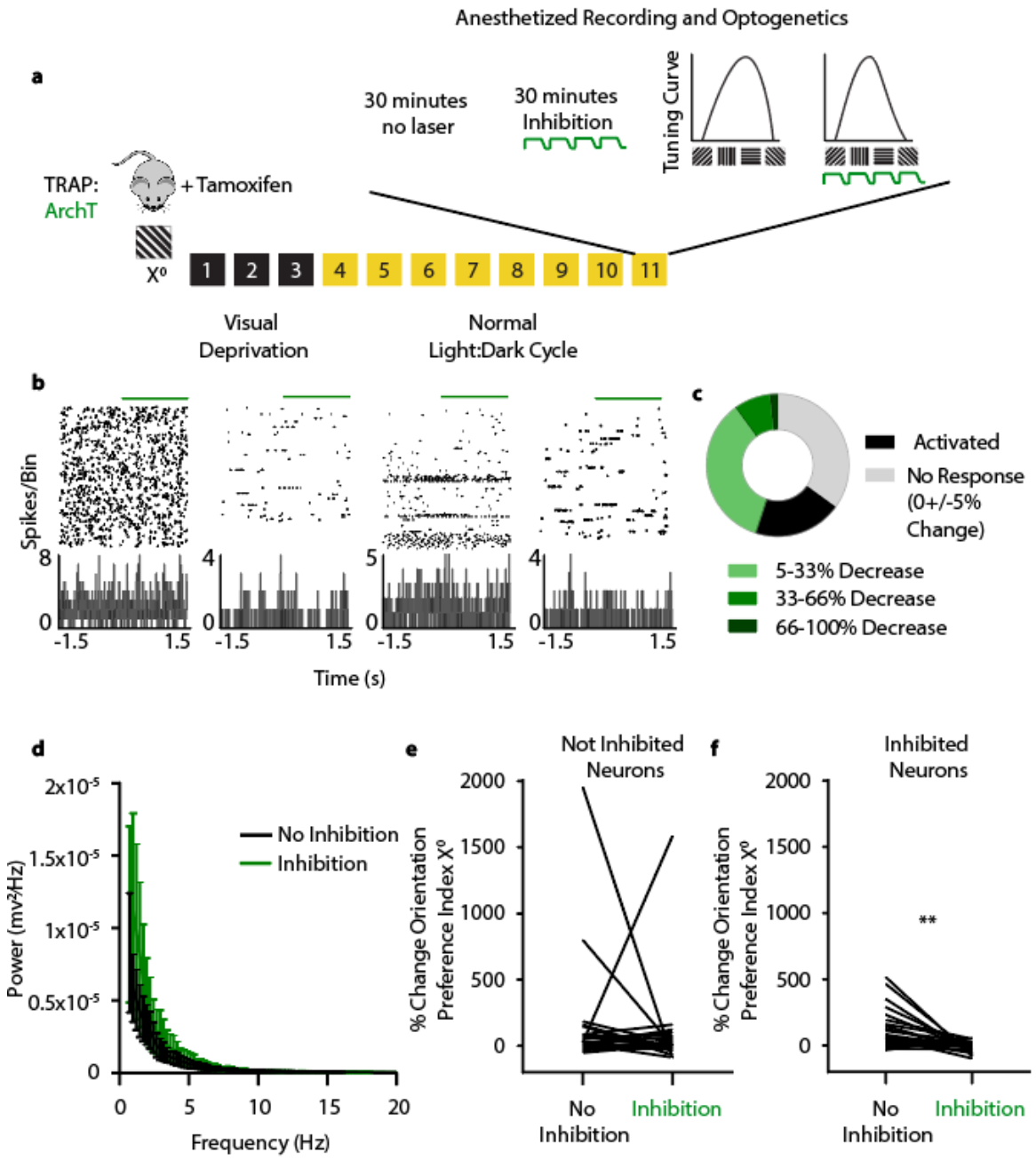

Figure 4.6. Optogenetic inhibition of orientation-selective TRAPed V1 ensembles alters orientation preference in surrounding V1 neurons. (a) *cFos::ArchT* mice were presented with an oriented grating (X°) for TRAP. 11 days later, V1 neurons were recorded from anesthetized mice across 30 minutes of optogenetic inhibition, and 30 minutes without inhibition. Afterward, orientation preference was assessed without optogenetic inhibition and with inhibition. **(b)** Representative rasters and perievent histograms for 4 simultaneously-recorded neurons, showing diverse firing responses during optogenetic inhibition. **(c)** Distributions of stably-recorded V1 neurons which were significantly inhibited, activated following light pulses, or unaffected by light delivery (n=5 mice, n=58 neurons). **(d)** Power spectra for V1 LFPs showed no significant change in rhythmic activity during periods of inhibition (*N.S.*, K-S test, n=5 mice). **(e-f)** During optogenetic inhibition, neurons that showed no decrease in firing rate showed no change in orientation preference (*N.S.*, nested t-test, n=5 mice, n=32 neurons). In contrast, neurons that were inhibited showed a reduced preference for gratings of the same orientation (X°) used for TRAP (** indicates p=0.0065 t=3.649 df=8, nested t-test, n=5 mice, n=26 neurons).

We next asked whether inhibition of V1 visual engram neurons (i.e., neurons encoding the orientation cues) during post-conditioning sleep disrupts consolidation of visually-cued fear. *cfos::ArchT* mice underwent visually-cued fear conditioning, using either the same orientation as the TRAPed ensemble (X°) or an alternate orientation (Y°) as the cue - either matching inhibition and cued information (X° inhibition - X° cue) or inhibiting non-cued information (X° inhibition - Y° cue) (**Figure 4.7A**). They were then returned to their home cages for *ad lib* sleep. For the first 6 hrs following conditioning, the TRAPed population was inhibited during sleep (quantification of state targeting success rates is in **Figure 4.S3**). As shown in **Figure 4.1**, this six hour window is a critical time window for consolidation of visually-cued fear. Importantly, this manipulation did not significantly alter sleep architecture or power spectra (**Figure 4.S4**) - indicating that the inhibition selectively disrupts reactivation without disrupting other features of sleep. Mice who were cued to the same orientation as the TRAPed ensemble showed high levels of generalized fear - indicating disrupted fear memory consolidation. In contrast, both control mice (not expressing ArchT), and mice shocked to an alternate cue, showed cued fear memory consolidation and discriminated between shock and neutral cues at ZT12 (**Figure 4.7b-c**). Together these data suggest that selective reactivation of V1 visual engram neurons during post-learning sleep provides an essential substrate for consolidation of an associative visually-cued memory.

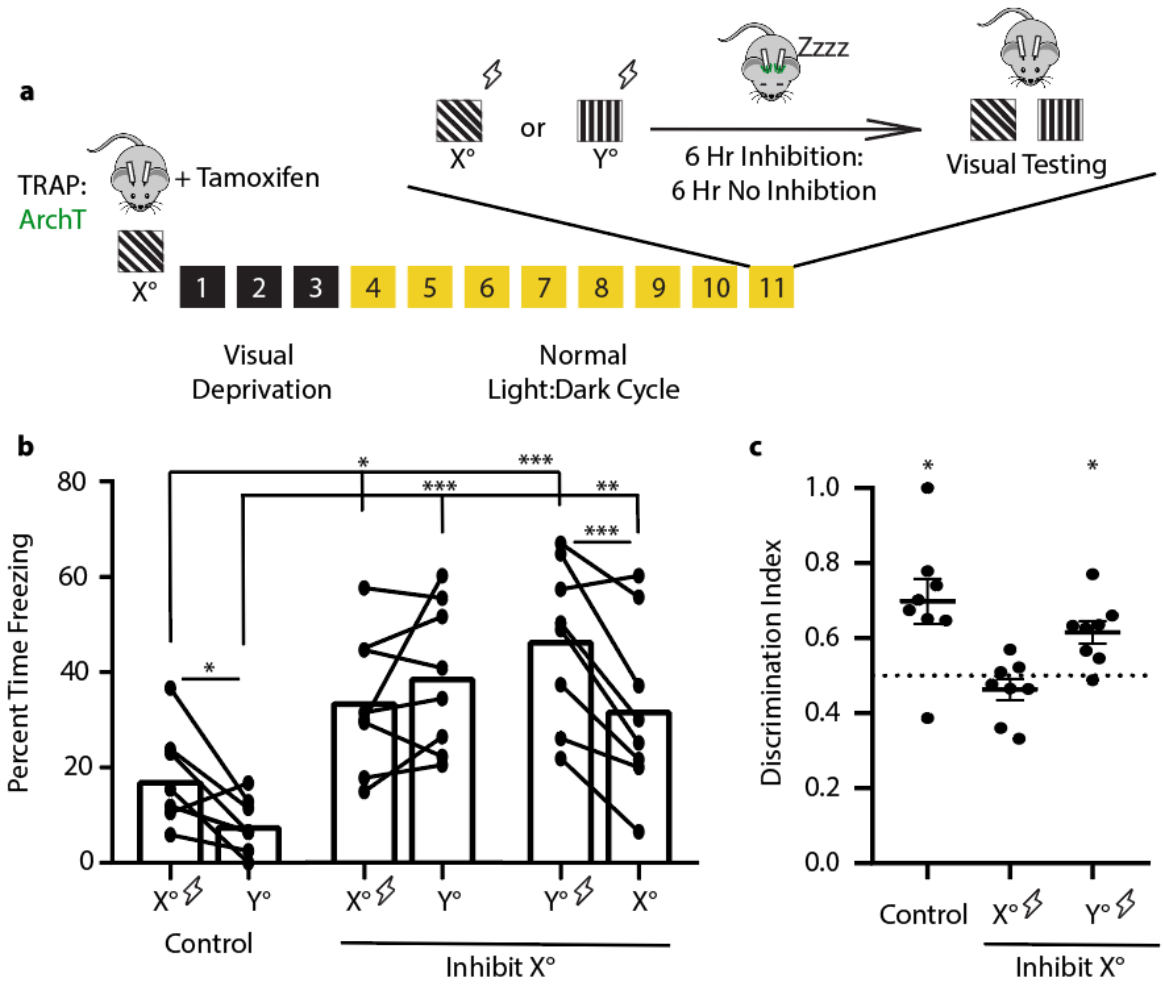

Figure 4.7. Sleep-specific inhibition of a V1 engram disrupts visually-cued fear memory consolidation. (a) *cFos::ArchT* mice implanted with bilateral V1 optical fibers and EEG/EMG electrodes were presented with X° for TRAP. 11 days later, mice were conditioned using either the same orientation (X°) or an alternate orientation (Y°). Post-conditioning, the mice slept, with sleep-specific inhibition during the first 6h. **(b)** The controls and mice cued to Y° showed higher freezing to the shock than the neutral cue (* controls p=0.017 t=2.599 df=21, *** Y°-cued p<0.001 t=3.995 df=21; Holm-Sidak *post hoc* test, RM two-way ANOVA), while the mice cued to X° did not (N.S. Holm-Sidak *post hoc* test). Both mice cued to X° (* shock cue p=0.028 t=2.321 df=42, *** neutral cue p<0.001 t=4.395 df=42; Holm-Sidak *post hoc* test) and mice cued to Y° showed higher freezing to both cues (*** shock cue p<0.001 t=4.147 df=42,** neutral cue p=0.002 t=3.423 df=42; Holm-Sidak *post hoc* test). The ANOVA effects: optogenetic condition (p<0.001 F=9.933 DF=2), cue condition (p=0.007 F=9.006 DF = 1), and opto condition x cue condition (p=0.003 F=7.828, DF=2). **(c)** Controls and mice cued to Y° show significant discrimination, while mice cued to X° did not (* indicates p=0.0156 for both control and Y° shock; Wilcoxon signed rank test).

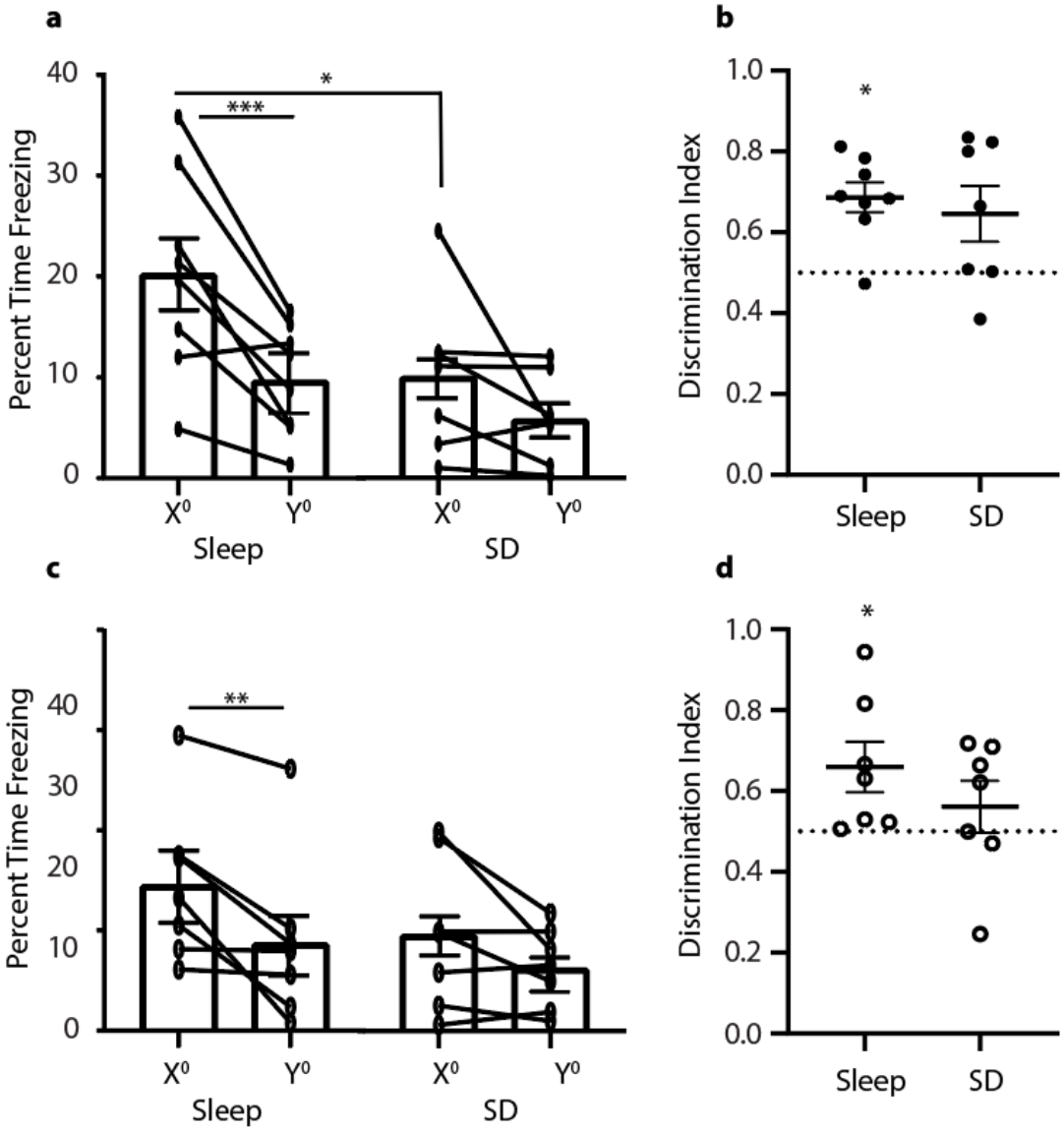

Figure 4.S1. Female and male freezing. (a) Male mice allowed to sleep froze significantly more to the shock cue (X°) than mice who were sleep deprived (* indicates p=0.014 t=2.673 df = 26, Holm-Sidak post hoc test; Two-way RM ANOVA). The sleep group froze significantly more to the shock cue than the neutral cue (*** indicates p=0.001 t=4.182 df=13, Holm-Sidak post hoc test; Two-way RM ANOVA).The ANOVA effects are as follows: effect of sleep condition (N.S.), effect of cue orientation (p= 0.002 F=16.027 df=1), effect of sleep condition x orientation interaction (N.S.). **(b)** Sleeping male mice showed cued discrimination above random chance (p=0.0156 Wilcoxon signed rank test vs chance). **(c)** Female mice who were allowed sleep froze significantly more to the shock cue than the neutral cue (** indicates p=0.007 t=3.251 df=12, Holm-Sidak post hoc test; Two-way RM ANOVA). The ANOVA effects are as follows: effect of sleep (N.S.), effect of cue orientation (p=0.0034 F=13.19 df=1), sleep condition x orientation interaction (N.S.). **(d)**Female mice allowed ad lib sleep showed significant discrimination, while sleep deprived mice did not (p=0.0156 Wilcoxon signed rank test vs chance).

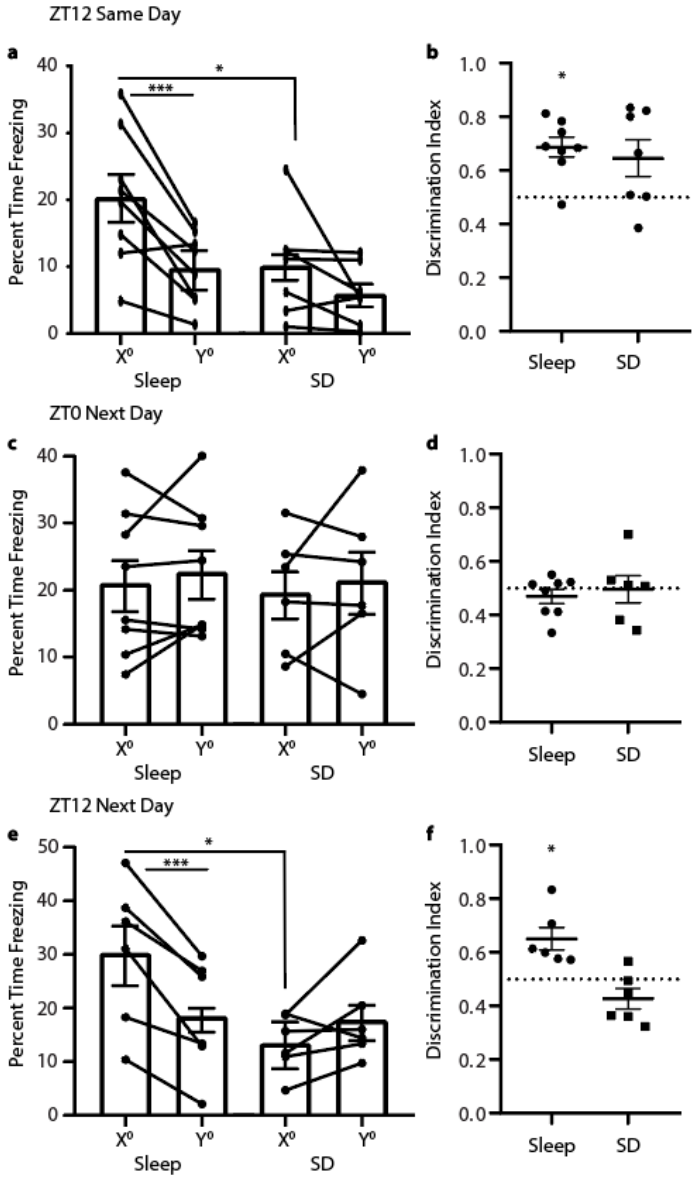

Figure 4.S2. Time course of freezing testing. (a) ZT12 test day of conditioning. Sleep mice froze more to the shock cue than SD mice (* indicates p=0.014 t=1.57 df=26, Holm-Sidak post hoc test; Two-way RM ANOVA). The sleep mice froze more to the shock cue than the neutral cue (***p=0.001 t=4.182 df=13, Holm-Sidak post hoc test). The ANOVA effects are: sleep condition (N.S.), cue orientation (p= 0.002 F=16.027 df=1), sleep condition x orientation interaction (N.S.).**(b)** Sleeping mice showed discrimination (* p=0.0156 Wilcoxon signed rank test vs chance) **(c)** ZT0 test the next day. There were no differences within groups or across groups (N.S., Holm-Sidak post hoc test; Two-way RM ANOVA). All ANOVA effects were not significant. **(d)** Neither group discriminated beyond chance (N.S., Wilcoxon signed rank test vs chance). **(e)** ZT 12 test the next day. Sleep mice froze more to the shock cue than SD mice (*p=0.013 t=2.934 df=20,Holm-Sidak post hoc test). Sleep mice froze more to the shock cue than the neutral cue (***p<0.001 t=4.881 df=10). The ANOVA effects are: sleep condition (N.S.), cue orientation (N.S.), sleep condition x orientation interaction (p<0.001 F=22.331 df=1). **(f)** Mice allowed ad lib sleep showed discrimination above random chance (*p=0.0313, Wilcoxan signed rank test vs chance)

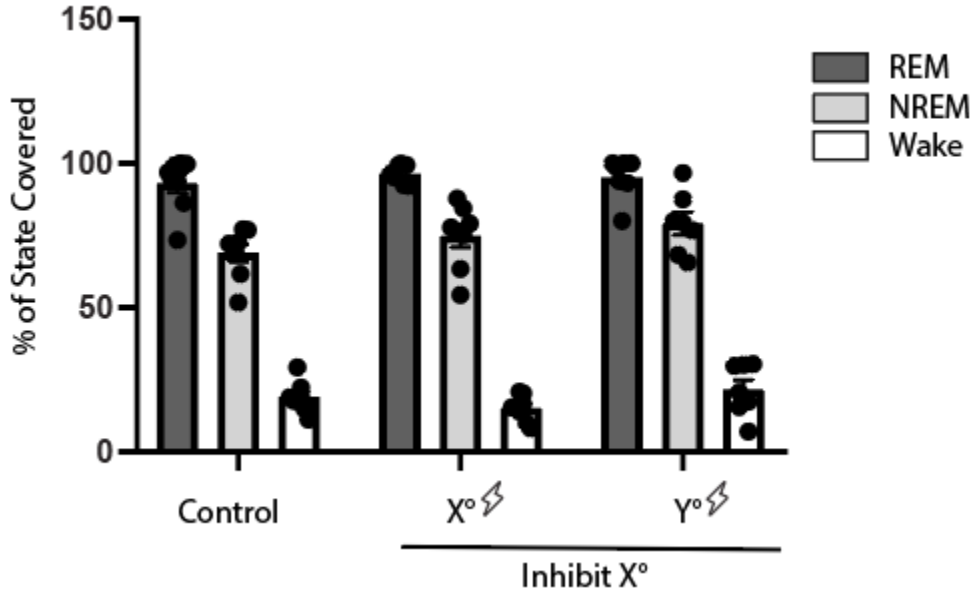

Figure 4.S3. Success rates of state-specific inhibition targeting. There were no significant differences in state coverage between different experimental groups (Two-way RM ANOVA, Holm-Sidak post hoc test; n=8 control, n=8 trained to X°, n=7 trained to Y°). In each group high levels of REM (average 93%+/-3, 96%+/-1, 96%+/-3) and NREM (69%+/-3, 75%+/-4, 79%+/-4) were covered. In each group low levels of wake were covered – Mostly reflecting microarousals (19%+/-2, 15%+/-2, 22%+/-3).

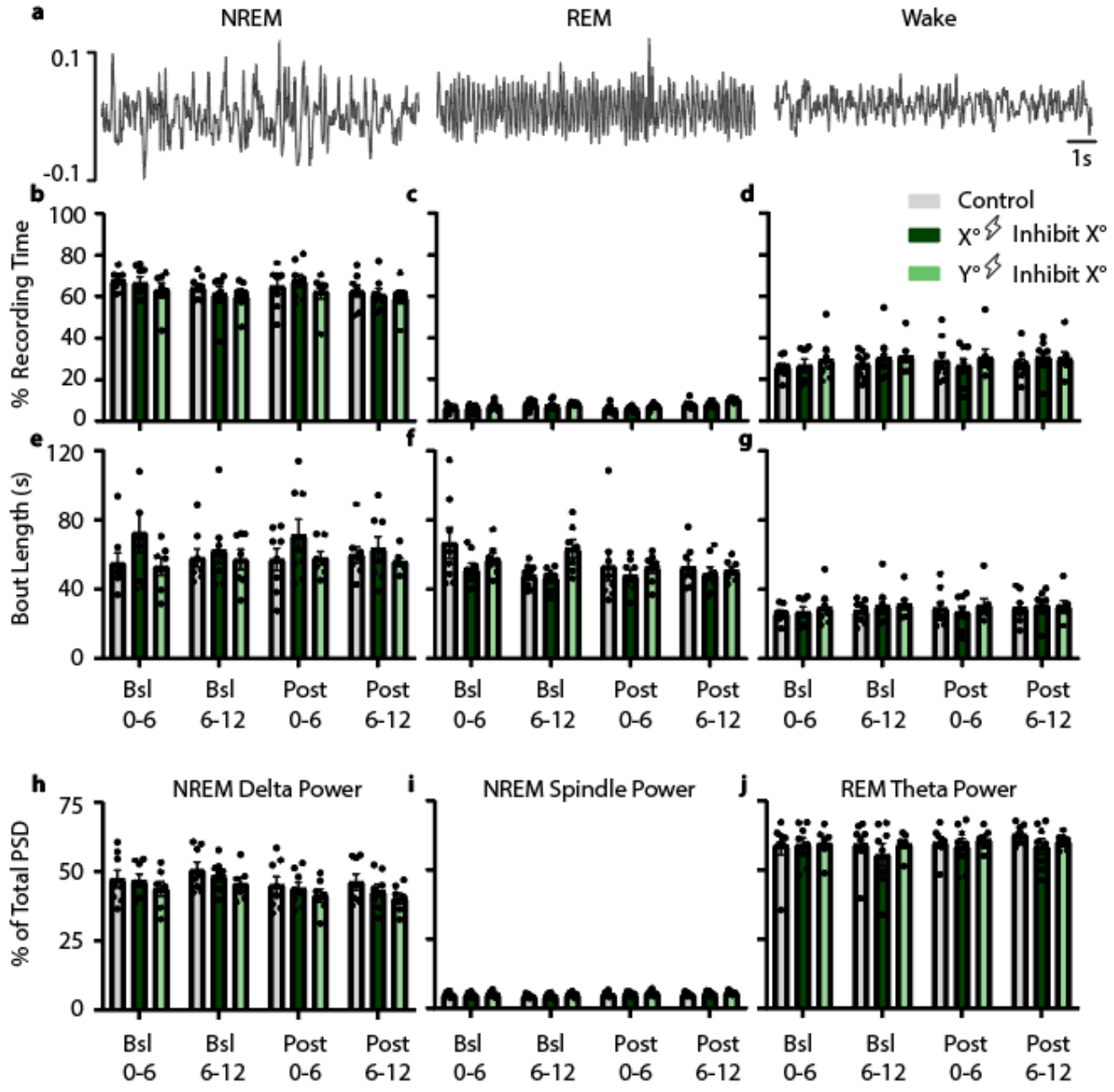

Figure 4.S4. Sleep architecture and power during baseline and inhibition. (a) Representative traces of EEG classified as NREM sleep, REM sleep, and wake. **(b-d)** Percent of recording time spent in each state across recording times and across experimental groups. There were no significant differences across experimental groups (n.s. Holm-Sidak post hoc test; Two-way RM ANOVA). **(e-g)** Average bout length for each state across recording times and across experimental groups. There were no significant differences across experimental groups (n.s. Holm-Sidak post hoc test; Two-way RM ANOVA). **(h-j)** Average power within NREM delta (0.5-4 Hz), NREM spindle (12-15 Hz), and REM theta (4-12 Hz) frequency bands across recording times and across experimental groups. There were no significant differences across experimental groups (n.s. Holm-Sidak post hoc test; Two-way RM ANOVA).

4.10 Discussion

Our present data demonstrate that orientation-selective V1 neurons involved in encoding a specific visually-cued fear memory (visual engram neurons) play an ongoing role in memory consolidation during subsequent sleep. After selective activation of these neurons during visually-cued fear conditioning, these neurons continue to be active during sleep in the subsequent hours (**Figure 4.4**) - a time window during which sleep plays a role in promoting consolidation (**Figure 4.1**). Activity in these neurons is sufficient to drive a percept which can substitute for the visual fear cue in mice during wake (**Figure 4.3**). It remains unclear how selective sleep-associated reactivation of these neurons affects the surrounding visual cortex (or interacts with circuitry engaged selectively by aversive conditioning). However, periodic optogenetic activation of these orientation-selective neurons is sufficient to drive shifts in orientation preference in surrounding neurons that show excitatory postsynaptic responses to their input (**Figure 4.5**). This leads to an increase in the representation of the visual engram neurons' preferred orientation in the surrounding V1 network. While the functions of such an increase in representation are currently unknown, this increase in representation for a specific orientation is seen in the visual cortex in mice[29,33,34,41,42], human subjects[43], and nonhuman primates as a result of orientation-specific experience and task training[44,45]. Thus, changes in representation in sensory cortex appear to be either a correlate, or a cause, of changes in orientation discrimination ability with experience.

We show conversely, that optogenetic inhibition of orientation-selective neurons acutely reduces the representation for the visual engram neurons' preferred orientation in the surrounding V1 network (**Figure 4.6**). Finally, we demonstrate that optogenetic

inhibition of these “visual engram” neurons during post-conditioning sleep dramatically disrupts consolidation of fear memories for specific visual cues (**Figure 4.7**). Mice with sleep-targeted inhibition of cue-activated neurons show high levels of general freezing behavior at testing, but no discrimination between cues of different orientations. Thus, their specific memory deficit seems to be due to an inability to link fear memory to a specific orientation cue during consolidation, rather than a disruption of fear memory *per se*.

This work links together two bodies of literature regarding the neural substrates of memory. One recent area of investigation has focused on the role of engram neurons which are activated by learning experiences, and whose activation is necessary and sufficient for memory recall[22,23,46]. However, the role these neurons play in the consolidation of memories following learning has been a matter of speculation. Here we show that the neurons engaged during learning play a necessary and instructive role over subsequent hours for long-term memory consolidation. A second body of literature has focused on replay of learning-associated activity patterns in specific neuronal ensembles as a mechanism for sleep-dependent facilitation of memory storage. While the phenomenon of replay during sleep has been widely reported[2,47,48], a causal role for sleep-dependent replay in memory consolidation has been difficult to prove. At least two technical obstacles have slowed progress toward understanding the role of replay in sleep-dependent consolidation. First, many tasks used in rodents to study replay phenomena (e.g. maze running) require several days of training prior to obtaining recordings of sequential firing patterns - a timescale incompatible with memory consolidation occurring across a single sleep period. Second, many prior studies aimed

at addressing the question of replay's necessity for consolidation have relied on disrupting circuit-level activity across windows of sleep or over several days[26,27]. Here we have taken advantage of recently-developed genetic tools to label cue-activated neurons and a new paradigm for studying sleep-dependent consolidation of memory for a specific sensory cue (**Figure 4.1**)[21]. These have allowed us to demonstrate that sleep-associated reactivation of cue-activated visual engram neurons plays a critical, instructive role in consolidating an associative memory linked to that cue.

A limitation of the present study is that inhibition of visual engram neurons in V1 occurred throughout all stages of sleep (i.e., both REM and NREM). Our prior work on experience-dependent plasticity in V1 (which has been linked to recognition memory for previously-viewed orientations[42])has demonstrated that thalamocortical oscillations coordinating activity between the lateral geniculate nucleus (LGN) and V1 during NREM sleep are essential for orientation preference shifts in V1[29].The pattern of optogenetic stimulation used on visual cue-activated neurons in this study (i.e., regular periodic activation at 1 Hz) is in some ways similar to what occurs in V1 during these NREM oscillations. Critically, this pattern of activation is sufficient to drive large V1 orientation preference shifts (**Figure 4.5**). However, a role for REM activity in cortical plasticity cannot be ruled out. REM plays a critical role in developmentally-regulated experience-dependent plasticity in V1[49]. In many species, REM is characterized by selective activation of LGN-V1 circuitry during pontine-geniculate-occipital (PGO) waves, which promote synaptic plasticity in various brain structures[50]. Future work will be aimed at both characterizing patterns of activity in orientation-selective populations during REM vs. NREM, and in targeting inhibition of this population to specific states.

The present findings may ultimately inform our understanding of how sensory cortical areas interact with structures such as the hippocampus and amygdala during sleep, and how these interactions inform consolidation of specific memories. Together our data indicate that primary sensory structures engaged in fear memory encoding communicate with structures conveying emotional valence information during post-learning sleep to promote long-lasting fear association with a specific cue. Whether this interregional communication is unique to one or more sleep states is a critical unanswered question. Answering this question may have important implications not only for understanding sleep's mechanistic role in memory consolidation, but also its mechanistic role in regulation of mood and affect. It will also have specific implications for treating disorders where fear is dysregulated or misattributed, including anxiety and panic disorders, acute stress disorder, and PTSD.

4.11 References

1. Pavlides, C. & Winson, J. Influences of Hippocampal Place Cell Firing in the Awake State on the Activity of These Cells During Subsequent Sleep Episodes. *Neuroscience* **9**, 2907–2918 (1989).

2. Wilson, M. A. & Mcnaughton, B. L. Reactivation of Hippocampal Ensemble Memories During Sleep. *Science (80-.).* **265**, 676–679 (1994).

3. Gerrard, J. L., Kudrimoti, H., McNaughton, B. L. & Barnes, C. A. Reactivation of hippocampal ensemble activity patterns in the aging rat. *Behav. Neurosci.* **115**, 1180–1192 (2001).

4. Kudrimoti, H. S., Barnes, C. A. & McNaughton, B. L. Reactivation of hippocampal cell assemblies: Effects of behavioral state, experience, and EEG dynamics. *J. Neurosci.* **19**, 4090–4101 (1999).

5. Skaggs, W. E. & McNaughton, B. L. Theta Phase Precession in Hippocampal Neurinak Populations abd the Compression of. *Hippocampus* **6**, 149–172 (1996).
6. Lee, A. K. & Wilson, M. A. Memory of sequential experience in the hippocampus during slow wave sleep. *Neuron* **36**, 1183–1194 (2002).

7. Louie, K. & Wilson, M. A. Temporally Structured Replay of Awake Hippocampal Ensemble Activity during Rapid Eye Movement Sleep. *Neuron* **29**, 145–156 (2001).

8. Nadasdy, Z., Hirase, H., Czurko, A., Csicsvari, J. & Buzsáki, G. Replay and Time Compression of Recurring Spike Sequences in the Hippocampus. *Neuroscience* **19**, 9497–9507 (1999).

9. Ji, D. & Wilson, M. A. Coordinated memory replay in the visual cortex and hippocampus during sleep. *Nat. Neurosci.* **10**, 100–107 (2007).

10. Euston, D. R., Tatsuno, M. & McNaughton, B. L. Fast-forward playback of recent memory sequences in prefrontal cortex during sleep. *Science (80-.).* **318**, 1147–1150 (2007).

11. Johnson, L. A., Euston, D. R., Tatsuno, M. & McNaughton, B. L. Stored-Trace Reactivation in Rat Prefrontal Cortex Is Correlated with Down-to-Up State Fluctuation Density. *J. Neurosci.* **30**, 2650–2661 (2010).

12. Peyrache, A., Khamassi, M., Benchenane, K., Wiener, S. I. & Battaglia, F. P. Replay of rule-learning related neural patterns in the prefrontal cortex during sleep. *Nat. Neurosci.* **12**, 919–926 (2009).

13. Hoffman, K. L. & McNaughton, B. L. Coordinated reactivation of distributed memory traces in primate neocortex. *Science (80-.).* **297**, 2070–2073 (2002).

14. Dave, A. S. & Margoliash, D. Song Replay During Sleep and Computational Rules for Sensorimotor Vocal Learning. *Science (80-.).* **290**, 812–816 (2000).

15. Pennartz, C. M. A. *et al.* The ventral striatum in off-line processing: Ensemble reactivation during sleep and modulation by hippocampal ripples. *J. Neurosci.* **24**, 6446–6456 (2004).

16. Lansink, C. S. *et al.* Preferential reactivation of motivationally relevant information in the ventral striatum. *J. Neurosci.* **28**, 6372–6382 (2008).

17. Lansink, C. S., Goltstein, P. M., Lankelma, J. V., McNaughton, B. L. & Pennartz, C. M. A. Hippocampus leads ventral striatum in replay of place-reward information. *PLoS Biol.* **7**, (2009).

18. Axmacher, N., Elger, C. E. & Fell, J. Ripples in the medial temporal lobe are relevant for human memory consolidation. *Brain* **131**, 1806–1817 (2008).

19. Rothschild, G., Eban, E. & Frank, L. M. A cortical – hippocampal – cortical loop of information processing during memory consolidation. *Nat. Neurosci.* **20**, 1–12 (2016).

20. Puentes-Mestril, C. & Aton, S. J. Linking network activity to synaptic plasticity during sleep: Hypotheses and recent data. *Front. Neural Circuits* **11**, 1–18 (2017).

21. Guenthner, C. J., Miyamichi, K., Yang, H. H., Heller, H. C. & Luo, L. Permanent genetic access to transiently active neurons via TRAP: Targeted recombination in active populations. *Neuron* **78**, 773–784 (2013).

22. Liu, X. *et al.* Optogenetic stimulation of a hippocampal engram activates fear memory recall. *Nature* **484**, 381–385 (2012).

23. Ryan, T. J., Roy, D. S., Pignatelli, M., Arons, A. & Tonegawa, S. Engram cells retain memory under retrograde amnesia. *Science (80-.).* **348**, 1007–1014 (2015).

24. Kitamura, T., Ogawa, S. K., Roy, D. S. & Okuyama, T. Engrams and circuits crucial for systems consolidation of a memory. **78**, 73–78 (2017).

25. Ego-Stengel, V. & Wilson, M. A. Disruption of ripple-associated hippocampal activity during rest impairs spatial learning in the rat. *Hippocampus* **20**, 1–10 (2010).

26. Girardeau, G., Benchenane, K., Wiener, S. I., Buzsáki, G. & Zugaro, M. B. Selective suppression of hippocampal ripples impairs spatial memory. *Nat. Neurosci.* **12**, 1222–1223 (2009).

27. Gridchyn, I. *et al.* Assembly-Specific Disruption of Hippocampal Replay Leads to Selective Memory Deficit Article Assembly-Specific Disruption of Hippocampal Replay Leads to Selective Memory Deficit. *Neuron* 1–10 (2020). doi:10.1016/j.neuron.2020.01.021

28. van de Ven, G. M., Trouche, S., McNamara, C. G., Allen, K. & Dupret, D. Hippocampal Offline Reactivation Consolidates Recently Formed Cell Assembly Patterns during Sharp Wave-Ripples. *Neuron* **92**, 968–974 (2016).

29. Durkin, J. *et al.* Cortically coordinated NREM thalamocortical oscillations play an essential , instructive role in visual system plasticity. *Proc. Natl. Acad. Sci.* 2–7 (2017). doi:10.1073/pnas.1710613114

30. Ognjanovski, N., Broussard, C., Zochowski, M. & Aton, S. J. Hippocampal Network Oscillations Rescue Memory Consolidation Deficits Caused by Sleep Loss. *Cereb. Cortex* 1–13 (2018). doi:10.1093/cercor/bhy174

31. Curzon, P., Rustay, N. & Browman, K. Cued and Contextual Fear Conditioning for Rodents. in *Methods of Behavior Analysis in Neuroscience.* (ed. Buccafusco, J.) 19–37 (CRC Press, 2009). doi:10.1201/noe1420052343.ch2

32. Ognjanovski, N. *et al.* Parvalbumin-expressing interneurons coordinate hippocampal network dynamics required for memory consolidation. *Nat. Commun.* **8**, 1–13 (2017).

33. Aton, S. J., Suresh, A., Broussard, C. & Frank, M. G. Sleep Promotes Cortical Response Potentiation Following Visual Experience. *Sleep* **37**, 1163–1170 (2014).

34. Durkin, J. & Aton, S. J. Sleep-Dependent Potentiation in the Visual System Is at Odds with the Synaptic Homeostasis Hypothesis. *Sleep* **39**, 155–159 (2016).

35. Clawson, B. C. *et al.* Sleep promotes, and sleep loss inhibits, selective changes in firing rate, response properties and functional connectivity of primary visual cortex neurons. *Front. Syst. Neurosci.* **12**, 1–16 (2018).

36. Ruskin, D. N., Liu, C., Dunn, K. E., Bazan, N. G. & LaHoste, G. J. Sleep deprivation impairs hippocampus-mediated contextual learning but not amygdala-mediated cued learning in rats. *Eur. J. Neurosci.* **19**, 3121–3124 (2004).

37. Cai, D. J., Shuman, T., Harrison, E. M., Sage, J. R. & Anagnostaras, S. G. Sleep deprivation and Pavlovian fear conditioning. *Learn. Mem.* **16**, 595–599 (2009).

38. Kumar, T. & Jha, S. K. Sleep Deprivation Impairs Consolidation of Cued Fear Memory in Rats. *PLoS One* **7**, (2012).

39. Graves, L. A., Heller, E. A., Pack, A. I. & Abel, T. Sleep deprivation selectively impairs memory consolidation for contextual fear conditioning. *Learn. Mem.* **10**, 168–176 (2003).

40. Marshel, J. H. *et al.* Cortical layer – specific critical dynamics triggering perception. *Science (80-.).* **365**, 1–23 (2019).

41. Frenkel, M. Y. *et al.* Instructive Effect of Visual Experience in Mouse Visual Cortex. *Neuron* **51**, 339–349 (2006).

42. Cooke, S. F., Komorowski, R. W., Kaplan, E. S., Gavornik, J. P. & Bear, M. F. Visual recognition memory, manifested as long-term habituation, requires synaptic plasticity in V1. *Nat. Neurosci.* **18**, 262–271 (2015).

43. Jehee, J. F. M., Ling, S., Swisher, J. D., van Bergen, R. S. & Tong, F. Perceptual learning selectively Refines orientation representations in early visual cortex. *J. Neurosci.* **32**, 16747–16753 (2012).

44. Adab, H. Z., Popivanov, I. D., Vanduffel, W. & Vogels, R. Perceptual Learning of Simple Modifies Stimulus Representations in Posterior Inferior Temporal Cortex. *J. Cogn. Neurosci.* **26**, 2187–2200 (2014).

45. Zivari Adab, H. & Vogels, R. Practicing coarse orientation discrimination improves orientation signals in macaque cortical area V4. *Curr. Biol.* **21**, 1661–1666 (2011).

46. Kitamura, T. *et al.* Engrams and circuits crucial for systems consolidation of a memory. *Science (80-.).* **356**, 73–78 (2017).

47. Ji, D. & Wilson, M. A. Coordinated memory replay in the visual cortex and hippocampus during sleep. *Nat. Neurosci.* **10**, 100–107 (2007).

48. Giri, B., Diba, K., Miyawaki, H., Cheng, S. & Mizuseki, K. Hippocampal Reactivation Extends for Several Hours Following Novel Experience. *J. Neurosci.* **39**, 866–875 (2018).

49. Bridi, M. C. D. *et al.* Rapid eye movement sleep promotes cortical plasticity in the developing brain. *Sci. Adv.* **1**, 1–8 (2015).

50. Puentes-Mestril, C., Roach, J., Niethard, N., Zochowski, M. & Aton, S. J. How rhythms of the sleeping brain tune memory and synaptic plasticity. *Sleep* **42**, 1–14 (2019).

CHAPTER V

Conclusion

5.1 In Sum

For almost 100 years we have known that sleep is critical for memory consolidation[1]. However, the sleep-associated neurobiological mechanisms underlying this effect are largely unknown. Prior work attempting to elucidate the activity-dependent mechanisms for sleep-dependent memory consolidation faced two major technical challenges. First, there were almost no behavioral paradigms where memory consolidation had been examined after a single period of sleep. Second, it was nearly impossible to examine sleep's effects at the level of a specific memory. **Chapters 3** and **4** of this dissertation use chronic *in vivo* electrophysiology and new genetic tools for engram labeling to begin to examine sleep's effects on visual system plasticity and visual memory.

In **Chapter 3**, we demonstrate that sleep bidirectionally modulates neuronal firing rates in the V1. Low firing rate, highly orientation-selective neurons show increases in firing rate across sleep, while high firing rate, minimally selective neurons have their activity selectively downregulated across sleep. This work suggests that sleep may refine networks by simultaneously increasing signal (e.g., activity among neurons whose firing has a high orientation encoding capacity) and decreasing noise (e.g., activity among neurons whose firing provides little feature-selective information).

In **Chapter 4**, we ask whether sleep-associated reactivation of memory encoding neurons is necessary for memory consolidation. We first characterized the sleep-

dependence of visually-cued fear memory consolidation—a memory which is encoded during a single training trial, pairing oriented gratings with foot shocks. Next, using recently developed genetic tools for engram labeling, we were able to visualize and manipulate orientation-selective V1 neurons. Rhythmic optogenetic activation of these neurons produces shifts in the orientation tuning of surrounding V1 neurons, leading to increased representation of the activated neurons' preferred orientation in the cortex. This labeled ensemble was selectively reactivated during *ad lib* sleep in the hours following training. Sleep-specific optogenetic inhibition of the labelled neurons leads to an inability to discriminate the foot shock cue stimulus from other stimuli, expressed as high levels of generalized fear.

This work examines sleep-dependent memory consolidation mechanisms in sensory cortex with unprecedented resolution—discriminating between changes occurring in memory encoding neurons compared to other neurons in the network. The network refinement that we see in **Chapter 3** aids in resolving a long-standing debate between proponents of SHY and ASC. Rather than having a unidirectional effect on the firing of cortical neurons, sleep facilitates bidirectional changes. Increases in firing occur selectively in neurons providing the most refined sensory information to the network, against a background of reduction in firing amongst neurons providing the least sensory information. In **Chapter 4,** we show for the first time that sleep-associated reactivation of V1 ensembles that encode sensory experience is necessary for sleep-dependent memory consolidation. These two processes (firing rate rescaling and selective reactivation of learning-associated neurons) may be linked. For example, firing rate data from mice exposed to visual stimuli to induce OSRP in **Chapter 3** suggest potentially larger firing

changes in these mice across sleep than in blank screen controls. Selective reactivation of populations of stimulus encoding populations may thus underlie the widely reported phenomenon of firing rate rescaling. However, further studies need to be conducted in order to directly link reactivation to firing rate rescaling.

To directly link reactivation and network renormalization the final experiment in **Chapter 4** should be repeated with tetrode recording in V1 rather than EEG to track the activity of individual neurons. This would allow assessment of whether firing rate renormalization is dependent on memory reactivation. Additionally, that data could be run through stability algorithms to get a deeper biophysical understanding of the network changes. It would be beneficial to also add a tetrode bundle in the LGN (similar to Durkin *et al*)[2]. This would allow for evaluation of information transfer between the LGN and V1. One may also consider a hippocampal tetrode bundle or LFP electrode to assay changes in SWRs and patterned hippocampal activity. Together these recordings could elucidate the links between memory reactivation, network renormalization, and two stage memory transfer (from initial hippocampal and thalamic inputs to cortical storage)

This work opens up a number of questions for future study. While our work addressed the necessity of reactivation for sleep-dependent memory consolidation, sufficiency of reactivation for memory consolidation (i.e., in the absence of other sleep-associated physiological changes) remains an open question. Testing sufficiency is likely to be more difficult: it is easier to break a toaster than to build one. Due to the complex electrochemical changes coordinated across many brain circuits during sleep, it is unlikely that reactivation of neuronal populations in V1 alone will be sufficient to produce proper visually-cued fear memory consolidation. However, augmentation of memory reactivation

during sleep may be feasible via closed-loop reactivation precisely coordinated with sleep's endogenous rhythms. Similarly sleep-targeted reactivation has been beneficial in human subjects in memory studies linking features of learned material to external sensory cues that can be re-presented to subjects during post-learning sleep[3-5].

Further studies must also be done to test the necessity of sleep-dependent reactivation for consolidation in other brain regions and across other memory paradigms. A greater understanding of when and where reactivation is beneficial for consolidation (and when and where it is not) will providing further insight into the neurobiological underpinnings of memory storage in the brain.

Another branch of future directions should center around changes occurring in individual engram neurons during sleep-dependent memory consolidation. This work can interrogate three key plasticity correlates: changes in structure, function, and molecular expression. To examine changes in structure and expression, our lab is currently examining sleep-dependent changes in dendritic spine density and ribosome-associated mRNAs in TRAPed neural ensembles. Further electrophysiological work will also be needed to fully evaluate functional changes in TRAPed neurons across sleep. This work should include measuring AMPA to NMDA ratios and evoked and spontaneous postsynaptic currents. The role of reactivation in this plasticity could also be studied at the level of specific connections both within and outside of the TRAPed ensemble. For example, optogenetically stimulating TRAPed neurons to evoke EPSCs in postsynaptic partners would provide unique access to studying plasticity in memory-specific synaptic connections. Together this work will begin to define a mechanism for how sleep alters specific memory traces at the cellular and molecular level.

Combining data dissecting circuitry and molecular mechanisms linked to replay may provide a more comprehensive view of how sleep alters memory. This would provide critical insights allowing for pharmacological treatment of disorders that are linked to alterations in sleep. Some such disorders, such as schizophrenia, show long term changes in sleep signatures linked to disordered executive function. These would require long-term treatment either pharmacologically stimulating replay or using targeted memory reactivation to induce replay where it was lacking before.[6] Others, such as PTSD, may be linked to a critical window during consolidation followed by extended sleep disturbance.[7] These may require rapid intervention during the acute stress phase – either pharmacologically inhibiting maladaptive replay of the traumatic memory or perhaps using targeted memory reactivation to occlude replay of the traumatic memory.

In the broad scheme of things, sleep is a highly conserved process critical for many body and brain functions - including maintaining proper cognition and memory consolidation. Whether it's a honeybee who needs to remember its waggle dance or a grad student who needs to remember the words to their dissertation defense, sleep plays a critical role in orchestrating our everyday lives. So now that you have read this, get some rest, and consolidate these memories while you sleep.

5.2 References

1. Jenkins, J. G. & Dallenbach, K. M. Obliviscence during Sleep and Waking. *Am. J. Psychol.* **35**, 605–612 (1924).

2. Durkin, J. *et al.* Cortically coordinated NREM thalamocortical oscillations play an essential , instructive role in visual system plasticity. *Proc. Natl. Acad. Sci.* 2–7 (2017). doi:10.1073/pnas.1710613114

3. Creery, J. D., Oudiette, D., Antony, J. W. & Paller, K. A. Targeted Memory Reactivation during Sleep Depends on Prior Learning. *Sleep* **38**, 755–763 (2015).

4. Rasch, B., Büchel, C., Gais, S. & Born, J. Odor cues during slow-wave sleep prompt declarative memory consolidation. *Science (80-.).* **315**, 1426–1429 (2007).

5. Hu, X., Cheng, L. Y., Chiu, M. H. & Paller, K. A. Promoting memory consolidation during sleep: A meta-analysis of targeted memory reactivation. *Psychol. Bull.* **146**, 218–244 (2020).

6. Manoach, D. S. & Stickgold, R. Sleep, Memory and Schizophrenia. *Sleep Med.* **16**, 553–554 (2015).

7. Goldstein, A.N. & Walker, M.P. The role of sleep in emotional brain function. *Annu Rev Clin Psychol.* **10**, 679-708 (2014).